

REINFORCEMENT OF POLYESTERS BY BORON MINERALS

A THESIS SUBMITTED TO
THE GRADUATE SCHOOL OF NATURAL AND APPLIED SCIENCES
OF
MIDDLE EAST TECHNICAL UNIVERSITY

BY

AYDIN MERT AKGÜN

IN PARTIAL FULFILMENT OF THE REQUIREMENTS
FOR
THE DEGREE OF DOCTOR OF PHILOSOPHY
IN
POLYMER SCIENCE AND TECHNOLOGY

SEPTEMBER 2015

Approval of the thesis:

REINFORCEMENT OF POLYESTERS BY BORON MINERALS

submitted by **AYDIN MERT AKGÜN** in partial fulfillment of the requirements for the degree of **Doctor of Philosophy in Polymer Science and Technology Department, Middle East Technical University** by,

Prof. Dr. Gülbin Dural Ünver

Director, Graduate School of **Natural and Applied Sciences**

Prof. Dr. Necati Özkan

Head of Department, **Polymer Science and Technology**

Prof. Dr. Ali Usanmaz (Deceased)

Supervisor, **Chemistry Dept., METU**

Prof. Dr. Teoman Tinçer

Supervisor, **Chemistry Dept., METU**

Assoc. Prof. Dr. Tonguç Özdemir

Co-Supervisor, **Chemical Eng. Dept., Mersin University**

Examining Committee Members:

Prof. Dr. Murat Şen

Chemistry Dept., Hacettepe University

Prof. Dr. Teoman Tinçer

Chemistry Dept., METU

Prof. Dr. Ahmet M. Önal

Chemistry Dept., METU

Assoc. Prof. Dr. Ali Çırpan

Chemistry Dept., METU

Asst. Prof. Dr. Elif Vargün

Chemistry Dept., Muğla Sıtkı Koçman University

Date: _____

I hereby declare that all information in this document has been obtained and presented in accordance with academic rules and ethical conduct. I also declare that, as required by these rules and conduct, I have fully cited and referenced all material and results that are not original to this work.

Name, Last name: Aydın Mert AKGÜN

Signature:

ABSTRACT

REINFORCEMENT OF POLYESTERS BY BORON MINERALS

Akgün, Aydın Mert

Ph.D., Department of Polymer Science and Technology

Supervisor: Prof. Dr. Teoman Tinçer

Co-Supervisor: Assoc. Prof. Dr. Tonguç Özdemir

September 2015, 109 pages

Polymers are used in areas where exposure to high-energy radiation might occur. Main effects of irradiation on polymers are crosslinking, chain scission and oxidation. Radiation resistance of polymers depends on structure, additives, or irradiation conditions. Since boron is highly effective material against radiation, especially against neutron radiation, with its high absorption cross section, boron products is used for radiation applications. The aim of this study is to investigate the effects of different types of boron minerals used as reinforcing fillers on mechanical properties, thermal properties and on radiation stability of unsaturated polyester resin.

Four different boron minerals (anhydrous borax, calcined tincal, concentrated tincal and ground colemanite) with various B_2O_3 content were used in this study. Unsaturated polyester composites were prepared with 2%, 5% and 10% of boron mineral by weight. They were exposed to gamma radiation with irradiation dose rates of 30 Gy/h and 2500 Gy/h. Samples were characterized by ATR-FTIR, TGA, DMA and SEM techniques as well as their mechanical properties.

Most satisfying mechanical test results were obtained for anhydrous borax which contains 68% of B_2O_3 . Polystyrene formation and oxidizing reactions especially at high doses were observed from ATR-FTIR spectra. T_g of neat polyester resin was shifted from 66.3 to 74.3 °C for high doses. Neat polyester resin was thermally degraded around 410 °C and thermal stability of composites was not significantly affected by irradiation or reinforcement as seen from TGA thermograms. Agglomeration derived from higher reinforcing filler ratio was seen from SEM micrographs.

Keywords: unsaturated polyester, boron minerals, irradiation, crosslinking, composite

ÖZ

POLİESTERLERİN BOR MİNERALLERİ İLE GÜÇLENDİRİLMESİ

Akgün, Aydın Mert

Doktora, Polimer Bilimi ve Teknolojisi Bölümü

Tez Yöneticisi: Prof. Dr. Teoman Tinçer

Ortak Tez Yöneticisi: Doç. Dr. Tonguç Özdemir

Eylül 2015, 109 sayfa

Polimerler, yüksek enerjili radyasyona maruz kaldıkları pek çok alanda kullanılır. Işınlamanın polimerler üzerindeki başlıca etkileri çapraz bağlanma, zincir kırılması ve oksitlenmedir. Polimerlerin radyasyon dirençleri yapılarına, katkı maddelerine veya ışınlama koşullarına bağlıdır. Bor, yüksek absorpsiyon tesir kesiti sebebiyle radyasyona, özellikle nötron radyasyonuna, karşı etkin bir malzemedir ve radyasyon uygulamalarında sıklıkla kullanılır. Bu çalışmanın amacı, güçlendirici olarak kullanılan farklı bor minerallerinin, doymamış poliester reçinenin mekanik özellikleri, termal özellikleri ve radyasyon kararlılığı üzerindeki etkilerini incelemektir.

Bu çalışmada, farklı B_2O_3 içeriğine sahip dört farklı bor minerali (susuz boraks, kalsine tinkal, konsantre tinkal, kolemanit) kullanılmıştır. Ağırlıkça %2, %5 ve %10 oranında bor minerali içeriğine sahip doymamış poliester kompozitler hazırlanmıştır. Bu malzemeler 30 Gy/h ve 2500 Gy/h doz hızına sahip kaynaklarda gama radyasyonuna maruz bırakılmıştır. Numuneler ATR-FTIR, TGA, DMA ve SEM tekniklerinin yanı sıra mekanik özellikleriyle de karakterize edilmişlerdir.

En tatmin edici mekanik test sonuçları, %68 oranında B₂O₃ içeren susuz boraks ile elde edilmiştir. ATR-FTIR spektrumlarından, özellikle yüksek dozlarda polistiren oluşumu ve oksitlenme reaksiyonları gözlenmiştir. Yüksek dozlarda, katkısız poliester reçinenin T_g'si 66.3 °C'den 74.3 °C'ye doğru kaymıştır. Katkısız polyester yaklaşık 410 °C'de termal bozunmaya uğramıştır ve TGA termogramlarından görüldüğü üzere kompozitlerin termal kararlılığı, ışınlamadan veya güçlendirmeden belirgin bir şekilde etkilenmemiştir. Yüksek katkı oranlarında oluşan topaklanma SEM mikrograflarından görülmüştür.

Anahtar Kelimeler: doymamış poliester, bor mineralleri, ışınlama, çapraz bağlanma, kompozit

To my parents and my grandfather,
(in memory of Prof. Dr. Ali USANMAZ)

ACKNOWLEDGEMENTS

I am very grateful to my thesis supervisor Prof. Dr. Ali Usanmaz for all his continuous support, helpful suggestions and guidance during my research work and for his interest in its progress. His positive approach and politeness always kept me focused on my study. I am also grateful to my thesis co-supervisor Assoc. Prof. Dr. Tongu Özdemir. He is such a mentor to me and he never stopped believing me.

I also give my special thanks to Prof. Dr. Teoman Tiner and Asst. Prof. Dr. Elif Vargün for their support, suggestions and critiques. This study found its way by their guidance.

I should mention my laboratory mates Yurdaer Babucuođlu and Fırat Hacıođlu for their help and suggestions. I especially would like to express my gratitude to them for their support and guidance.

I would like to thank Prof. Dr. Uđur Adnan Sevil from Hitit University for their help in the irradiation procedure of samples. Besides, I would also like to express my acknowledgments to Ümit Tayfun and technician Osman Yaslıtaş in Chemistry Department for their assistance and guidance to me during experimental work.

It is great honor for me to express my sincere appreciation to my mother Kamelya Akgün and my father Razi Akgün who encouraged me to begin and to finish my doctoral study. Finally, my grandfather, I know you are watching me over from up there with a smile in your face.

TABLE OF CONTENTS

ABSTRACT	v
ÖZ	vii
ACKNOWLEDGEMENTS	x
TABLE OF CONTENTS	xi
LIST OF TABLES	xiv
LIST OF FIGURES	xvi
LIST OF SYMBOLS AND ABBREVIATIONS	xx
CHAPTERS	
1. INTRODUCTION	1
1.1. Polyesters	1
1.1.1. Unsaturated Polyesters	2
1.1.1.1. Raw Materials of Unsaturated Polyesters	2
1.1.1.2. Production of Unsaturated Polyesters	3
1.1.1.3. Types of Unsaturated Polyester Resins	4
1.1.1.4. Crosslinking Mechanism of Unsaturated Polyester Resins	5
1.1.1.5. Properties of Unsaturated Polyester Resins	7
1.2. Reinforcement of Polyesters	9
1.3. Effects of Ionizing Radiation on Polymers	16
1.4. Boron and Boron Minerals	19
1.5. Aim of the Study	23
2. EXPERIMENTAL	25
2.1. Boron Minerals	25
2.2. Boron Minerals-Polyester Composites	25
2.3. Irradiation of Samples	26
2.4. Characterization of Samples	27
3. RESULTS AND DISCUSSION	31
3.1. Physical Appearances of the Samples	31

3.2. Tensile Tests.....	32
3.2.1. Tensile Tests of Samples Irradiated Open to Atmosphere	33
3.2.1.1. Young’s Modulus.....	33
3.2.1.2. Tensile Strength.....	39
3.2.1.3. Elongation at Break.....	41
3.2.2. Tensile Tests of Samples Irradiated by High Dose Rate Gamma Source under Vacuum.....	50
3.2.2.1. Young’s Modulus.....	50
3.2.2.2. Tensile Strength.....	53
3.2.2.3. Elongation at Break.....	55
3.3. Attenuated Total Reflectance - Fourier Transform Infrared Spectroscopy	58
3.3.1. ATR-FTIR Results of Boron Minerals.....	59
3.3.2. ATR-FTIR Results of Samples Irradiated by Low Dose Rate Gamma Source.....	60
3.3.3. ATR-FTIR Results of Samples Irradiated by High Dose Rate Gamma Source Open to Atmosphere.....	64
3.3.4. ATR-FTIR Results of Samples Irradiated by High Dose Rate Gamma Source under Vacuum.....	66
3.4. Dynamic Mechanical Analysis.....	69
3.4.1. DMA Results of Neat Polyester Resin Samples Non-irradiated and Irradiated	69
3.4.2. DMA Results of Polyester Resin Reinforced with Different Boron Minerals.....	70
3.4.3. DMA Results of Polyester Resin Reinforced with Different Compositions.....	71
3.5. Thermogravimetric Analysis.....	72
3.5.1. TGA Results of Boron Minerals.....	72
3.5.2. TGA Results of Neat Polyester Resin Samples Non-irradiated and Irradiated	73
3.5.3. TGA Results of Polyester Resin Reinforced with Different Boron Minerals.....	75
3.5.4. TGA Results of Polyester Resin Reinforced with Different Compositions.....	76

3.6. Scanning Electron Microscopy Study	78
4. CONCLUSIONS	83
REFERENCES	85
APPENDICES	95
A: CONTENTS OF BORON MINERALS USED IN THE STUDY	95
B: PROPERTIES OF UNSATURATED POLYESTER RESIN USED IN THE STUDY	97
C: TABLES OF TENSILE TEST RESULTS	99
D: TABLES OF NORMALIZED ABSORBANCE VALUES OF ATR-FTIR SPECTRA	103
CURRICULUM VITAE	107

LIST OF TABLES

TABLES

Table 2.1: Boron Minerals Used In This Study.....	25
Table 2.2: Preparation of Polyester Composites.....	26
Table 2.3: Absorbed Dose Values for Irradiated Samples.....	27
Table A.1: Contents of Etibor-68 (Anhydrous Borax).....	95
Table A.2: Contents of Calcined Tincal.....	95
Table A.3: Contents of Concentrated Tincal.....	96
Table A.4: Contents of Ground Colemanite.....	96
Table B.1: Properties of Unsaturated Polyester Resin.....	97
Table C.1: Young's Modulus Results of Tensile Tests.....	99
Table C.2: Tensile Strength Results of Tensile Tests.....	100
Table C.3: Elongation at Break Results of Tensile Tests.....	101
Table D.1: ATR-FTIR Results of Boron Minerals.....	103
Table D.2: ATR-FTIR Results of POL Irradiated by Low Dose Rate Gamma Source	103
Table D.3: ATR-FTIR Results of Reinforced Samples Irradiated by Low Dose Rate Gamma Source (Absorbed Dose of 245 kGy).....	103
Table D.4: ATR-FTIR Results of PANB with Different Compositions Irradiated by Low Dose Rate Gamma Source (Absorbed Dose of 245 kGy).....	104
Table D.5: ATR-FTIR Results of POL Irradiated by High Dose Rate Gamma Source Open to Atmosphere.....	104
Table D.6: ATR-FTIR Results of Reinforced Samples Irradiated by High Dose Rate Gamma Source Open to Atmosphere (Absorbed Dose of 2500 kGy).....	104
Table D.7: ATR-FTIR Results of PANB with Different Compositions Irradiated by High Dose Rate Gamma Source Open to Atmosphere (Absorbed Dose of 2500 kGy)	104

Table D.8: ATR-FTIR Results of POL Irradiated by High Dose Rate Gamma Source under Vacuum.....	105
Table D.9: ATR-FTIR Results of Reinforced Samples Irradiated by High Dose Rate Gamma Source under Vacuum (Absorbed Dose of 2500 kGy).....	105
Table D.10: ATR-FTIR Results of PANB with Different Compositions Irradiated by High Dose Rate Gamma Source under Vacuum (Absorbed Dose of 2500 kGy)....	105

LIST OF FIGURES

FIGURES

Figure 1.1: General Representation of Formation of Polyester.....	1
Figure 1.2: Crosslinked Unsaturated Polyester Resin.....	7
Figure 1.3: Polymerization of Polyester Resin with Reinforcement.....	11
Figure 1.4: Chemical Structures of Tincal and Colemanite.....	20
Figure 2.1: Lloyd Instruments LR 5K Universal Testing Machine.....	28
Figure 2.2: Thermo Nicolet iS10 ATR-FTIR Spectrometer.....	28
Figure 2.3: LECO TGA701 Thermogravimetric Analyzer.....	29
Figure 3.1: Physical Appearances of a) PANB b) PCAT c) PCOT and d) PCOL.....	31
Figure 3.2: Physical Appearance of Neat Polyester Resin Irradiated by Low Dose Rate Gamma Source with Increasing Doses.....	32
Figure 3.3: Physical Appearance of Neat Polyester Resin Irradiated by Low Dose Rate Gamma Source with Increasing Doses a) in Air and b) under Vacuum.....	33
Figure 3.4: Young's Moduli of PANB Samples Irradiated by a) Low Dose Rate Gamma Source b) High Dose Rate Gamma Source.....	35
Figure 3.5: Young's Moduli of PCOT Samples Irradiated by a) Low Dose Rate Gamma Source b) High Dose Rate Gamma Source.....	36
Figure 3.6: Young's Moduli of PCAT Samples Irradiated by a) Low Dose Rate Gamma Source b) High Dose Rate Gamma Source.....	37
Figure 3.7: Young's Moduli of PCOL Samples Irradiated by a) Low Dose Rate Gamma Source b) High Dose Rate Gamma Source.....	38
Figure 3.8: Tensile Strengths of PANB Samples Irradiated by a) Low Dose Rate Gamma Source b) High Dose Rate Gamma Source.....	40
Figure 3.9: Tensile Strengths of PCOT Samples Irradiated by a) Low Dose Rate Gamma Source b) High Dose Rate Gamma Source.....	42
Figure 3.10: Tensile Strengths of PCAT Samples Irradiated by a) Low Dose Rate Gamma Source b) High Dose Rate Gamma Source.....	43

Figure 3.11: Tensile Strengths of PCOL Samples Irradiated by a) Low Dose Rate Gamma Source b) High Dose Rate Gamma Source.....	44
Figure 3.12: Elongation at Break of PANB Samples Irradiated by a) Low Dose Rate Gamma Source b) High Dose Rate Gamma Source.....	46
Figure 3.13: Elongation at Break of PCOT Samples Irradiated by a) Low Dose Rate Gamma Source b) High Dose Rate Gamma Source.....	47
Figure 3.14: Elongation at Break of PCAT Samples Irradiated by a) Low Dose Rate Gamma Source b) High Dose Rate Gamma Source.....	48
Figure 3.15: Elongation at Break of PCOL Samples Irradiated by a) Low Dose Rate Gamma Source b) High Dose Rate Gamma Source.....	49
Figure 3.16: Young’s Moduli of PANB Samples Irradiated by High Dose Rate Gamma Source under Vacuum.....	51
Figure 3.17 Young’s Moduli of PCOT Samples Irradiated by High Dose Rate Gamma Source under Vacuum.....	51
Figure 3.18: Young’s Moduli of PCAT Samples Irradiated by High Dose Rate Gamma Source under Vacuum.....	52
Figure 3.19: Young’s Moduli of PCOL Samples Irradiated by High Dose Rate Gamma Source under Vacuum.....	52
Figure 3.20: Tensile Strengths of PANB Samples Irradiated by High Dose Rate Gamma Source under Vacuum.....	53
Figure 3.21: Tensile Strengths of PCOT Samples Irradiated by High Dose Rate Gamma Source under Vacuum.....	54
Figure 3.22: Tensile Strengths of PCAT Samples Irradiated by High Dose Rate Gamma Source under Vacuum.....	54
Figure 3.23: Tensile Strengths of PCOL Samples Irradiated by High Dose Rate Gamma Source under Vacuum.....	55
Figure 3.24: Elongation of PANB Samples at Break Irradiated by High Dose Rate Gamma Source under Vacuum.....	56
Figure 3.25: Elongation of PCOT Samples at Break Irradiated by High Dose Rate Gamma Source under Vacuum.....	56
Figure 3.26: Elongation of PCAT Samples at Break Irradiated by High Dose Rate Gamma Source under Vacuum.....	57
Figure 3.27: Elongation of PCOL Samples at Break Irradiated by High Dose Rate Gamma Source under Vacuum.....	58

Figure 3.28: ATR-FTIR Spectra of Boron Minerals.....	59
Figure 3.29: ATR-FTIR Spectra of POL Irradiated by Low Dose Rate Gamma Source.....	62
Figure 3.30: ATR-FTIR Spectra of Reinforced Samples Irradiated by Low Dose Rate Gamma Source.....	63
Figure 3.31: ATR-FTIR Spectra of PANB with Different Compositions Irradiated by Low Dose Rate Gamma Source.....	63
Figure 3.32: ATR-FTIR Spectra of POL Irradiated by High Dose Rate Gamma Source Open to Atmosphere.....	64
Figure 3.33: ATR-FTIR Spectra of Reinforced Samples Irradiated by High Dose Rate Gamma Source Open to Atmosphere.....	65
Figure 3.34: ATR-FTIR Spectra of PANB with Different Compositions Irradiated by High Dose Rate Gamma Source Open to Atmosphere.....	66
Figure 3.35: ATR-FTIR Spectra of POL Irradiated by High Dose Rate Gamma Source under Vacuum.....	67
Figure 3.36: ATR-FTIR Spectra of Reinforced Samples Irradiated by High Dose Rate Gamma Source under Vacuum.....	68
Figure 3.37: ATR-FTIR Spectra of PANB with Different Compositions Irradiated by High Dose Rate Gamma Source under Vacuum.....	68
Figure 3.38: $\tan\delta$ Curves of Neat Polyester Resin Samples Non-irradiated and Irradiated.....	69
Figure 3.39: $\tan\delta$ Curves of Polyester Resin Reinforced with Different Boron Minerals.....	70
Figure 3.40: $\tan\delta$ Curves of Polyester Resin Reinforced with Anhydrous Borax in Different Compositions.....	71
Figure 3.41: TGA Thermograms of Boron Minerals.....	73
Figure 3.42: TGA Thermograms of Neat Polyester Resin Samples Non-irradiated and Irradiated.....	74
Figure 3.43: DTG Curves of Neat Polyester Resin Samples Non-irradiated and Irradiated.....	75
Figure 3.44: TGA Thermograms of Non-irradiated Polyester Resin Samples Reinforced with 5% of Boron Minerals.....	76
Figure 3.45: TGA Thermograms of Polyester Resin Reinforced with Anhydrous Borax in Different Compositions.....	77

Figure 3.46: DTG Curves of Polyester Resin Reinforced with Anhydrous Borax in Different Compositions	77
Figure 3.47: SEM Micrograph of Non-irradiated Neat Polyester Resin.....	78
Figure 3.48: SEM Micrograph of Neat Polyester Resin Irradiated by Low Dose Rate Gamma Source with Absorbed Dose of 54 kGy	79
Figure 3.49: SEM Micrograph of Non-irradiated PCOT5	80
Figure 3.50: SEM Micrograph of PCOT5 Irradiated by Low Dose Rate Gamma Source with Absorbed Dose of 54 kGy.....	80
Figure 3.51: SEM Micrograph of Non-irradiated PCOT10	81
Figure 3.52: SEM Micrograph of PCOT10 Irradiated by Low Dose Rate Gamma Source with Absorbed Dose of 54 kGy.....	81

LIST OF SYMBOLS AND ABBREVIATIONS

%	Percent elongation at break with respect to its initial state
%	Reinforcing filler ratio by weight
°C	Degree Celsius, temperature
cm ⁻¹	FT-IR wavenumber
Gy	Gray
kGy	Kilogray
MPa	Megapascal
ATR-FTIR	Fourier transform infrared spectrometer equipped with attenuated total reflection
DMA	Dynamic mechanical analysis
HDR	Irradiation by high dose rate gamma source
LDR	Irradiation by low dose rate gamma source
MEKP	Methyl ethyl ketone peroxide
POL	Neat unsaturated polyester resin
PANB	Unsaturated polyester resin reinforced with anhydrous borax
PCAT	Unsaturated polyester resin reinforced with calcined tincal
PCOL	Unsaturated polyester resin reinforced with colemanite
PCOT	Unsaturated polyester resin reinforced with concentrated tincal
SEM	Scanning electron microscopy
T _g	Glass transition temperature
TGA	Thermogravimetric analysis
DSC	Differential scanning calorimetry

CHAPTER 1

INTRODUCTION

1.1. Polyesters

Polymers are one of the most used materials in today's industry and their usage increases day by day. They grow up by new technologies and discoveries. Polyesters are one of the most important type of polymers in use today [Schiers and Long, 2003] and they are used in varied parts of our lives such as construction, automotive, marine, packaging, furnishing or textile. Polyesters are used to produce fabrics, carpets, tire cords, medical accessories, seat belts, electronic items, packaging materials, bottles, and so on.

Polyesters are molecules containing ester groups in the backbone and produced by polycondensation reaction of a glycol with a difunctional carboxylic acid (or diacids) as shown in Figure 1.1. Even though hundreds of polyesters exist due to combinations of glycols and diacids, only about a dozen of them have commercial importance.

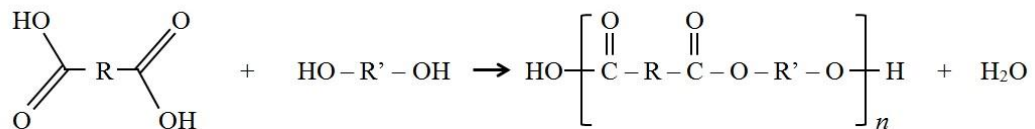


Figure 1.1: General Representation of Formation of Polyester

Polyesters are typically crystalline thermoplastics with excellent chemical resistance, relatively low water absorption and excellent tensile and electrical

properties [Sastri, 2010]. They can be either transparent or opaque depending upon their chemical structure, the additives used or the processing conditions. In our modern life, polyesters are used ranging from bottles for drinks, to fibers for shirts [Schiers and Long, 2003].

1.1.1. Unsaturated Polyesters

Unsaturated polyesters are condensation polymers formed by the reaction of polyols and polycarboxylic acids but their difference from saturated polyesters such as polyethylene terephthalate (PET) is reactive unsaturation provided from one of the reactants, usually the acids [Goodman, 1998]. This reactive unsaturation can then be used to form thermosetting crosslinked polyesters with vinyl monomers. The resulting polymer is a hybrid of a condensation and vinyl type polymer.

Thermoset resins such as unsaturated polyester have a distinct advantage over linear polymers [Sorenson et al., 2001]. Their relatively low molecular weight and low viscosity provide void-free structures whereas linear resins with high viscosity are inefficient.

First unsaturated polyester resins produced in the early 1940's were used with glass fiber as reinforcement to produce first composite plastics. Applications of these resins continue to grow and this is due to their diversity. Consumption of unsaturated polyesters by industrialized countries is about 20% of total thermoset consumption and is about 3% of total plastic consumption [Biron, 2004]. They are mainly used for their favorable ratio of cost vs. mechanical and thermal properties, low investment costs, durability and corrosion resistance, design freedom, repairing possibilities, and electric and thermal insulation. Main applications of unsaturated polyesters are in automotive industry, building and civil engineering, shipbuilding, electronics, furniture and transportation.

1.1.1.1. Raw Materials of Unsaturated Polyesters

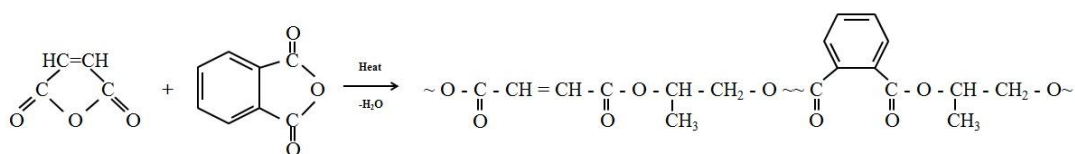
Unsaturated polyesters are formed by step-growth esterification of glycols and dibasic acids and the properties of products can be affected widely by the choice

of raw materials [Mark, 2003]. The majority of commercial resins is derived from maleic anhydride as the unsaturated component in the polymer, and styrene as the co-reactant monomer. Propylene glycol is the glycol used in most compositions, and orthophthalic anhydride is the dibasic acid incorporated to moderate the reactivity and performance of the final resins.

There are also other raw materials used for specific requirements [Mark, 2003]. For example, isophthalic acid is selected to improve thermal resistance as well as to produce stronger, more resilient crosslinked plastics that demonstrate improved resistance to chemical attack. Terephthalic acid provides similar properties and it is also used for corrosion resistance. Ethylene glycol is used to reduce cost, since diethylene glycol produces a more flexible polymer that can resist cracking when impacted. Neopentyl glycol is used to improve UV and water resistance. Adipic acid gives the material flexibility and impact resistance. Use of recycled PET as a raw material component is increasing with increasing demands for environmentally compatible resins.

1.1.1.2. Production of Unsaturated Polyesters

The reaction of glycols with dibasic acid anhydrides proceeds at above 100 °C, ending with the exothermic formation of the acid half-ester produced by the opening of the anhydride ring [Mark, 2003]. This exothermic reaction rises the temperature of reactants to over 150 °C. Viscosity of the reactants increases and it prevents the release of water as the reaction continues. So, the temperature must be increased to 220 °C to maintain a steady evolution of condensate water. Because polyesterification reaction is reversible since it is influenced by the presence of condensate water in equilibrium with the reactants and the polymer. The removal of water in the latter part of the reaction process is essential for the development of optimum molecular weight which is important since structural performance depends on it. This process is carried out in the presence of an inert gas, such as N₂ or CO₂, to prevent discoloration. The production reaction of unsaturated polyester resin from maleic anhydride – phthalic anhydride mixture and propylene glycol is shown below.



The viscosity of the final polymer melt usually limits the progress of molecular weight development, and number-average molecular weight is generally between 1800 and 2500 g/gmol. Other side reactions also modify molecular weight growth and these side reactions are affected by the choice of reactants. For example, ethylene glycol can form cyclic esters with phthalic anhydride. Maleic anhydride can produce addition products with lower glycols that lead to high molecular weight branched polymers. Or, fumaric acid is used to maintain maximum unsaturation.

1.1.1.3. Types of Unsaturated Polyester Resins

Resins based on orthophthalic anhydride contain the largest group of polyester resins and are used in a variety of commercially applications such as marine craft, simulated-marble vanity sets, or buttons [Mark, 2003]. Most laminating and casting processes also rely on both colored and clear gel coats to provide some surface protection. The glycol generally controls the required performance and the phthalic–maleic anhydride ratio is adjusted to modify the reactivity according to physical properties required. Phthalic resins are polymers with a number average molecular weight of 1800–2000 g/gmol. Hydroquinone stabilizer is added to prevent premature gelation during blending process with styrene.

Isophthalic acid can be replaced with phthalic anhydride to enhance mechanical and thermal performance and improve resistance to corrosive environments [Mark, 2003]. Significant products from these resins include underground gasoline storage tanks and large diameter sewer and water pipes. When compared with phthalic resins, isophthalic resins are more widely used in products employing high temperature forming processes. Isophthalic resins intended for corrosion application are processed to a number average molecular weight of 2200–2500 g/gmol. Stabilizers such as toluhydroquinone and benzoquinone are more

effective gelation inhibitors for the higher styrene blending temperatures used for these resins.

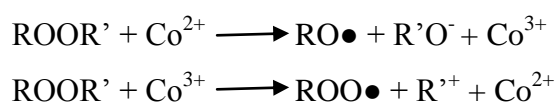
Dicyclopentadiene can be used as a reactive component in reactions with maleic anhydride. These resins have largely displaced orthophthalic resins in marine applications because of beneficial shrinkage properties. The low viscosity of these polymers also allows for the use of high levels of fillers. Dicyclopentadiene can be esterified with propylene glycol to produce resins suitable for electrical components.

Flame retardant resins are resins produced from halogenated intermediates and they are formulated to conform to fire safety specifications. Derivatives of bisphenol A form resin groups that demonstrate superior thermal and corrosion resistance.

1.1.1.4. Crosslinking Mechanism of Unsaturated Polyester Resins

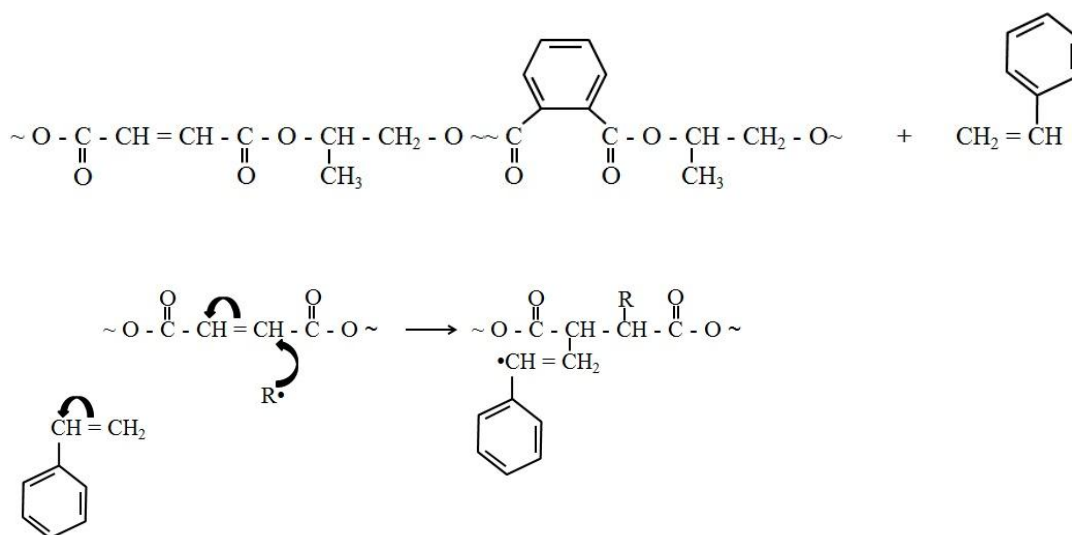
Unsaturated polyester resins are crosslinked by free radicals. These free radicals are obtained from decomposition of peroxides such as methyl ethyl ketone peroxide (MEKP) and these peroxides are generally called initiators or hardeners. Hardeners can give more rapid decomposition by using compounds called as accelerators or activators. Tertiary amines or metal soaps (such as cobalt octoate or naphthenate) are generally used as accelerators.

Polymerization mechanism of unsaturated polyester resin containing styrene monomer can be summarized as follows: before polymerization, accelerator and resin are mixed. Hardener is then added to this mixture. Firstly, redox reaction between peroxide-based hardener and cobalt soap accelerator occurs [Marais et al., 1999].

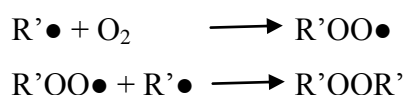


The free radicals initially formed are neutralized by the quinone stabilizers. Stabilizers delay the crosslinking reaction between the styrene and the fumarate sites

(-O-CO-CH=CH-CO-O-) in the polyester chain temporarily [Mark, 2003]. This temporary induction period is called as gelation time and it can be controlled by varying amounts of stabilizer and accelerator. As the quinone stabilizer is consumed, the peroxy radicals initiate the addition chain propagation reactions through styrene as shown below.



Air restrains this free radical mechanism since initiator radicals react with oxygen and chain termination occurs.



After curing process, the structure of crosslinked polyester can be introduced as shown in Figure 1.2.

Generally, optimum strength characteristics are obtained in resins having a styrene/fumarate molar ratio of 2:1 [Mark, 2003]. Most resins are formulated with styrene content consistent with this relationship. In resins having equivalent molar ratios of dibasic and unsaturated acid, this equates to resin polymer solutions containing around 40% styrene. However, this imposes some limitation on viscosity and most commercial resins contain between 40 and 45% styrene to achieve lower application viscosities.

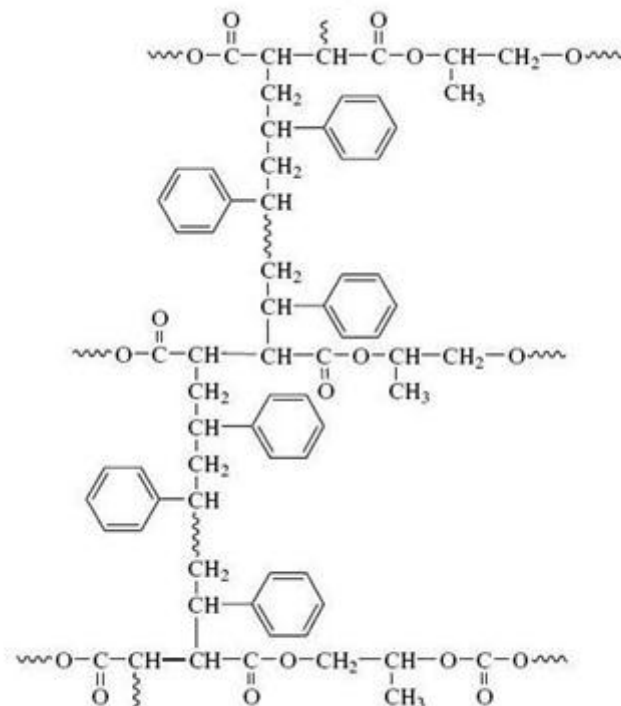


Figure 1.2: Crosslinked Unsaturated Polyester Resin

Choices of chemical constituents, additives, fillers or reinforcers for unsaturated polyester resin preparation can modify resin performance [Schiers and Long, 2003]. Cure rate, viscosity or shrinkage can easily be controlled by additives, fillers can reduce cost of production and reinforcers enhance the physical strength of final products.

1.1.1.5. Properties of Unsaturated Polyester Resins

The highly crosslinked structure of cured unsaturated polyester resins produces thermoset characteristics in which the resistance to softening and deformation is greatly enhanced at elevated temperatures. During heating, the crosslinked network shows structural transition in which the rigid crystalline structure transforms to a softer amorphous structure at its glass transition temperature (T_g). Aromatic constituents enhance the T_g , since aliphatic derivatives and reduced fumarate levels decrease T_g [Mark, 2003]. Resins containing high adipic acid levels display rubbery or elastomeric properties at below ambient temperatures.

Although reinforcement can improve the structural behavior of the composite at elevated temperature, polyester resin begins to disassociate chemically in the presence of oxygen and this situation is not affected by its composition. All resins depolymerize spontaneously at around 300 °C as the ester groups disassociate from the polymer network, and by-products that include lactones, dimer esters, and glycols are produced. Oxidative disassociation at elevated temperature can be suppressed with antioxidants, but these eventually interfere with the catalyst's activity, thus cure rate is reduced.

Crosslinked polyester composites have a relatively low coefficient of thermal conductivity, which can provide beneficial property retention in thick laminates at high temperatures as well as remove the need for secondary insulation.

Polyester resins are nonconductors [Mark, 2003]. They have relatively low dipolar characteristics and they provide high dielectric strength and surface resistivity. But at high voltage or high current, crosslinked plastics fail due to carbon arcing or tracking caused by the charring of the polymer surface into a conductive carbonaceous residue. High temperature electrical applications usually specify bisphenol fumarate resins or high molecular weight isophthalic resins having high fumarate reactivity.

The three dimensional crosslinked network resists penetration and attack by most corrosive chemicals and nonpolar solvents, although weak alkalies and especially polar solvents such as lower ketones, chlorinated aliphatics, and aromatics readily attack orthophthalic, isophthalic, and dicyclopentadiene resins. Water has wide ranging effects on different resin compositions as it penetrates into the plastic network. Crosslinking density and the presence of steric constituents local to the ester groups can enhance water resistance. Isophthalic resins have better water absorption characteristics than orthophthalic resins. Ethylene and diethylene glycols demonstrate high water absorption and that leads to the loss of mechanical strength.

Corrosion attack on the polymer is influenced by permeation rate, as well as internal stresses or fatigue. Localized corrosion failure in large tanks or piping systems can be explained by stress induced corrosion failure. Nonpolar solvents have

little effect on polyester resins and have been used extensively for underground storage of gasoline. However, with the reformulation to unleaded gasoline, the higher aromatic fuels require resins that have higher crosslinking density. This is provided by high fumarate isophthalic or terephthalic derivatives.

Polyester resin products ignite and burn by emitting sooty smoke [Mark, 2003]. Flammability can be reduced significantly through halogen modified components either formulated into the polyester polymer, or as part of the monomer system.

Polyester resins in the form of laminates, coatings, and castings perform well in outdoor exposures such as marine craft, tanks, and pipes. In direct sunlight, polyesters show some change in their surface features such as discoloration or yellowing. Dulling and microcrazing occur only in products not appropriately formulated for the exposure.

1.2. Reinforcement of Polymers

In today's world, materials and structures are required to be stronger, lighter or cheaper. These requirements are often provided through the concept of combining different materials in a composite structure. The goal of this concept is to achieve improved performance from the composite that is not available from the separate constituents. This improved performance includes increased strength or reinforcement of one material by the addition of another material [Kirk-Othmer, 2001].

Many polymer resins are mixed with additives to either improve properties, or reduce the cost of the final product [Peacock and Calhoun, 2006]. The type of additive and the addition process determine the effectiveness of the additive.

The reinforcement of linear and crosslinked polymers is a process of their compatibilization with various solid, liquid, and gaseous substances which are uniformly distributed in the bulk of polymer and have a pronounced phase border with polymeric phase (matrix) [Lipatov, 1995]. Filling or reinforcement of polymers

is one of the most important and popular methods of production of plastics, rubbers, coatings, adhesives, etc., which must possess the necessary mechanical and physical properties such as color, processing stability, strength, or elasticity for any given practical application.

Wide range of materials can be used to reinforce unsaturated polyester resin. For example, carbon fibers make composites which have higher modulus characteristics. Resins filled with ground limestone are useful in solid-cast products. Fiber reinforced resins show good performance against concentrated hydrochloric and phosphoric acids. Alumina trihydrate suppresses surface char formation and enhances flame retardancy of composites. Fillers such as talcs or clays prevent the wearing effects of direct sunlight.

The mostly used method to polymerize the polyester resins with reinforcement in the literature is shown in Figure 1.3. Firstly, polyester resin is mixed with fillers or additives up to 60 minutes. The mixture is degassed to remove bubbles in a vacuum chamber or in an ultrasonic bath. After this step, MEKP solution as hardener and cobalt naphthenate or cobalt octoate solution as accelerator are added. They are generally used in concentrations of 1-4% and 0.1-2% by weight, respectively. They are mixed for a couple of minutes. Finally, the product is cured at room temperature or in an oven at desired temperature to accelerate curing.

There are so many studies about polyester resins in the literature. In these studies, different types of fillers or additives are used and effects of these materials on mechanical and morphological properties of polyesters are investigated. The adhesion at the polymer-solid interface is the most important factor determining the properties of filled and reinforced polymers. Strong interaction is the necessary condition for improving and changing polymer properties by reinforcement. Generally two types of materials are used to reinforce the resin: Fibers and powder fillers.

Powder fillers are used to enhance some properties of polyester resins such as mechanical strength or chemical resistance. They make the resin stiffer and more brittle but on the other hand, they have advantage of cost reduction.

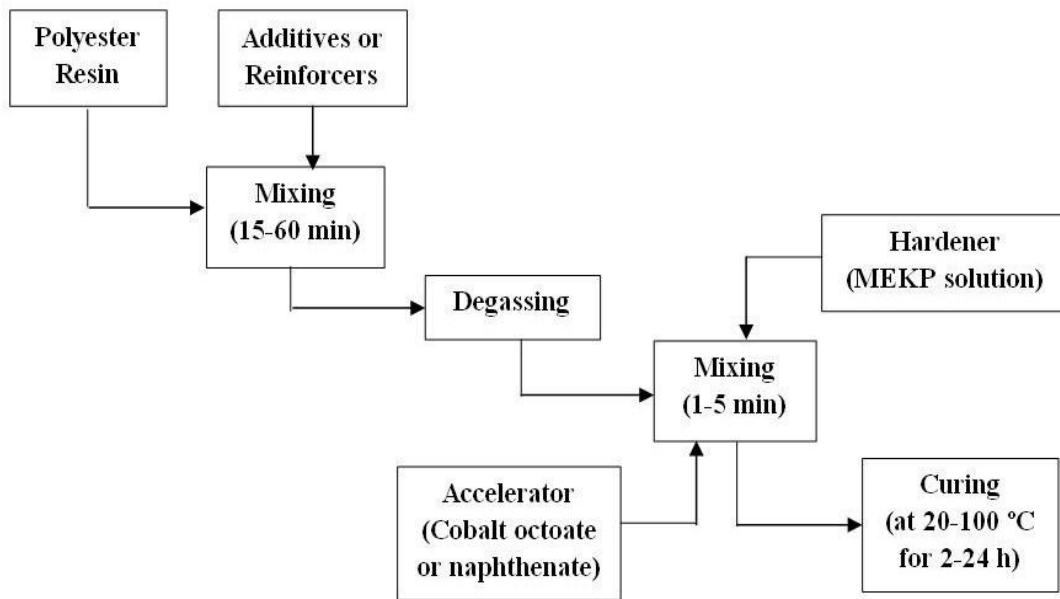


Figure 1.3: Polymerization of Polyester Resin with Reinforcement

Evans et al. (1997) investigated the effects of different fillers such as silica, calcium carbonate or glass fibers and different curing regimes on degradation of polyester resins. The products were analyzed by TGA, DTA, DSC and Pyrolysis-GC. As a result of their study, different curing regimes didn't affect the stability of polyesters significantly. Addition of fillers reduced the stability of polyesters but these changes were relatively low.

Şen and Nugay (2001) studied on the effect of replacement of fly ash with mica in terms of processability and mechanical properties of polyester resins. Fly ash and mica were added into commercial polyester resin in different portions. Products were characterized with DSC, DMTA, viscosity and mechanical tests. Addition of mica into fly ash reinforced polyester increased tensile strength and elongation ability of composite materials but brittleness was not affected.

Fernandes Jr. et al. (2002) produced composite materials by commercial polyester resins containing decabromodiphenyl oxide and antimony trioxide. Thermal degradation of these products was studied by UL-94 flammability test, TGA and DSC. Char formation of flame retardant system used in this work did not

increase. DSC curves indicated that additives were effective for limiting combustion. TGA results showed that activation energy for degradation of polyester containing additives was much larger than that of untreated resin.

Zhang and Singh (2004) used aluminum oxide as reinforcement to enhance mechanical properties of commercial polyester resins. Composite materials were also treated with organofunctional silane to investigate the effect of particle-matrix adhesion. The products were characterized by fracture testing. Fracture toughness decreased as volume fraction of untreated aluminum oxide particles was increased. Silane-treated particles gave the composite toughness and enhancement of fracture toughness was strongly influenced by particle-matrix adhesion.

Madugu et al. (2009) studied the effects of iron filling particles on the structure and properties of fiber-polyester composites. Physical and mechanical properties of products such as porosity, density, tensile strength, impact strength or hardness were investigated. Porosity slightly increased with increase in fraction of iron fillings. Tensile strength and compressive strength increased with increasing percentage of iron fillings to a maximum point and then decreased. Hardness increased with increase in fraction of iron fillings. Impact energy decreased with increase in fraction of iron fillings.

Tibiletti et al. (2011) added nano-sized alumina and submicron-sized alumina trihydrate particles into commercial polyester resins in different loadings. Thermal degradation of composite materials was studied by TGA and Pyrolysis-GC/MS. Each kind of particles has little influence on thermal stability but mixture of additives gives the composite highest thermal stability. When the degradation kinetics was investigated, the samples which contain only alumina have highest degradation activation energies. Fire behavior of materials was also studied and results showed that mixture of additives increased the ignition time.

Ateş and Barnes (2012) investigated the effects of temperature of curing treatment on mechanical properties of polyester resin composites. For this purpose, quartz was chosen as filler material in the composite structure. Changes in the compression strength of composite material cured at elevated temperatures were

analyzed. The elevated temperature compression strength values were generally lower when compared with room temperature compression strength values.

Hassan et al. (2012) used maize stalk ash to produce reinforced polyester composites. Final products were analyzed by SEM, XRD, Charpy impact test and tensile tests. SEM results showed significant microstructural change in composite as addition of maize stalk ash particles. The tensile modulus and tensile strength increased with increase in weight percent of maize stalk ash and this situation might be attributed to higher crosslink density and good distribution of ash particles in polyester matrix. Impact tests showed that impact energy of composites decreased with addition of ash particles since these particles provided points of stress concentration.

Seki et al. (2012) used huntite mineral as reinforcement for unsaturated polyester. Huntite mineral was turned into powder form and added into the resin. The highest values of tensile and flexural strength were found for the composite with 3% huntite which may be attributed to the more uniform distribution of the fillers. TGA results showed that degradation temperature of polyester matrix was improved by adding huntite. DSC curves showed that curing behavior of polyester resin was not influenced by huntite filling.

Fibers are also used to reinforce polyester resins. These fibers can be organic or inorganic. The objective of using fibers is to enhance strength, stiffness, resistance or strength to weight ratio. They can also be chemically treated to improve adhesion in fiber-polymer interface.

Mishra et al. (2003) added small amounts of glass fiber to pineapple leaf fiber and sisal fiber reinforced-polyester matrix. Sisal fibers were also modified by different chemical treatments such as alkali treatment, cyanoethylation and acetylation. Final products were characterized by mechanical tests, SEM and water absorption tests. Tensile tests showed that tensile strength of pineapple leaf fiber-reinforced polyester composite was improved by incorporation of glass fiber. The highest tensile strength was obtained by alkali-treated sisal fiber reinforced-polyester because of improvement in the interfacial bonding. Chemically treated sisal/glass

hybrid polyester composites had much more stronger interfacial adhesion as shown by SEM.

Sreekumar et al. (2007) investigated the tensile and flexural behavior of sisal fiber-reinforced polyester resins as a function of fiber loading and fiber length. Composite materials were produced by resin transfer and compression molding techniques. Mechanical tests and water sorption experiments were performed. Mechanical properties increased with increase in fiber length and further increase in fiber loading decreased these properties. In general, mechanical properties of resin transfer samples were higher than that of compression molding samples.

Bessadok et al. (2009) studied reinforcement of unsaturated polyester resins by Alfa fibers. These fibers were modified by different chemicals such as maleic anhydride, acrylic acid, styrene and acetic anhydride. Chemically-treated fibers were characterized by FT-IR, SEM and mechanical tests. Chemical treatment of Alfa fibers were led to increase in mechanical properties of fibers because of increase in moisture resistance. On the other hand, chemical treatment did not affect mechanical behavior of composite materials significantly.

Mulinari et al. (2011) reinforced polyester resins with chemically modified coconut fibers. Fibers were characterized by SEM, FT-IR, XRD and TGA. Composite materials were produced by compression molding technique. Mechanical properties of composites were investigated. Chemical treatment improved crystallinity, adhesion performance and thermal stability of fibers. Decrease in fatigue life was observed when great tension was applied to composites. This situation occurred due to poor dispersion of fibers in the polyester matrix and poor bonding interfacial.

Ramanaiah et al. (2012) used waste grass broom natural fibers as reinforcement and polyester resin as matrix to produce partially biodegradable green composites. Thermal conductivity, thermal diffusivity and specific heat capacity of composites were investigated. Thermal conductivity and specific heat capacity of composites decreased as fiber content increased because of lower thermal conductivity and lower specific heat capacity of grass broom fiber. Tensile strength

and tensile modulus increased with increasing fiber content since polyester resin transmitted distributed the applied stress to the broom grass fibers. The results were analogous for impact tests.

Sathishkumar et al. (2012) studied about tensile and flexural properties of snake grass natural fiber reinforced polyester composites. Tensile strength of composites increased with increase in fiber content up to 25% but when fiber content was 30%, load and stress transfer between fiber and matrix reduced significantly due to insufficient matrix content. It was also noted that the flexural strength depends upon the fiber length. SEM micrographs of tensile and flexural tested specimens showed that composites had good interfacial properties, high wetting and less fiber pull-out.

Sawpan et al. (2012) reinforced polylactide and unsaturated polyester with hemp fiber. Fibers were chemically treated with sodium hydroxide and silane solution. Flexural strength of polylactide-hemp fiber composite decreased with increase in fiber content. This behavior was explained by weak spots in fibers acted as sites of potential crack initiation. In contrast to flexural strength, flexural modulus of the composites increased as the fiber content increased because hemp fibers are very stiff compared to polylactide matrix. Flexural strength and flexural modulus of unsaturated polyester-hemp fiber composites showed similar trends to polylactide-hemp fiber composites. Unsaturated polyester had better results when compared with polylactide. SEM micrographs showed that fibers were well connected to the polymer matrix.

Sreenivasan et al. (2012) treated *Sansevieria cylindrica* fibers with solutions of sodium hydroxide, benzoyl peroxide, potassium permanganate and stearic acid to improve interfacial interactions between fibers and polyester matrix. Tensile tests of chemically-treated fibers showed that tensile strength was found to be higher for all of the treated fibers compared with untreated fibers because of removal of some substances and increase in ratio of cellulose in the material. Among the treated fibers-polyester composites, maximum tensile strength and flexural strength were observed in composite reinforced with potassium permanganate treated-fiber due to good interfacial bond between fibers and polyester matrix. There was no significant

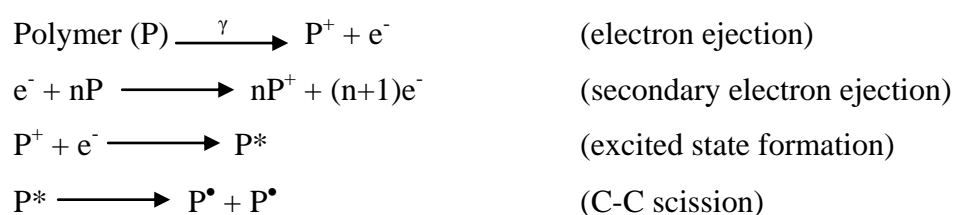
change in impact strength of chemically treated-fiber reinforced polyester except potassium permanganate treated-fiber reinforced polyester which had much better impact strength. Finally, composites reinforced with chemically treated-fiber showed lower water absorption compared with untreated fiber-reinforced composites.

1.3. Effects of Ionizing Radiation on Polymers

Polymers are used in many areas where exposure to high-energy radiation can occur [Scott, 1990]. Applications include nuclear power plants, radiation equipment such as X-ray sources, sterilization systems such as medical equipment and particle-physics generators. High-energy radiation can also be used to modify polymers for molecular weight control, crosslinking or branching.

Radiation resistance of polymers mainly depends on their chemical structure [Ivanov, 1992]. Since polymers contain double bonds and aromatic rings, they are more resistant to ionizing radiation than polymers containing saturated bonds and this fact is called dissipation of ionizing radiation. Dissipation is observed on structures with aromatic rings more likely. The resonance structures of aromatic rings submit a wide range of energy levels and this makes dissipation of absorbed energy easier. On the other hand, bonds such as C-Si, C-F or C-O have lower resistance against radiation. Polymer structure also affects mechanism of radiation-chemical processes which can be crosslinking or degradation.

Typical reactions occurred as a result of radiation exposure (such as gamma radiation) of polymer are shown below. Interaction of gamma-ray photon with polymer yields fast electrons and these electrons cause ejection of secondary electrons at some distance from primary event. Ion-electron combination gives excited states. These excited states dissipate some excess energy by bond scission to give free radicals.





Formed free radicals and reactive intermediates lead to constructive or destructive changes in the polymer such as crosslinking, formation of new bonds, disproportionation or degradation [Hacıoğlu, 2010]. These changes or modifications depend on structure of polymer, additives, temperature or irradiation conditions.

In general, main effects of irradiation on polymers are classified as crosslinking, chain scission and oxidation [Ivanov, 1992]. Crosslinking by irradiation has some advantages. Stability of the polymer increases and it provides high strength, high impact and chemical resistance to the polymer. Crosslinked polymers preserve their shapes at high temperatures and their molecular weight increase. On the other hand, degradation of the polymers by irradiation results in chain scission, oxidation and decrease in molecular weight. The mechanical and chemical properties of polymers are diminished.

Various studies about irradiation of polyester resins are available in literature. These studies are generally focused on effects of irradiation on mechanical properties of polyesters. These studies are differed from each other by irradiation conditions and additives used.

Segovia et al. (2001) exposed glass fiber reinforced unsaturated polyester composites to sunlight radiation. Effects of curing temperature, commercial resin type and fiber type on mechanical properties and degree of aging were investigated. Results of this study showed that elastic modulus, tensile strength and toughness decreased with increase in exposure time. Mechanical properties of composite materials were inversely proportional to curing temperature. Tensile strength and modulus were not affected by fiber type significantly but loss in toughness was quite different for different types of glass fibers.

Ajji (2005) prepared composite materials by commercial polyester resin and gypsum. These materials were cured by gamma radiation at different rates and they were characterized by DSC, TMA, TGA and mechanical tests. There was no significant effect of radiation on T_g of neat polymer or composites. Only filler

particles increased T_g . Thermal degradation temperature was not influenced by radiation significantly. Hardness was not affected by gamma radiation but compression strength increased with increase in irradiation.

Jurkin and Pucic (2006) investigated post irradiation crosslinking of unsaturated polyester resins. Commercial polyester resin samples were prepared without any accelerator or hardener and they were irradiated at different doses. They were monitored for 15 days by extraction analysis, FT-IR and DSC. Significant post-irradiation crosslinking was detected and it lasted up to 5 days after the irradiation. DSC was the most sensitive technique to detect post-irradiation changes. Some additional information such as behavior of styrene or polyester components of resin could be gained by DSC. On the other hand, FT-IR was found not to be appropriate for monitoring of the post-irradiation changes.

Czayka et al. (2007) investigated the effects of irradiation on polyester resin and dose rate on the degree of crosslinking. After preparation of commercial polyester resin samples with or without accelerator, they were irradiated at room temperature at different dose rates. Chemically-cured samples were also prepared. The samples were characterized by DSC, FT-IR, compressive tests and tensile tests. Contribution of irradiation to crosslinking was observed by DSC results. Mechanical tests showed that irradiated samples had higher modulus, maximum tensile strength and elongation at break than that of chemically-cured samples. Primary mechanism for change in mechanical properties was due to crosslinking.

Gu (2008) produced multilayer laminates from glass fibers and unsaturated polyester resins. The samples were irradiated by ultraviolet radiation and they were subjected to tensile strength testing. Penetration of radiation into composites was very limited. Tensile strength of composites decreased with long period exposure to ultraviolet radiation. But short period ultraviolet radiation had no significant effect on composites. Resistance to radiation increased with increase in the amount of layers.

Martinez-Barrera et al. (2008) developed polymer concrete by using different concentrations of silica sand and commercial unsaturated polyester resin. Polymer

concrete samples were irradiated by gamma source. Compressive strength increased with increasing polyester concentration. On the other hand, it was almost independent of irradiation dosage. Compressive strain values showed periodical behavior since irradiation dose increased and this behavior was explained by the fact that irradiation causes chain scission but it also produces relaxation and cage breaking. SEM micrographs showed that under irradiation by gamma source, crack formation of resin and separation between sand particles and resin were observed.

Peng et al. (2008) prepared unsaturated polyester composites reinforced with glass fiber and nano-sized ZnO and resistance of composites to UV radiation were investigated. Bending strength of composites decreased with addition of ZnO. Exposure time to UV radiation also affected bending strength negatively but decrease of bending strength of ZnO added composites was slower than that of neat resin. These results indicated that ZnO could reduce UV degradation of polyester matrix. Impact strength of the samples increased after ZnO was added. DSC results showed that ZnO could retard the crosslinking of resin which coincided with bending strength results. ZnO particles could hinder crack growth and induce more cracks as seen from SEM micrographs.

1.4. Boron and Boron Minerals

Boron is an important element for today's world. There are more than 200 of borate minerals occurred naturally but only a few of these minerals such as ulexite ($\text{NaCaB}_5\text{O}_9 \cdot 8\text{H}_2\text{O}$), colemanite ($\text{Ca}_2\text{B}_6\text{O}_{11} \cdot 5\text{H}_2\text{O}$) or tincal ($\text{Na}_2\text{B}_4\text{O}_7 \cdot 10\text{H}_2\text{O}$) are commercially important [Garrett, 1998]. More than 70% of known deposits of boron are in Turkey and half of world production is provided also from Turkey.

Major uses of boron include the industries of glass and ceramics, detergents and bleaching, fertilizers and agricultural chemicals, flame retardants, electronics and engineering, and insulation. Some final boron products and their main application areas can be summarized as borax pentahydrate ($\text{Na}_2\text{B}_4\text{O}_7 \cdot 5\text{H}_2\text{O}$) to produce cosmetics and pesticides; borax decahydrate ($\text{Na}_2\text{B}_4\text{O}_7 \cdot 10\text{H}_2\text{O}$) for adhesives; anhydrous borax ($\text{Na}_2\text{B}_4\text{O}_7$) for fertilizers and flame retardants; boric acid (H_3BO_3)

for antiseptics and nuclear applications; and boron trioxide (B_2O_3) for borosilicate glasses and optical fibers.

All boron minerals contain triangular (BO_3) and/or tetragonal (BO_4) structural units [Garrett, 1998]. B-O groups tend to form ring structures and boron minerals can also polymerize to result in chains or networks. For example, structure of colemanite contains long B-O chains including a ring of one triangular and two tetragonal units as can be seen from Figure 1.4. Tincal is formulated as $Na_2B_4O_7 \cdot 10H_2O$ but $Na_2[B_4O_5(OH)_4] \cdot 8H_2O$ could be a better formula since tincal's structure contains two triangular and two tetragonal units. Some variables such as temperature can affect structure.

The shielding ability of a material against radiation can be explained by cross section concept. When gamma-rays or neutrons are directed into a material, some of them can pass through the material, some of them can be scattered as a result of collision with a nucleus and some of them can be absorbed by nuclei. All of these incidents have a probability [Murray, 2000]. For example, the probability of absorption of a neutron is the ratio of number of neutrons absorbed to the number of neutrons originally presented. The absorption cross section is the probability of absorption divided by number of nuclei per unit area of the material. The sum of all these cross sections is called total cross section and it describes the probability of interactions between radiation and the shielding material.

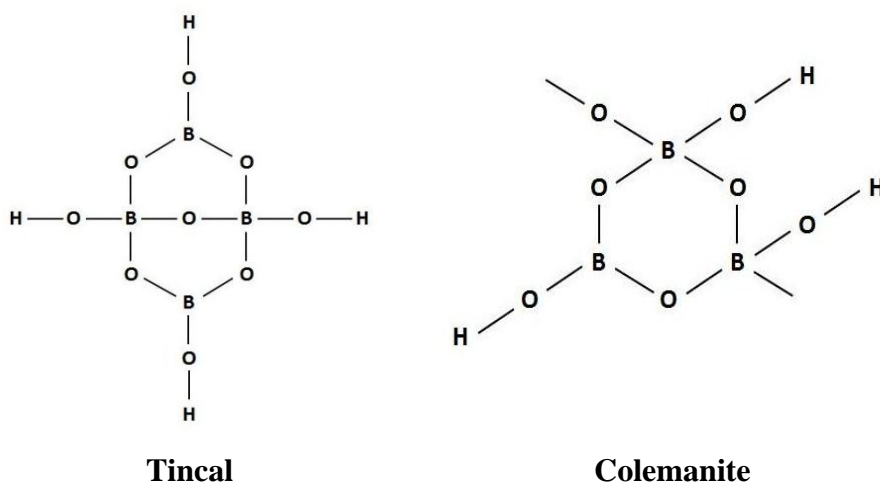


Figure 1.4: Chemical Structures of Tincal and Colemanite

Boron has high absorption cross section and materials containing boron become highly effective for radiation applications. For example, boron carbide (B_4C) is used as a control rod in nuclear reactors and in neutron shielding systems [Büyük and Tuğrul, 2014]. Boric acid dissolved in cooling water of nuclear reactor helps to control the speed of fission reactions.

Since end products of boron minerals such as boron carbide or boron nitride are highly priced materials, unprocessed boron minerals can be used not only to improve radiation stability of composites but also to produce cost effective material. There are distinctive amount of such studies in literature.

Baştuğ et al. (2010) prepared lead (II) oxide-borax and uranyl nitrate-borax mixtures in different ratios and pellets of these mixtures were exposed to ^{241}Am source. Effective atomic numbers and mass attenuation coefficients, which can be defined as a measure of how easy energy or matter penetrates through the material, of these mixtures were determined theoretically and experimentally. Results showed that presence of borax in a mixture decreased radiation permeability of the mixture. Uranyl nitrate was worse regarding to radiation shielding than lead (II) oxide since it had lower effective mass number but uranium is less toxic than lead.

Demir (2010) determined mass attenuation coefficients of ulexite, colemanite and tincal ores both experimentally and theoretically. The results were compared with that of lead (II) oxide and paraffin wax as reference materials. Mass attenuation coefficients of boron ores were quite lower than that of lead (II) oxide but higher than that of paraffin wax. This result is reasonable since Pb has a larger size when compared with, B, O, Ca, or Na. Colemanite had the highest; tincal had the lowest mass attenuation coefficient among boron ores. Theoretical and experimental results were comparable with each other.

Un and Şahin (2011) determined mass attenuation coefficients, effective atomic numbers, total mass cross sections and mean free paths of barite, tincal, ulexite and colemanite for different energies of gamma rays both experimentally and theoretically. In general, barite showed the best performance against radiation when compared with boron ores. Colemanite had the highest total atomic cross section and

total attenuation coefficient and the lowest mean free path among boron ores. Tincal showed the poorest performance.

Derun and Kıpçak (2012) studied with inyoite, borax, inderite, colemanite and kurnakovite as boron minerals. Those minerals were characterized by acid-base titration, flame photometer, XRF and XRD techniques. Sample pellets were exposed to thermal neutrons from ^{239}Pu -Be source and neutron permeability of samples were measured to calculate total macroscopic cross section. Kurnakovite mineral showed lowest neutron permeability. Boron oxide content of kurnakovite mineral was not high when compared with other minerals but hydrogen atoms inside the mineral were considered to help the neutron shielding performance. Total macroscopic cross section of samples of same minerals kept for 12 years were also determined and compared with these samples. Samples used in current study showed better performance and this situation were related to formation of micro cracks and loss of water during 12 years.

Korkut et al. (2012) exposed colemanite, ulexite and tincal samples to ^{241}Am -Be source to measure neutron total macroscopic cross sections. Monte Carlo simulation was also used to simulate total macroscopic cross sections of samples. Experimental and simulation results were comparable with each other. Results showed that macroscopic cross sections increased with increase in boron atoms per unit volume. According to those results, colemanite has better neutron shielding.

Demir and Un (2013) investigated radiation performances of boron minerals such as tincalconite, colemanite and ulexite. Samples were prepared as pellets and linear accelerator with ionization chamber was used to determine radiation transmission of samples. Mass attenuation coefficients of samples were calculated from measurements. Mass attenuation coefficients of samples were found lower when compared with that of Pb and paraffin wax as references. Tincalconite, colemanite and ulexite were considered as good absorbers to prevent photon and neutron particles.

Kıpçak et al. (2013) investigated neutron shielding behaviors of dehydrated magnesium borates. They were synthesized by solid-state method from MgO and

B_2O_3 and 7 different synthetic dehydrated magnesium borates were obtained. Samples were characterized by XRD, FT-IR, Raman, SEM, and acid-base titration. Neutrons from $^{241}\text{Am-Be}$ source were counted by neutron detector and total neutron transmissions and total macroscopic cross sections were calculated. The results reported showed that kotoite ($\text{Mg}_3(\text{BO}_3)_2$) had the lowest neutron transmission value since it has highest XRD crystal score.

Binici et al. (2014) used colemanite, barite, ground basaltic pumice and ground blast furnace slag as additives in mortars. Bending and compressive strengths of composites were investigated. Samples were also exposed to gamma radiation. Linear absorption coefficients of samples were increased with increase in barite ratio in sample. On the other hand, colemanite showed inverse ratio with linear absorption coefficient and shielding of gamma rays for colemanite samples was lower when compared with reference material which is Portland cement with standard fine aggregates. Barite, colemanite and blast furnace slag were found to be effective to prevent gamma radiation.

Kıpçak et al. (2014) also used sodium-calcium borates such as ulexite and probertite and sodium borates such as borax and tincalconite from different regions of Turkey to perform neutron absorption. Characterization tests were performed by using XRD, FT-IR, Raman, DTA/TGA and SEM techniques. Neutron transmission values and total macroscopic cross-sections were determined by using $^{239}\text{Pu-Be}$ source. Results showed that neutron transmission was highly affected by pellet thickness and particle size. It can be said from the results that both B_2O_3 and structural water contents of minerals are effective on their neutron absorption performance. Secondary ulexite from Kırka showed the best performance with its moderate B_2O_3 and structural water contents among boron minerals. In general, sodium-calcium borates had better neutron transmission values relative to sodium borates.

1.5. Aim of the Study

Nuclear technology is in use in several fields from energy to agriculture. Since this technology is to become widespread, synthesis of new materials and

improvement of conventional materials that are used for purposes such as nuclear waste management or radiation protection are essential. Unsaturated polyester resin is a cheap and widely-used product which has favorable mechanical properties. The aim of this study is to investigate the effects of different types of boron minerals, which contain B_2O_3 in different weight ratios, used as reinforcing fillers on mechanical properties, thermal properties and on radiation stability of polyester resin.

CHAPTER 2

EXPERIMENTAL

2.1. Boron Minerals

In the Table 2.1 below, boron minerals that were used in this study can be seen. Their chemical formulas and their B₂O₃ content were also given (“Bor Ürünleri”, 2012). All boron minerals were provided from Eti Maden Company. Contents of these boron minerals were given in Appendix A.

Table 2.1: Boron Minerals Used in This Study

Boron Mineral	Chemical Formula	B₂O₃ Content (% wt.)
Etibor-68 (Anhydrous Borax)	Na ₂ B ₄ O ₇	68
Calcined Tincal	Na ₂ [B ₄ O ₅ (OH) ₄]	52
Ground Colemanite	CaB ₃ O ₄ (OH) ₃ .H ₂ O	40
Concentrated Tincal	Na ₂ [B ₄ O ₅ (OH) ₄].8H ₂ O	29

2.2. Boron Mineral-Polyester Composites

Preparation of reinforced polyester resins was performed as illustrated in Figure 1.3. All boron minerals were ground in a ball mill and sieved before usage. Powders with particle size of minus 230 mesh (63 µm) were used. Different types of boron minerals in different weight fractions were added into pre-accelerated, orthophthalic based cast type commercial polyester resin (ES 1060 DK, Eskim A.Ş., Eskişehir). This commercial polyester resin contains 35% of styrene monomer. Molecular structure of the resin was given in Section 1.1.1.2. Some properties of the resin can be seen in Appendix B. Weight fractions of boron minerals and

abbreviations of composites were given in the Table 2.2 below. After addition of boron minerals into polyester resin, they were stirred mechanically for 20 minutes and the mixture was degassed in vacuum chamber for 5 minutes. Methyl ethyl ketone peroxide (MEKP) used as hardener was added and stirred for another 2 minutes. Mixtures were poured into silicon rubber molds with dimensions of 115 x 19 x 3,5 mm according to the ASTM D638 standard. After composites were hardened, they were cured in an oven at the temperature of 60 °C for 2 hours.

Table 2.2: Preparation of Polyester Composites

Boron Mineral	Polyester Resin (g)	Boron Mineral (g)	Hardener (ml)	Abbreviation
(Neat)	100	-	3	POL
Etibor-68 (Anh. Borax)	100	2 / 5 / 10	3	PANB2-5-10
Calcined Tincal	100	2 / 5 / 10	3	PCAT2-5-10
Ground Colemanite	100	2 / 5 / 10	3	PCOL2-5-10
Conc. Tincal	100	2 / 5 / 10	3	PCOT2-5-10

2.3. Irradiation of Samples

Low dose rate (LDR) irradiations were performed in Gammacell 220 model including ^{60}Co source in the presence of air. This gamma source has half-life of 5.26 years and an initial activity of 12400 Ci (in 1968). Dose rate of low dose rate gamma source was 30 Gy/h when the samples were placed. High dose rate (HDR) irradiations were performed in Nordion JS 9600 model including ^{60}Co source in GAMMA-PAK Company (Çerkezköy, Tekirdağ). This gamma source has an initial activity of 300000 Ci (in 2012). Dose rate of high dose rate gamma source was 2500 Gy/h. Irradiation by low dose rate and high dose rate gamma source were performed in the presence of air but irradiation by high dose rate gamma source was also performed under vacuum. The samples were placed into pyrex tubes under the pressure of 10^{-3} torr before irradiation.

Polyester composites which were untreated and reinforced with Etibor-68, with concentrated tincal, with calcined tincal and with ground colemanite (POL,

PANB, PCOT, PCAT and PCOL samples, respectively) have being irradiated up to 3 different total dose values for each irradiation rate. These total dose values are given in Table 2.3 below.

Table 2.3: Absorbed Dose Values for Irradiated Samples

Irradiation Process	Irradiation by Low Dose Rate Gamma Source			Irradiation by High Dose Rate Gamma Source		
	LDR1 (kGy)	LDR2 (kGy)	LDR3 (kGy)	HDR1 (kGy)	HDR2 (kGy)	HDR3 (kGy)
Dose Absorbed	54	138	245	500	1000	2500

2.4. Characterization of Samples

The samples exposed to desired total doses and removed from gamma sources were characterized by mechanical tests. For this purpose, tensile tests were performed. These tests were performed by Lloyd Instruments LR 5K Universal Testing Machine as can be seen from Figure 2.1. They were performed according to BS EN ISO 527-1 and BS2782 Part 3 Method 322 standards with testing speed of 1 mm/min. These tests gave results for Young's modulus, tensile strength and elongation at break.

Samples were also analyzed by ATR-FTIR technique to investigate their chemical structure. Thermo Nicolet iS10 FT-IR Spectrometer equipped with ATR accessory was used for these analyses. Spectra of the samples were noted at room temperature and samples were scanned from 4000 cm^{-1} to 600 cm^{-1} with a resolution of 8 cm^{-1} . All FT-IR spectra of samples were normalized around the strongest band to eliminate path length variations of samples and to reduce differences between measurements [Smith, 2011]. To normalize the spectra, absorbances of spectra were divided by the absorbance of selected peak. Band of 820 cm^{-1} which represents tetragonal boron units (BO_4) and band of 1255 cm^{-1} which represents ester C–O single bond were chosen for boron minerals and for composites, respectively.

Thermogravimetric analysis (TGA) was performed to determine changes in weight with changes in temperature and for these tests, LECO TGA701 was used. Samples which have 0.5 g of weight were heated from room temperature to 900 °C in an inert (N₂) atmosphere with constant heating rate of 3 °C/min.



Figure 2.1: Lloyd Instruments LR 5K Universal Testing Machine



Figure 2.2: Thermo Nicolet iS10 ATR-FTIR Spectrometer

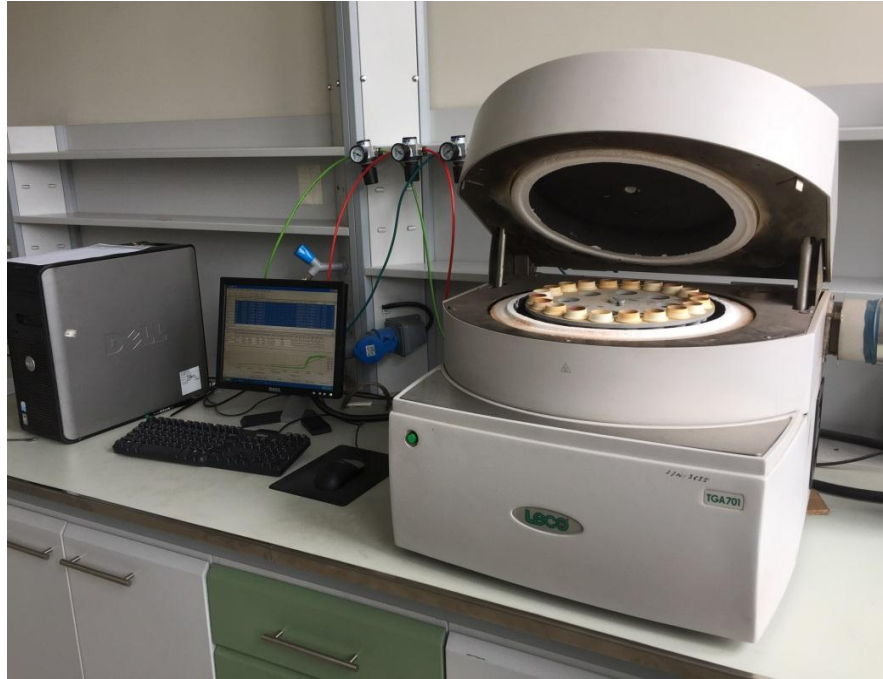


Figure 2.3: LECO TGA701 Thermogravimetric Analyzer

Dynamic mechanical analysis (DMA) was used to study viscoelastic behavior of composites. Samples which have dimensions of 3 x 13 x 55 mm were heated from -150 °C to degradation temperature with constant heating rate of 5 °C/min and they were tested at a frequency of 1 Hz.

Scanning electron microscope (SEM) micrographs of outer surfaces of neat polyester resin and composite materials were taken by Zeiss Supra 55 to obtain information about their surface features.

CHAPTER 3

RESULTS AND DISCUSSION

3.1. Physical Appearances of the Samples

After reinforcement of unsaturated polyester resin with different boron minerals, appearances of composites before irradiation were given in Figure 3.1. First sample in each picture is neat polyester resin and samples became darker with increase in reinforcing filler ratio as can be seen from the figure, from left to right. Anhydrous borax, calcined tincal and concentrated tincal are white powder. On the other hand, ground colemanite powder is grey-green, so it gives its color to composites as shown in Figure 3.1.d.

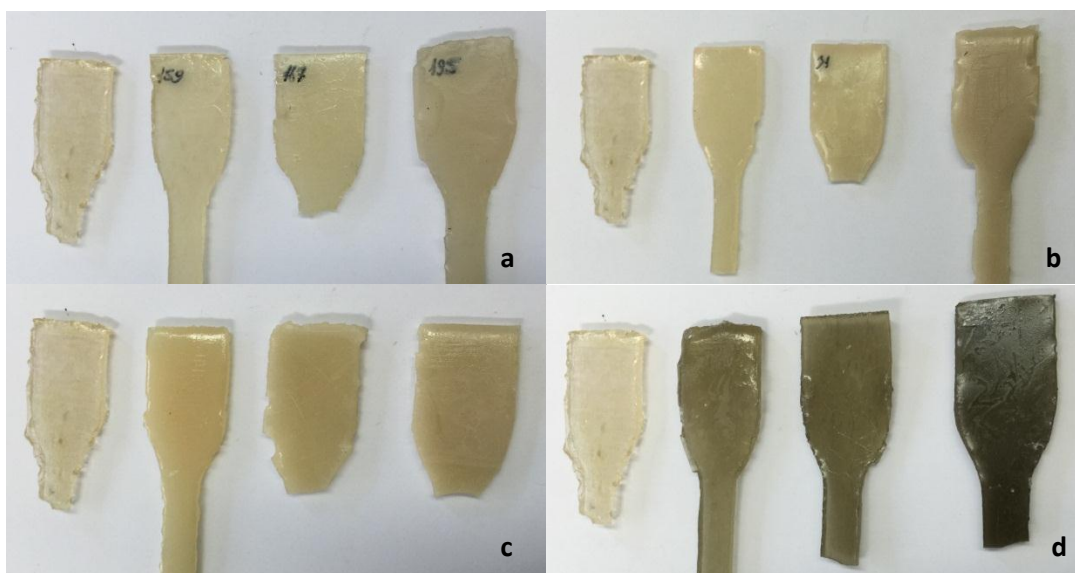


Figure 3.1: Physical Appearances of a) PANB b) PCAT c) PCOT and d) PCOL

When composites were irradiated with low dose rate gamma source, samples turned yellow. Samples became more and more yellowish with increasing absorbed

dose from zero to 245 kGy and this can be observed from Figure 3.2, from left to right. This color change is due to chromophore units in a molecule and these units are responsible for color of the material. Chromophore units contain conjugated double bonds and structure of these units determines the color of the material. When a polymer is exposed to light or radiation, degradation occurs and this results formation of conjugated double bonds along the chain and leads to yellow discoloration of the material [Mark, 2007].



Figure 3.2: Physical Appearance of Neat Polyester Resin Irradiated by Low Dose Rate Gamma Source with Increasing Doses

Figure 3.3 shows change in color of samples irradiated by high dose rate gamma source. These samples were more yellowish when compared with Figure 3.2 and this could be sign of increased effects of gamma irradiation than low doses [Kojima et al., 1981, Croonenborghs et al., 2007 and Fintzou et al., 2007]. As will be mentioned in Section 3.2 and 3.3, samples were degraded more at high doses and increasing degradation causes increasing discoloration. There were not significant differences in color of samples for irradiation open to atmosphere and under vacuum.

3.2. Tensile Tests

Tensile tests for the samples that were removed from gamma source after completion of irradiation process were performed. From these tests, data for Young's modulus, tensile strength and elongation at break were obtained. All numerical data of tensile tests can be seen in Appendix C.

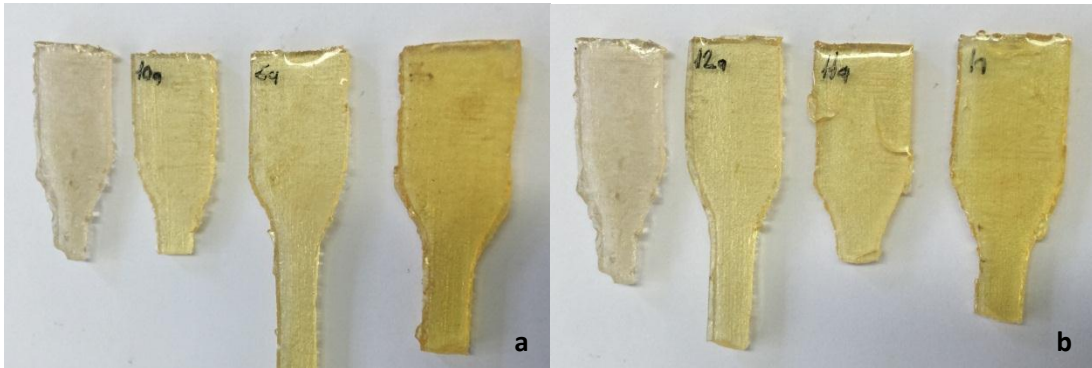


Figure 3.3: Physical Appearance of Neat Polyester Resin Irradiated by Low Dose Rate Gamma Source with Increasing Doses **a)** in Air and **b)** under Vacuum

3.2.1. Tensile Tests of Samples Irradiated Open to Atmosphere

3.2.1.1. Young's Modulus

Young's modulus represents stiffness of the material. This means that Young's modulus of the material increases with decrease in elasticity of the material. Changes in Young's moduli of samples irradiated by low dose rate (30 Gy/h) and by high dose rate (2500 Gy/h) gamma source with respect to total dose absorbed are given in Figures 3.4 to 3.7.

As seen from Figure 3.4.a, 2% of anhydrous borax (ETIBOR-68) caused 25% increase in Young's modulus when compared with POL before irradiation. But when anhydrous borax was added more than 2% into polyester resin, Young's modulus decreased. During irradiation by low dose rate gamma source up to 138 kGy, Young's moduli of all PANB samples decreased. When chain scission occurs due to oxidative degradation, network structure of the composite was diminished. It loses its stiffness and Young's modulus of composite decreases.

But after that point, they started to increase when crosslinking by irradiation became the predominant mechanism occurred. Stiffness was regained because of reformation of network. Change in Young's modulus of PANB10 was lower than that of other PANB samples. This result was reasonable since highly crystalline molecules such as boron minerals give the composite material some stiffness. Figure

3.4.b shows that when irradiation by high dose rate gamma source was concluded, loss in Young's moduli of PANB samples were higher as compared with low doses. This could be due to destructive effect of high doses on polymer chains. Since degradation mechanism is dominant, polymer chains start to fail and composite materials to lose their stiffness.

When concentrated tincal was added into unsaturated polyester resin, Young's modulus increases with increase in reinforcing filler ratio as seen from Figure 3.5. In the earlier period of low dose rate irradiation process, Young's moduli of samples reinforced with concentrated tincal increased. As the process continued, Young's moduli of PCOT samples started to decrease. The reason for this could be the competitive crosslinking and chain scission reactions during irradiation, that's why this periodical behavior was observed [Martinez-Barrera et al., 2008]. On the other hand, when PCOT samples were irradiated with high dose rate, decrease in Young's modulus was higher when compared with low dose rate and this decrease was inversely proportional to concentrated tincal ratio as seen from Figure 3.5.b.

Figure 3.6.a shows that non-irradiated PCAT2 had the highest Young's modulus value among PCAT samples and it decreased with increase in reinforcing filler ratio. This can be explained by retardation of crosslinking by the presence of filler [Simitzis et al., 1997]. It can be seen that when PCAT samples were irradiated up to 245 kGy as shown in Figure 3.6.a, Young's modulus of PCAT2 showed decreasing trend but PCAT5 remained almost the same. On the other hand, Young's modulus of PCAT10 increased with increase in absorbed dose. When PCAT samples irradiated with high dose rate, Young's moduli of PCAT2 and PCAT5 decreased sharply but PCAT10 resisted against radiation.

All non-irradiated samples reinforced with colemanite had lower Young's modulus than neat polyester resin and this shows poor interfacial adhesion between colemanite and polyester. During low dose rate irradiation, Young's moduli of PCOL2 and PCOL5 samples decreased slightly as can be seen from Figure 3.7.a. But Young's modulus of PCOL10 sample had increasing trend. Figure 3.7.b shows that when samples were irradiated at high dose rate, all PCOL samples exhibited lower Young's modulus as compared to neat polyester resin.

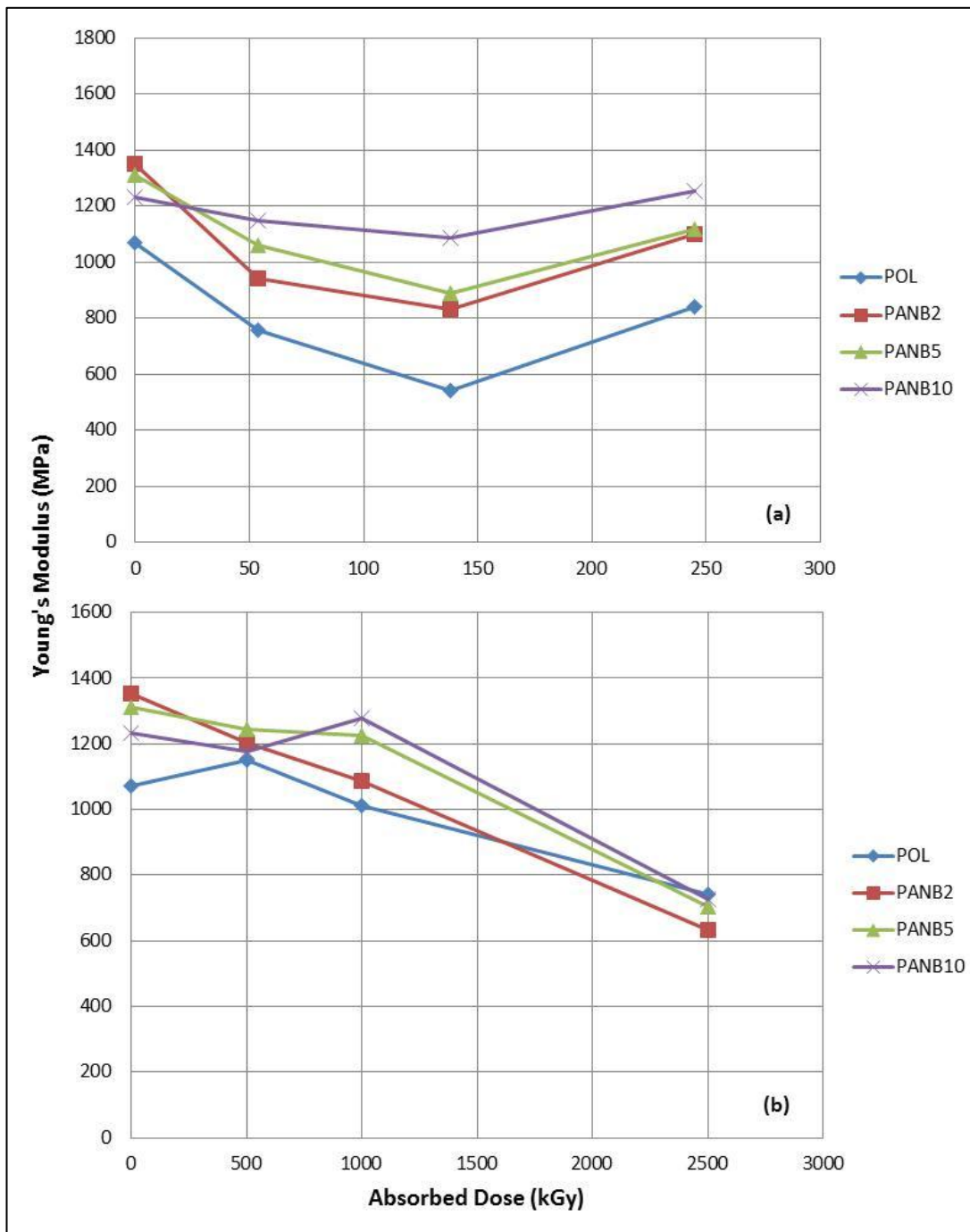


Figure 3.4: Young's Moduli of PANB Samples Irradiated by **a)** Low Dose Rate Gamma Source **b)** High Dose Rate Gamma Source

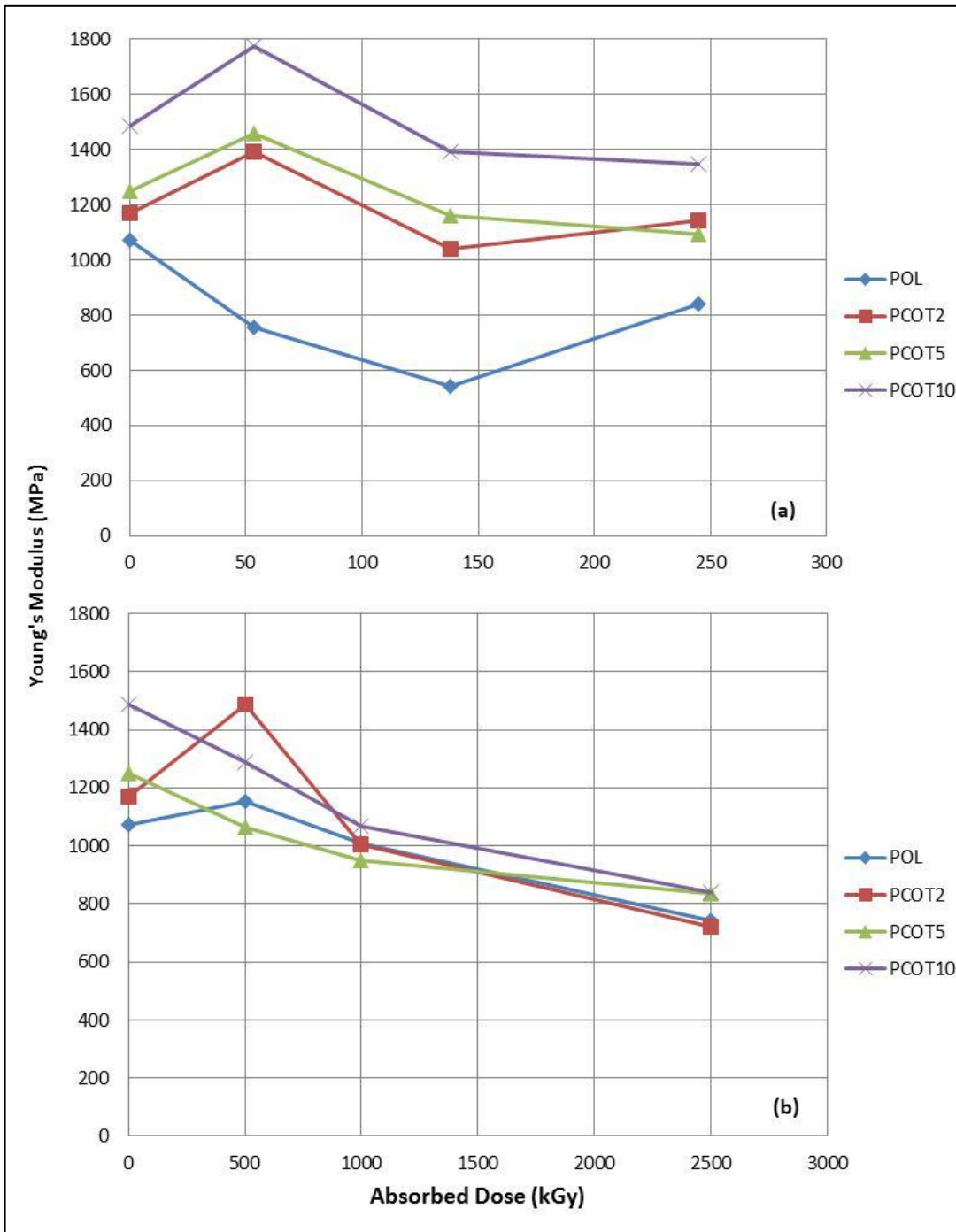


Figure 3.5: Young's Moduli of PCOT Samples Irradiated by **a)** Low Dose Rate Gamma Source **b)** High Dose Rate Gamma Source

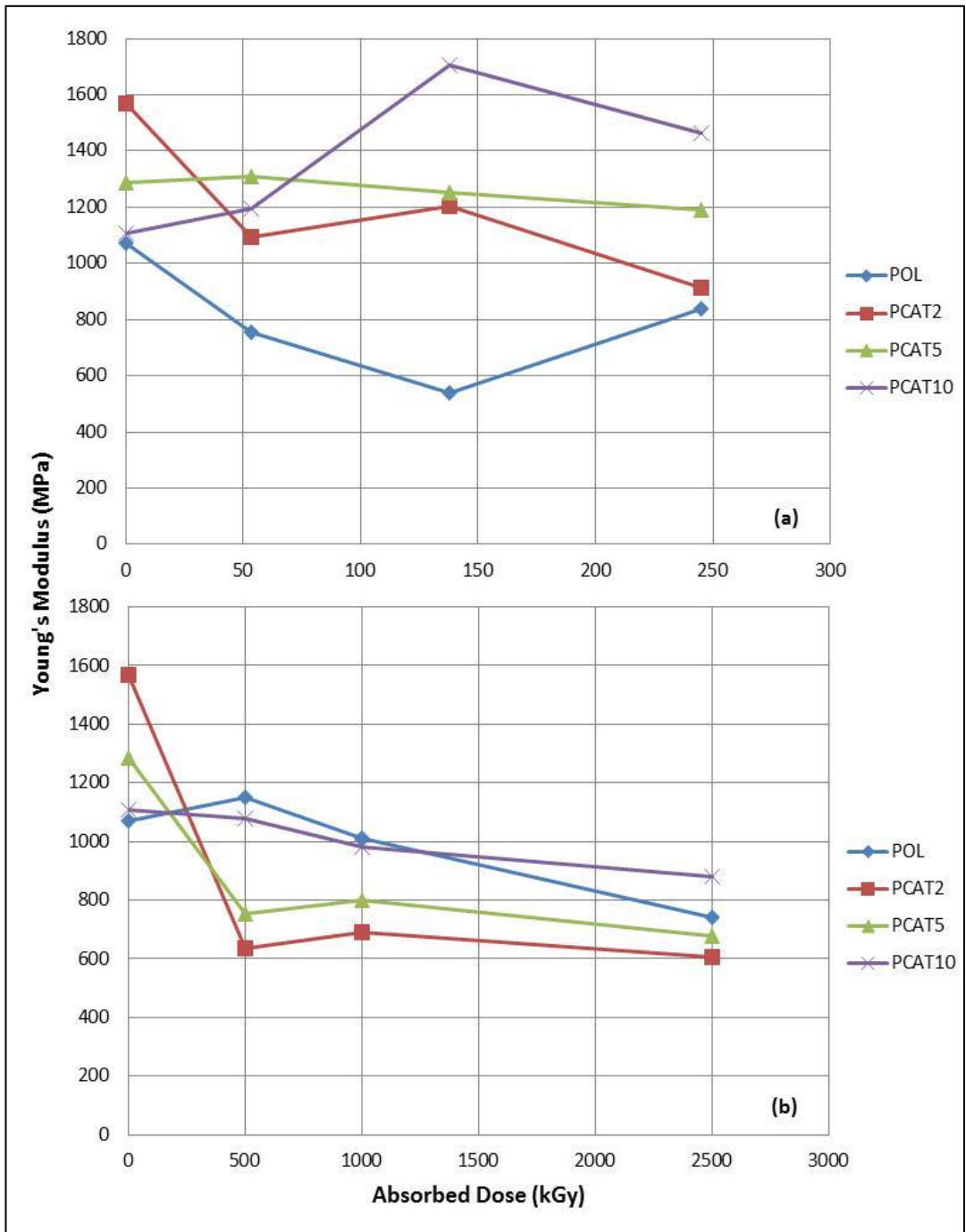


Figure 3.6: Young's Moduli of PCAT Samples Irradiated by a) Low Dose Rate Gamma Source b) High Dose Rate Gamma Source

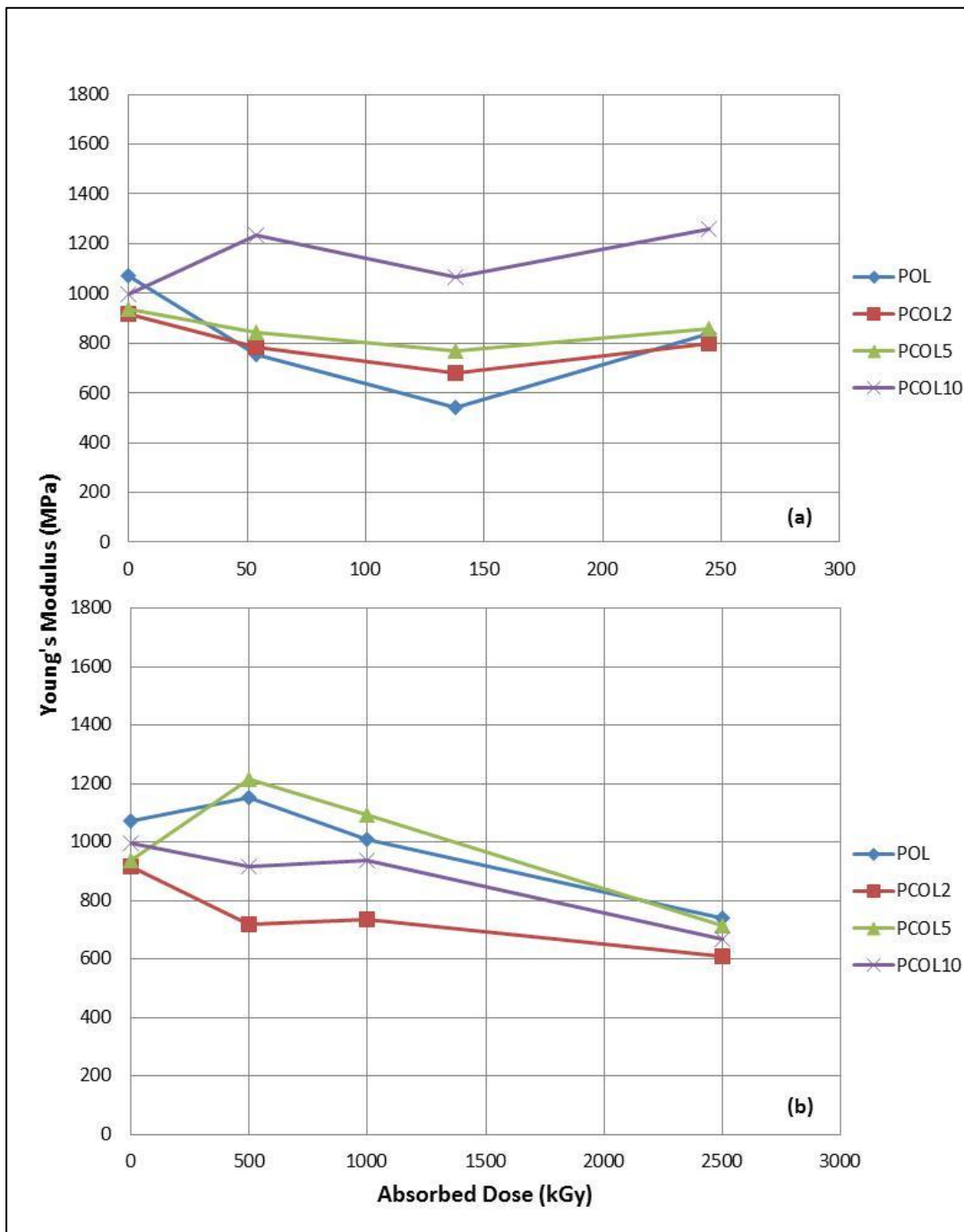


Figure 3.7: Young's Moduli of PCOL Samples Irradiated by **a)** Low Dose Rate Gamma Source **b)** High Dose Rate Gamma Source

3.2.1.2. Tensile Strength

Tensile strength represents how much force a material withstands before it fails. In other words, it is how much load a material can accommodate before it loses its integrity. Effects of irradiation on tensile strength of composite materials are given in Figure 3.8 to Figure 3.11.

All non-irradiated polyester resin samples reinforced with anhydrous borax had lower tensile strength than neat polyester resin. Since uniform distribution of filler in polymer matrix is the key factor for improvement of mechanical properties of composites, this decrease in tensile strength may indicate either poor dispersion of boron mineral, agglomeration or existence of voids [Seki et al., 2013]. But it can be seen from Figure 3.8.a that, decrease in tensile strength of PANB samples was relatively low when compared with neat polyester resin after absorbed dose was reached to 245 kGy.

But when PANB samples were irradiated by high dose rate gamma source up to 2500 kGy, it can be seen from Figure 3.8.b that the decrease in tensile strengths of PANB samples was much higher when compared with tensile strength of neat polyester resin. It can be said that, irradiation by low dose rate gamma source is a long-time process to reach to the desired absorbed dose. During this long period, there is enough time for oxidation [Clegg and Collyer, 1991]. Neat polyester resin was degraded due to oxidative degradation while boron minerals in reinforced composites prevented this oxidation to a certain extent. As a result, reinforced composites had better mechanical properties.

On the other hand, samples are exposed to high amount of radiation in a short time during irradiation by high dose rate gamma source. Radicals could be formed because of high amount of energy but oxidation could not occur adequately during this short period. Radicals are recombined with each other and effects of degradation on polymer could be reduced. These recombination reactions might have been prevented in the presence of boron minerals in reinforced samples and that's why reinforced samples had lower mechanical properties than neat polyester resin.

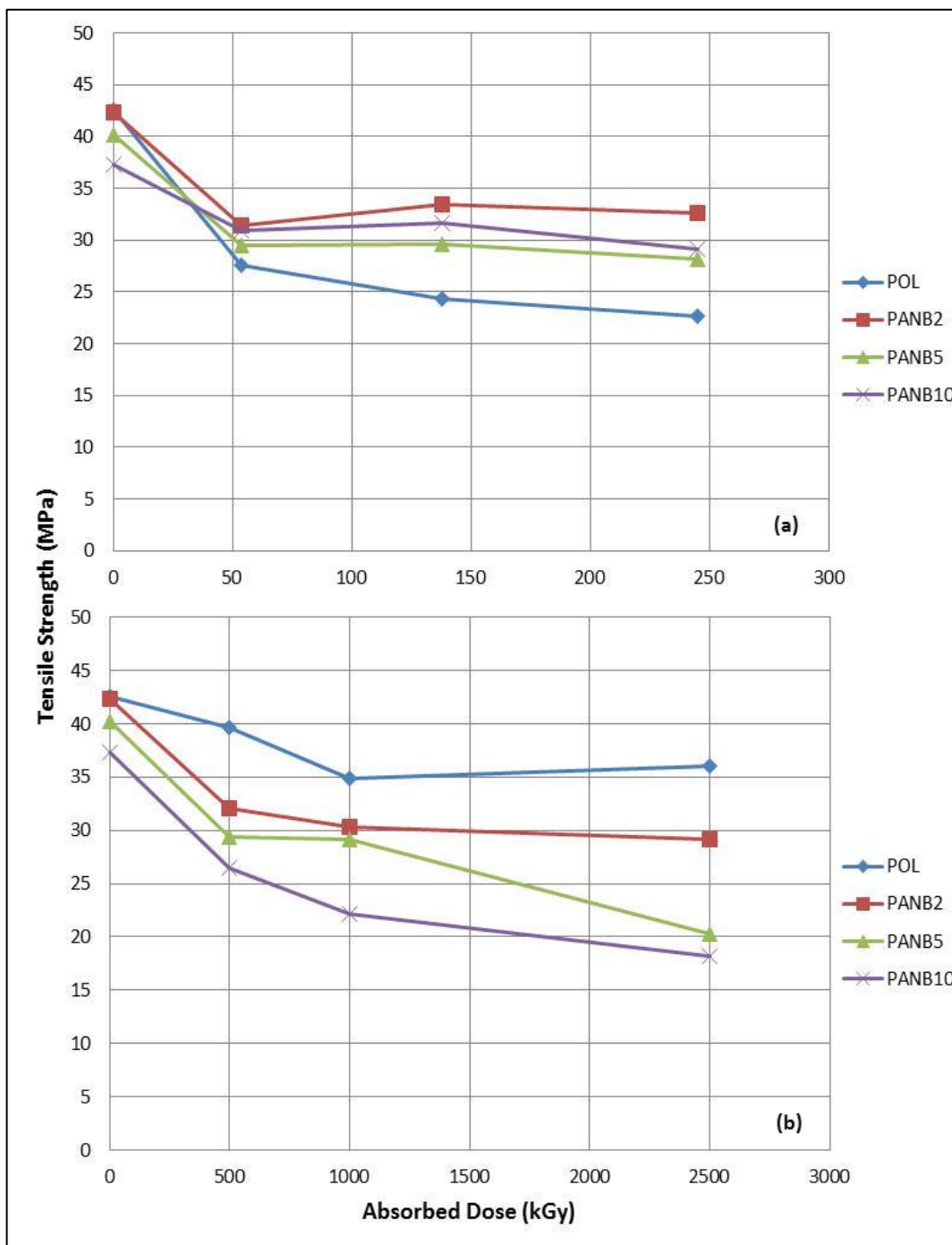


Figure 3.8: Tensile Strengths of PANB Samples Irradiated by **a)** Low Dose Rate Gamma Source **b)** High Dose Rate Gamma Source

Figure 3.9 shows that only PCOT5 sample among PCOT samples had higher tensile strength than neat polyester resin before irradiation and this could be attributed to more uniform distribution of filler [Seki et al., 2013]. As will be mentioned in Section 3.6, agglomeration could be occurred with increasing reinforcing filler ratio and this could be the main reason for decrease in mechanical properties. Loss in tensile strength of neat polyester resin was much higher at low doses. PCOT5 sample had also the highest tensile strength after irradiation up to 245 kGy. When PCOT samples irradiated by high dose rate gamma source, loss in tensile strengths of PCOT5 and PCOT10 samples were more than 50% but tensile strength of PCOT2 was almost the same as seen from Figure 3.9.b.

As can be seen from Figure 3.10, PCAT2 had higher tensile strength than PCAT5 and PCAT10 before irradiation. All PCAT samples had loss in their tensile strengths during irradiation up to 54 kGy by low dose rate gamma source. But after that point, when PCAT2 and PCAT5 samples were going on losing their tensile strengths, tensile strength of PCAT10 remained almost constant. Similar trends can also be seen in Figure 3.10.b. Although decrease during irradiation was low, tensile strength of PCAT10 was the lowest after irradiation because of poor interfacial adhesion.

Figure 3.11 shows that all PCOL samples had lower tensile strength than that of neat polyester resin before irradiation. There was loss in tensile strength of all PCOL samples when absorbed dose rate was reached to 138 kGy. After that, there were slight increases for PCOL5 and PCOL10 when tensile strength of PCOL2 remained almost constant. This increase could not be seen at high doses. All PCOL samples had lower tensile strength than that of neat polyester resin.

3.2.1.3. Elongation at Break

Elongation at break is the ratio between change in length after failure and initial length of the material and it is a measure of ductility of material. Elongation at break results of composite materials can be seen in Figure 3.12 to Figure 3.15.

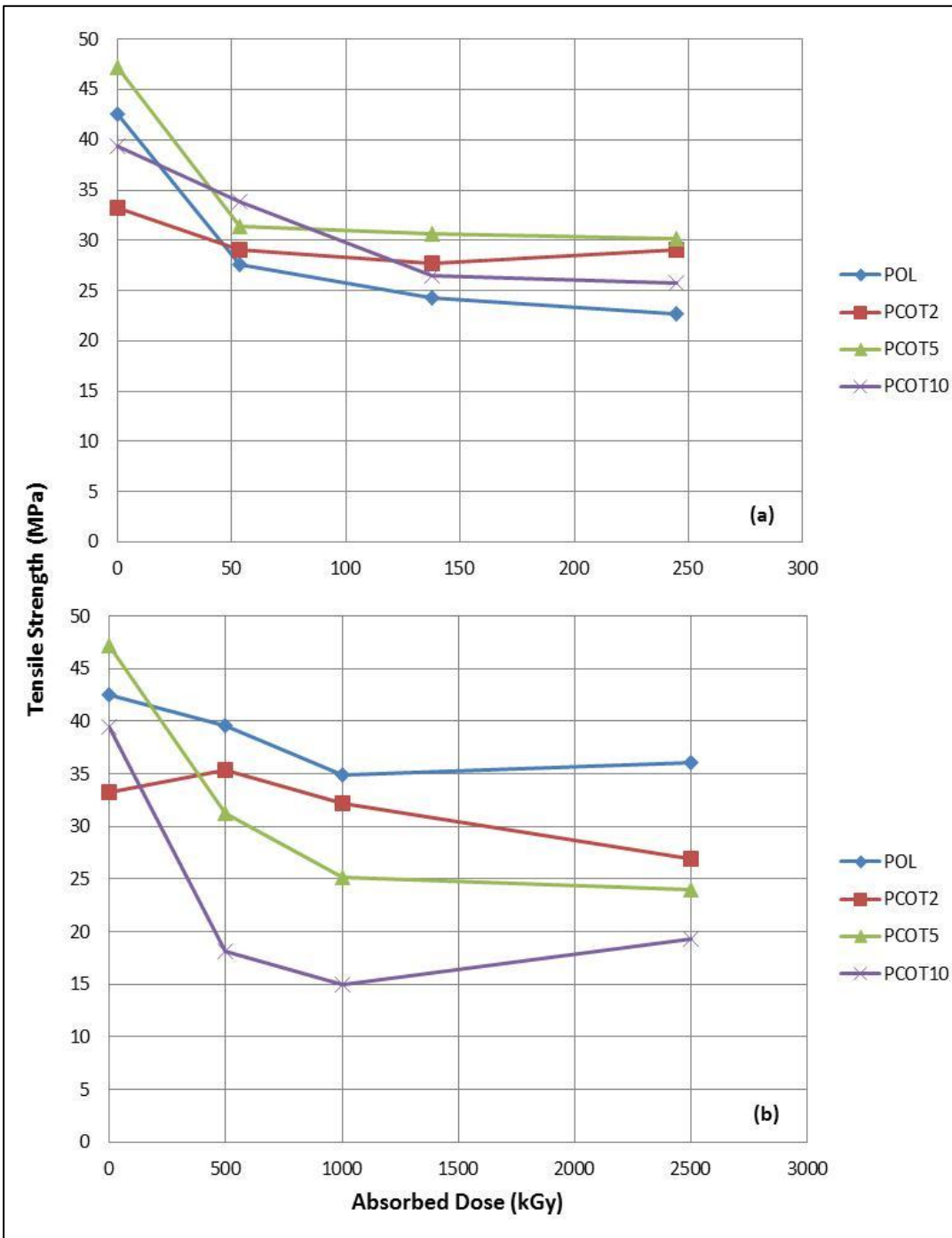


Figure 3.9: Tensile Strengths of PCOT Samples Irradiated by **a)** Low Dose Rate Gamma Source **b)** High Dose Rate Gamma Source

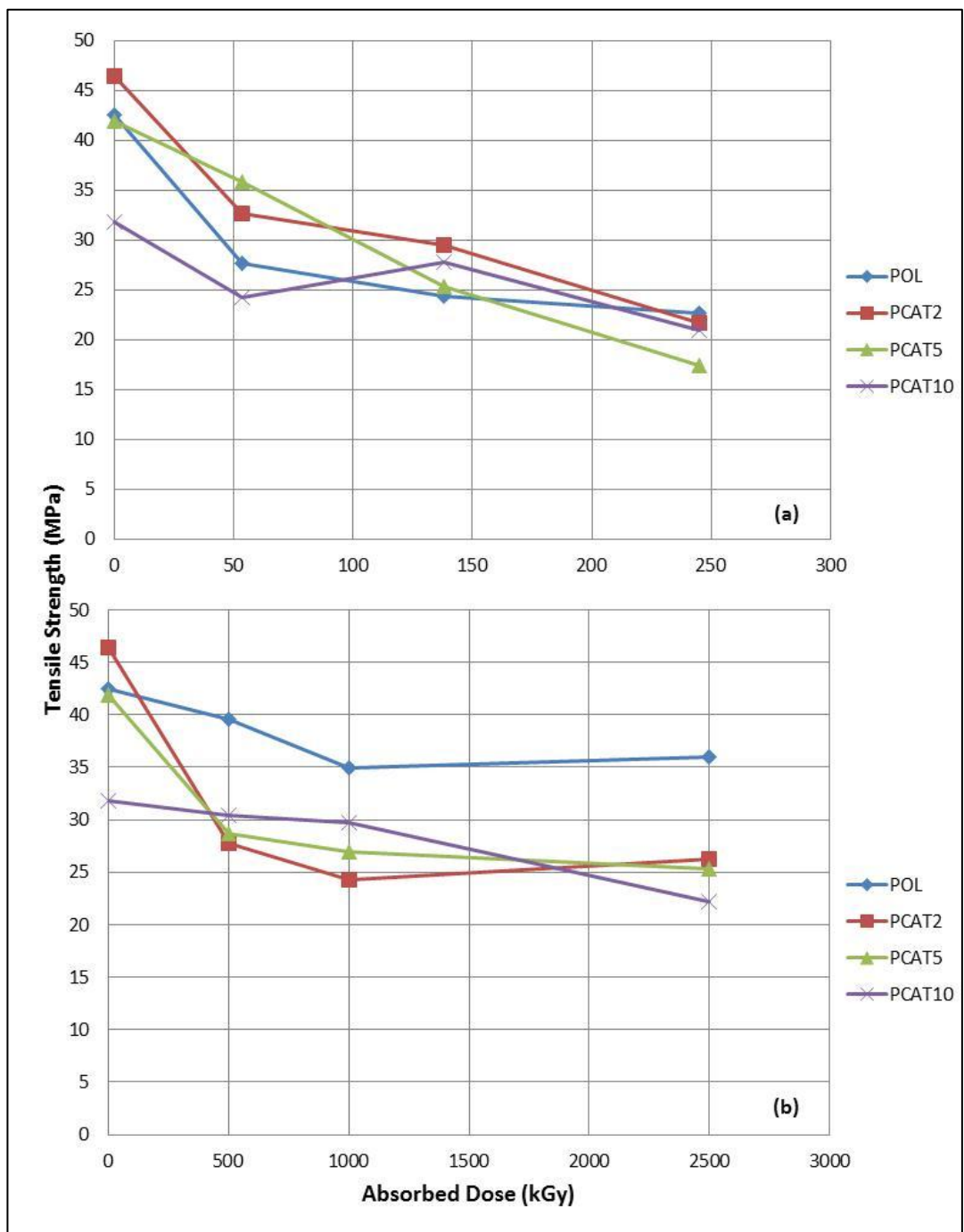


Figure 3.10: Tensile Strengths of PCAT Samples Irradiated by a) Low Dose Rate Gamma Source b) High Dose Rate Gamma Source

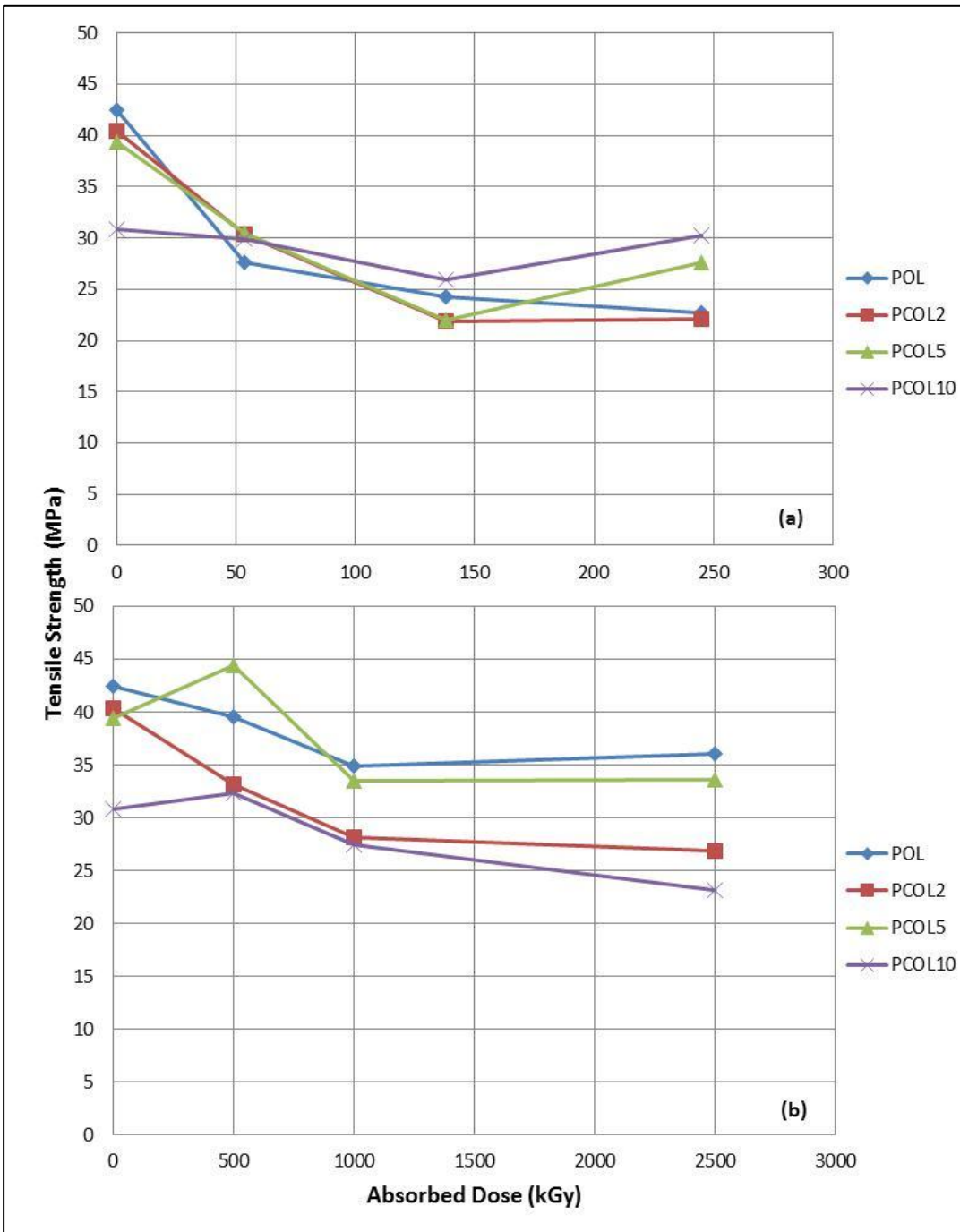


Figure 3.11: Tensile Strengths of PCOL Samples Irradiated by a) Low Dose Rate Gamma Source b) High Dose Rate Gamma Source

Elongation of non-irradiated PANB samples at break decreased with increase in reinforcing filler ratio. During irradiation by low dose rate gamma source, elongation of neat polyester resin at break firstly increased and then it decreased and these results are compatible with Young's modulus and tensile strength results. But PANB samples showed very little change as seen from Figure 3.12.a. Figure 3.12.b shows that elongation of neat polyester resin and PANB samples at break were increasing during irradiation by high dose rate gamma source.

Similar with PANB samples, elongation of PCOT samples at break remained almost constant during irradiation by low dose rate gamma source as can be seen from Figure 3.13.a. These results can be explained by chain scission and crosslinking reactions occurring simultaneously. Whereas for the case of high doses, there were slight increases in elongation of PCOT samples at break. This was probably due to the rate of chain scission is higher than that of crosslinking.

When polyester resin was reinforced with calcined tincal, PCAT samples became more brittle as seen from Figure 3.14. After irradiation by low dose rate gamma source, elongations of PCAT2 and PCAT10 at break remained constant whereas PCAT5 showed a slight decrease. On the other hand, as shown in Figure 3.14.b, PCAT samples became more ductile at high doses.

When PCOL samples were irradiated by low dose rate gamma source up to 138 kGy, elongation of PCOL2 and PCOL5 samples at break remained almost constant but after that point they started to increase. On the other hand, PCOL10 showed increasing trend during all irradiation process as seen from Figure 3.15.a. But Figure 3.15.b shows that elongation at break results of PCOL samples showed periodical behavior during irradiation by high dose rate gamma source.

After all, it can be said that boron minerals gave resistance to polyester resin against low doses. Composite materials had better mechanical properties. But at high doses, degradation was the dominant mechanism and boron minerals could not show any significant shielding effect. Defects in boron mineral-polyester interface also enhanced degradative effects of radiation and composites had lower mechanical properties than neat polyester resin.

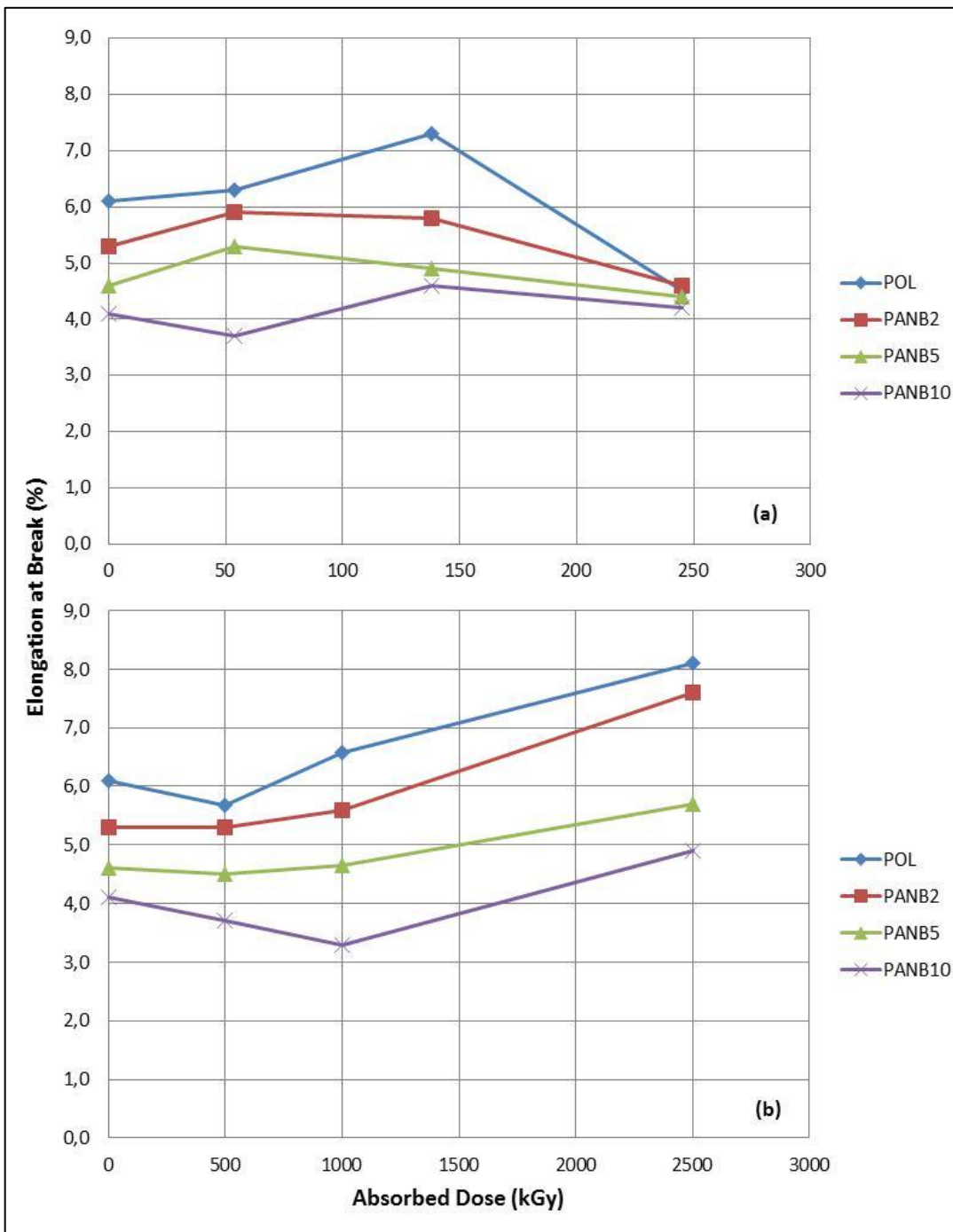


Figure 3.12: Elongation at Break of PANB Samples Irradiated by **a)** Low Dose Rate Gamma Source **b)** High Dose Rate Gamma Source

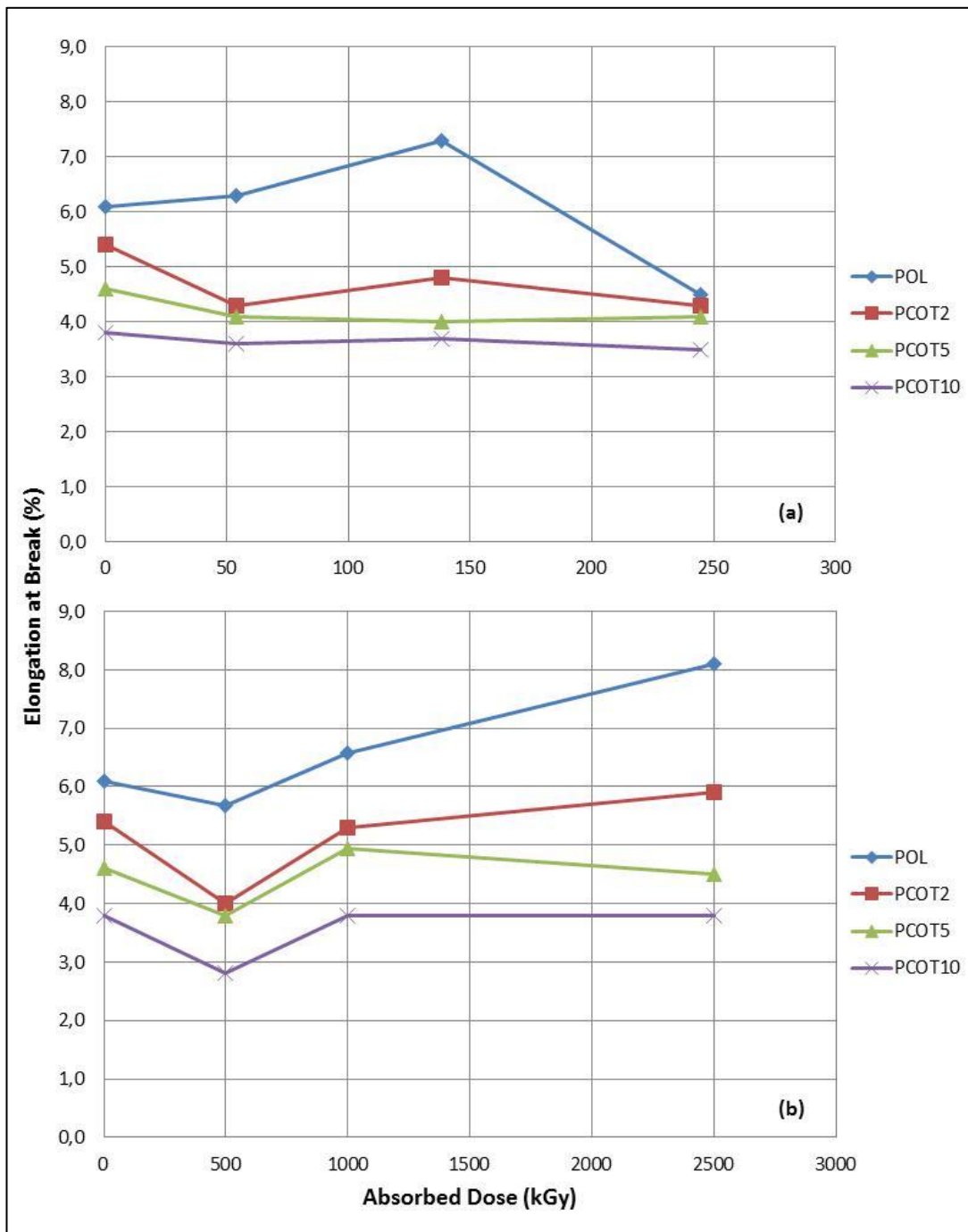


Figure 3.13: Elongation at Break of PCOT Samples Irradiated by **a)** Low Dose Rate Gamma Source **b)** High Dose Rate Gamma Source

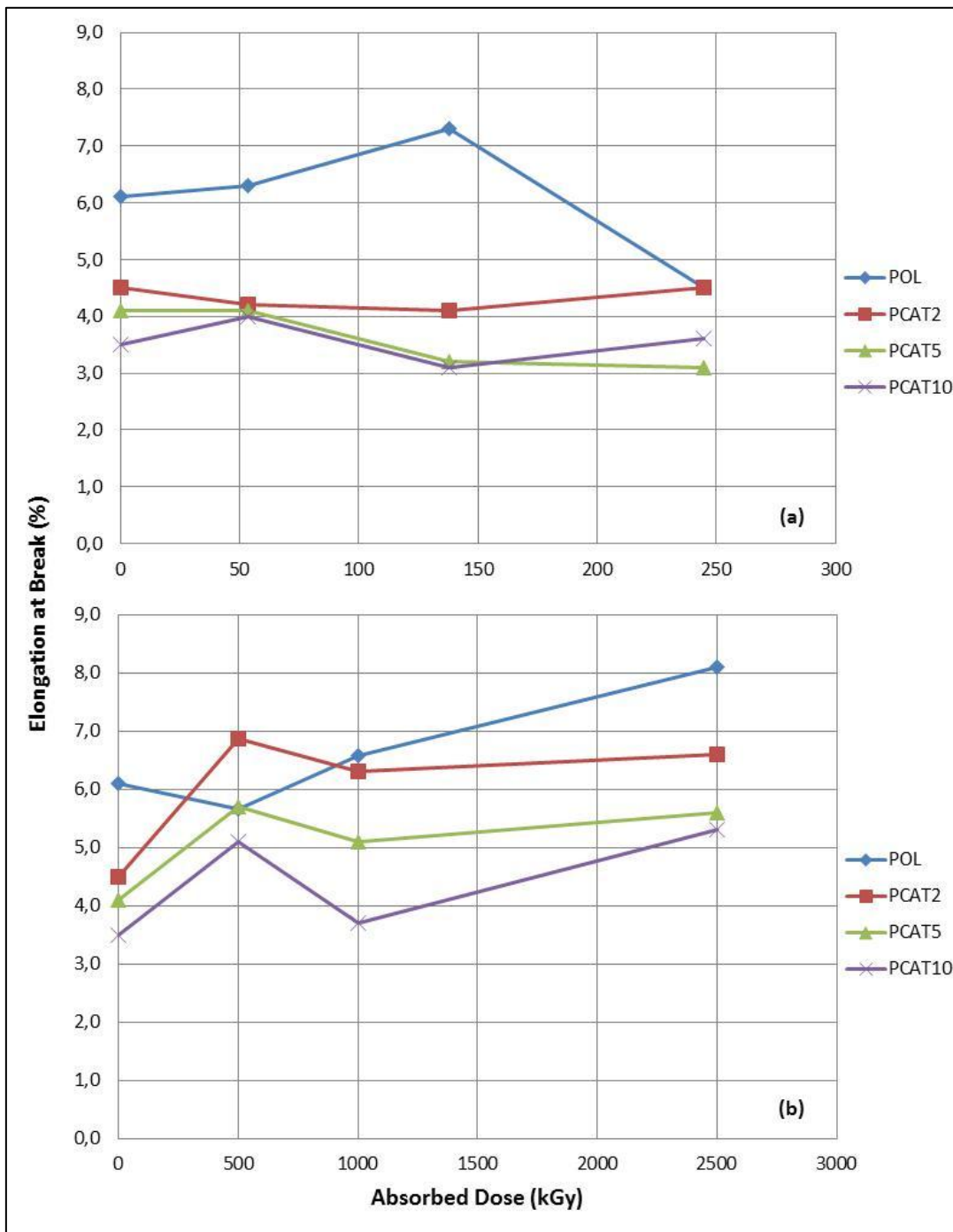


Figure 3.14: Elongation at Break of PCAT Samples Irradiated by **a)** Low Dose Rate Gamma Source **b)** High Dose Rate Gamma Source

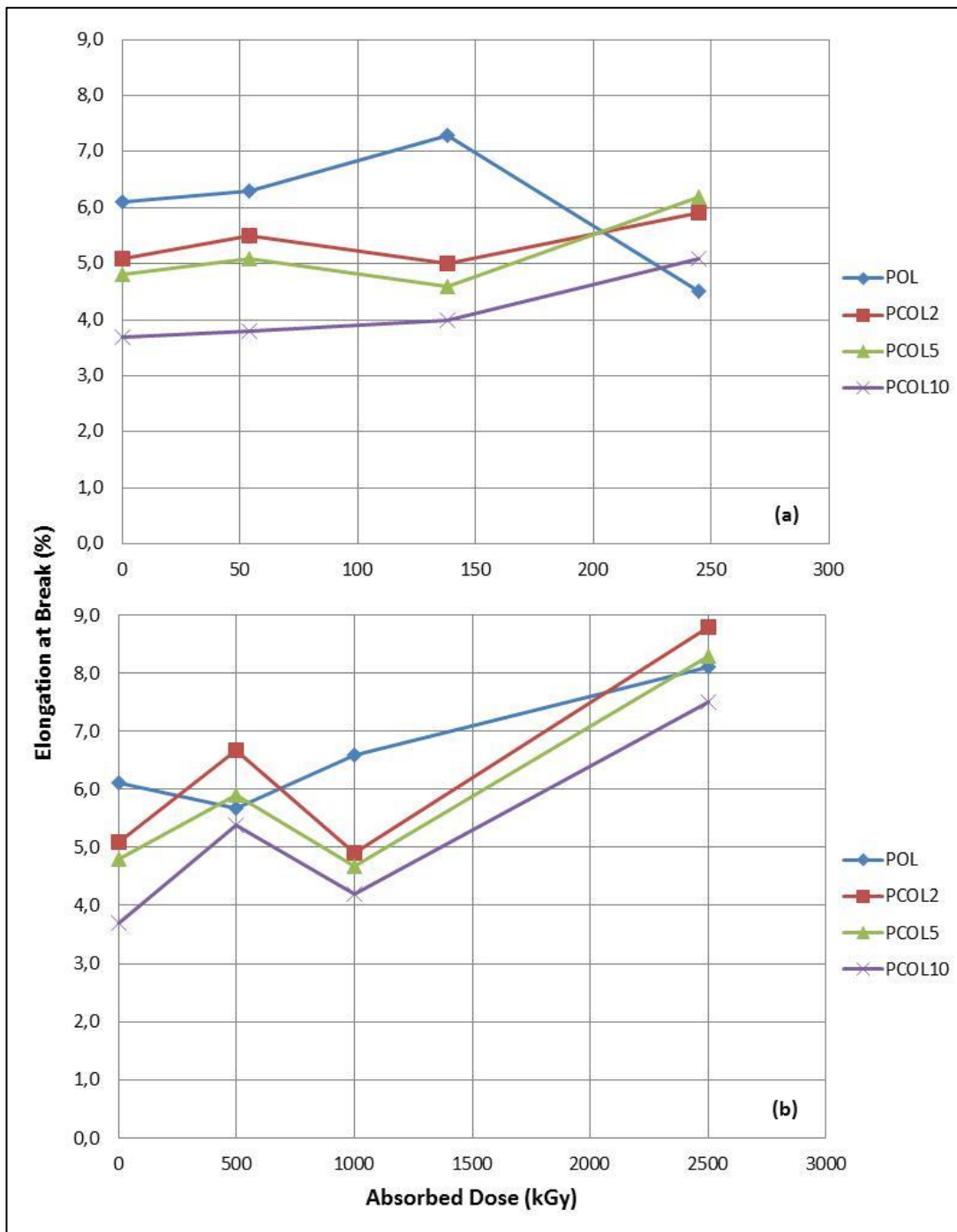


Figure 3.15: Elongation at Break of PCOL Samples Irradiated by **a)** Low Dose Rate Gamma Source **b)** High Dose Rate Gamma Source

Most satisfying results were obtained from anhydrous borax. This could be explained by its highest boron content which makes composite material able to resist against radiation. On the other hand, colemanite had the worst performance on the contrary of its moderate boron content. Molecules of colemanite were much bigger than other boron minerals used in this study and this situation could interrupt curing and crosslinking of polyester resin.

3.2.2. Tensile Tests of Samples Irradiated by High Dose Rate Gamma Source Under Vacuum

Irradiation by high dose rate gamma source was also performed in vacuum conditions. By this way, it was intended to observe the effect of air on irradiation.

3.2.2.1. Young's Modulus

Figure 3.16 shows how Young's moduli of PANB samples changed at high doses under vacuum. PANB2 and PANB5 showed some resistance against radiation after absorbed dose of 2500 kGy since Young's moduli of PANB10 decreased to about half of its starting value.

In the earlier period of irradiation under vacuum, Young's moduli of samples reinforced with concentrated tincal decreased. Even though there were some increase was observed as the process continued, Young's moduli of PCOT samples were lower than that of values before irradiation as seen from Figure 3.17.

After reinforcement of polyester resin with calcined tincal, Young's moduli of PCAT samples were higher than that of neat polyester resin. When PCAT samples were irradiated under vacuum, PCAT10 showed some increase during process but Young's moduli of all PCAT samples decreased after all. Figure 3.18 shows that neat polyester resin had higher Young's modulus than PCAT samples after irradiation.

All PCOL samples had lower Young's modulus than neat polyester resin before irradiation. But after irradiation under vacuum, only Young's modulus of PCOL5 was higher than that of neat polyester resin as shown in Figure 3.19.

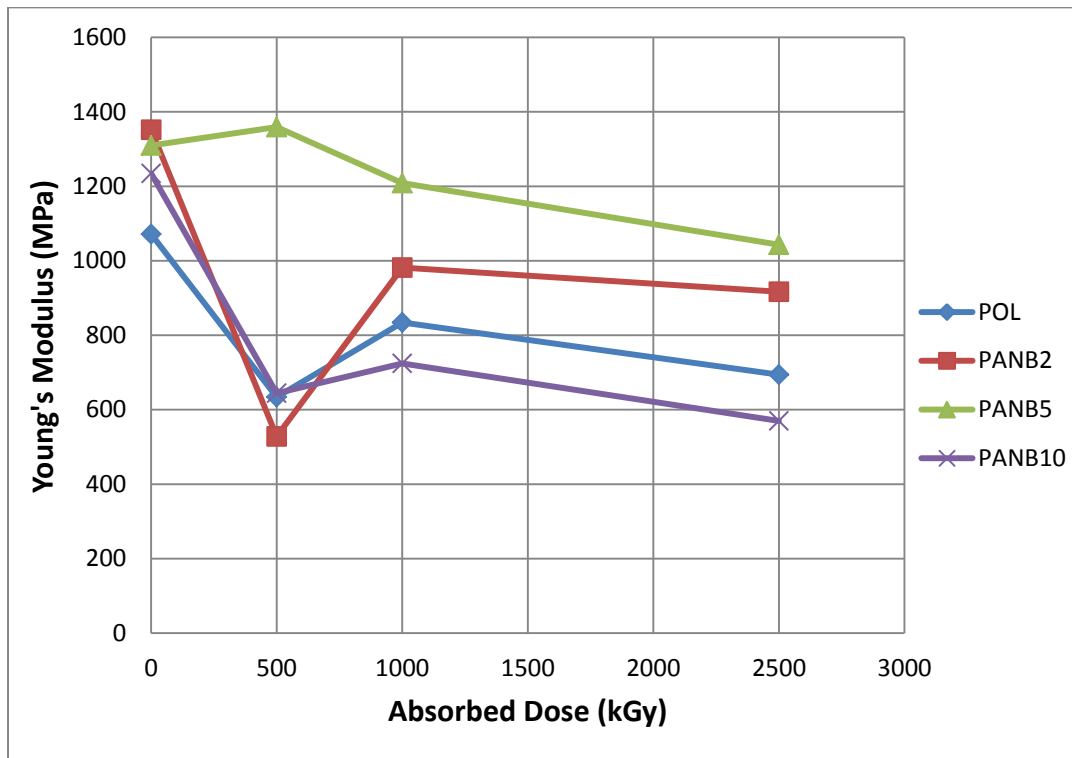


Figure 3.16: Young's Moduli of PANB Samples Irradiated by High Dose Rate Gamma Source under Vacuum

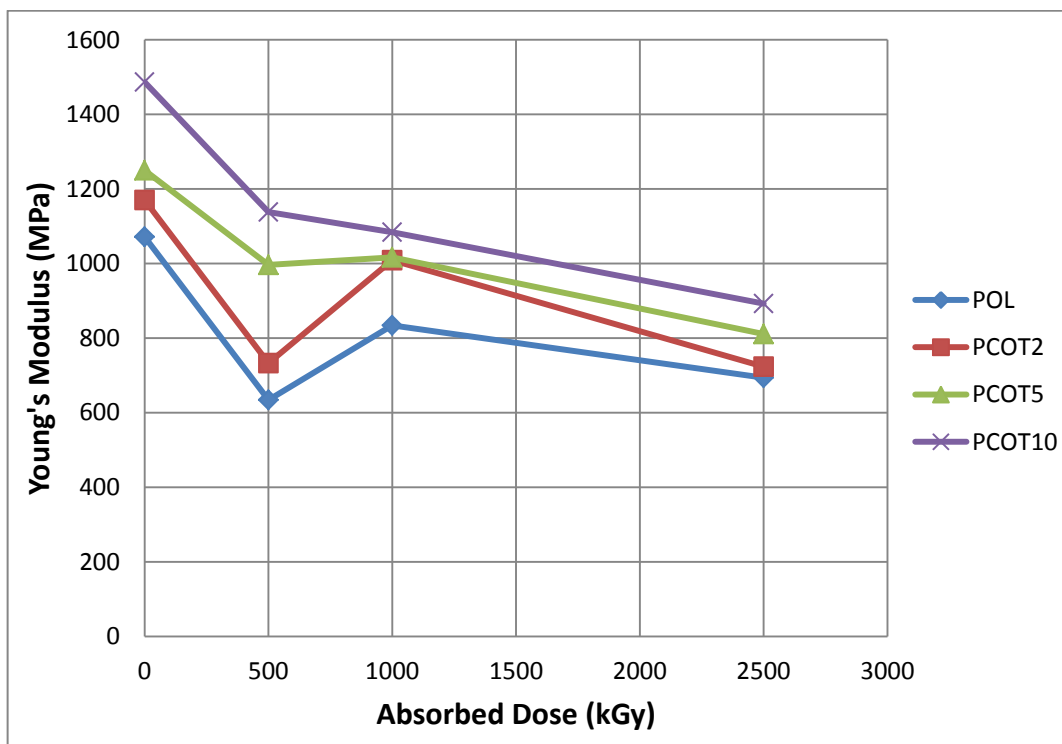


Figure 3.17 Young's Moduli of PCOT Samples Irradiated by High Dose Rate Gamma Source under Vacuum

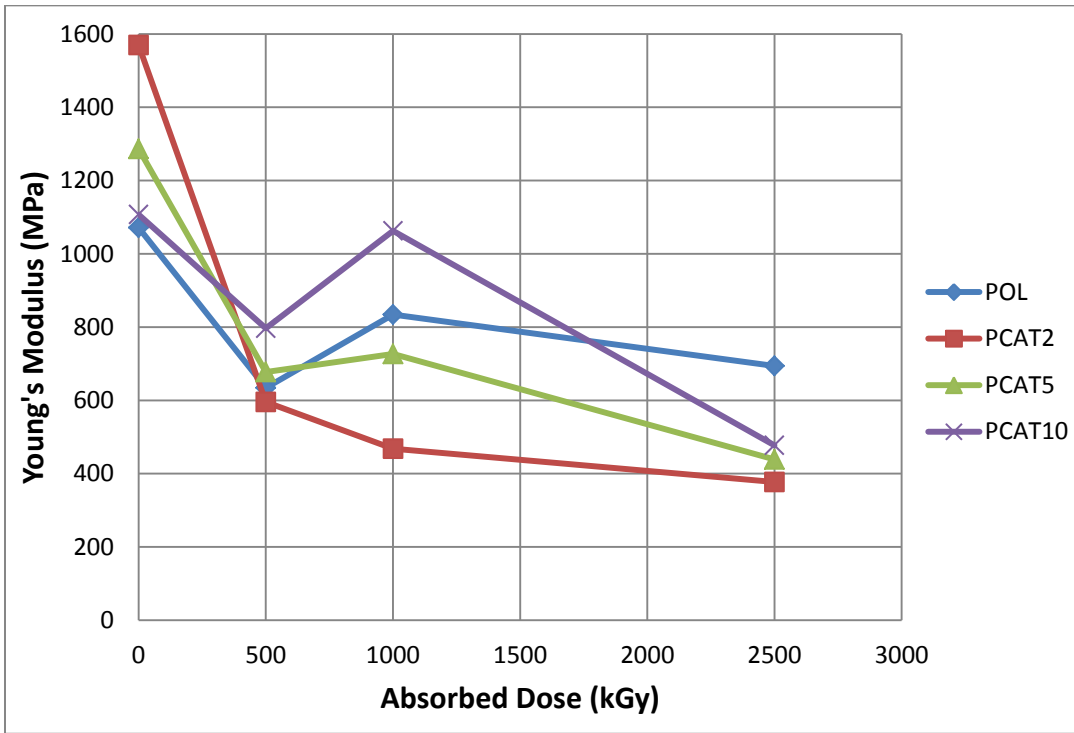


Figure 3.18: Young's Moduli of PCAT Samples Irradiated by High Dose Rate Gamma Source under Vacuum

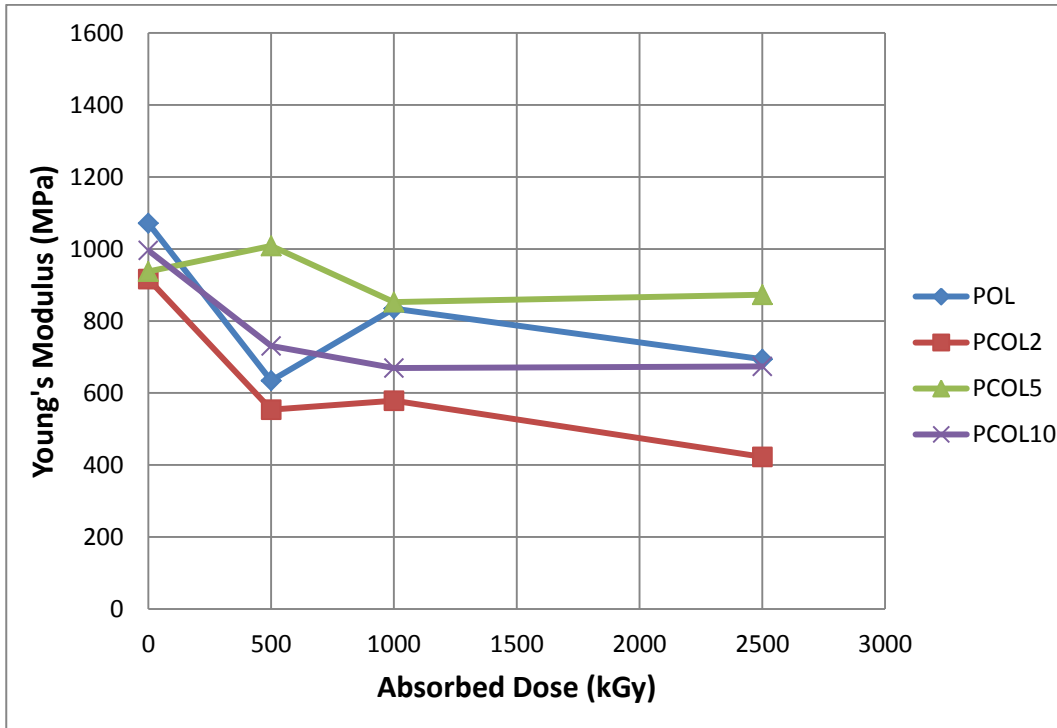


Figure 3.19: Young's Moduli of PCOL Samples Irradiated by High Dose Rate Gamma Source under Vacuum

3.2.2.2. Tensile Strength

Figure 3.20 shows periodical behavior in tensile strengths of PANB samples against high doses under vacuum. All PANB samples had lower tensile strength than neat polyester resin before irradiation. But after irradiation under vacuum, PANB5 showed higher tensile strength than neat polyester resin.

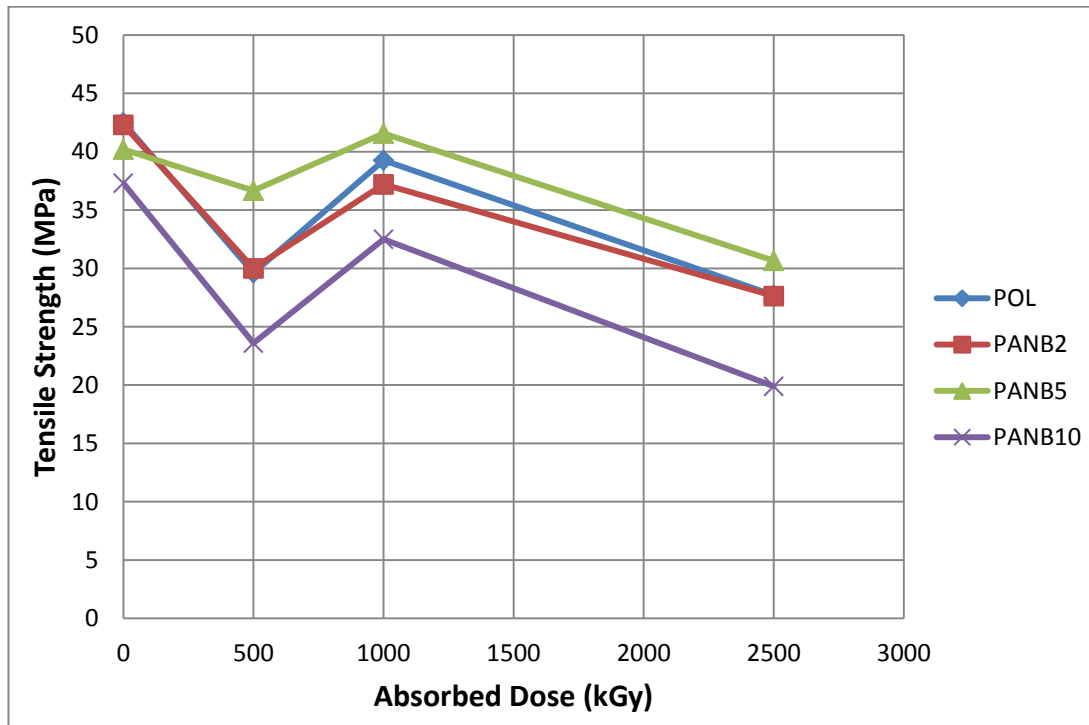


Figure 3.20: Tensile Strengths of PANB Samples Irradiated by High Dose Rate Gamma Source under Vacuum

Before irradiation of PCOT samples, only PCOT5 had higher tensile strength than neat polyester resin. When PCOT samples were irradiated under vacuum, tensile strengths of PCOT5 and PCOT10 decreased sharply and then they increased as seen from Figure 3.21. Tensile strength of PCOT2 had limited change during irradiation.

When neat polyester resin was irradiated with high dose rate under vacuum, tensile strength had periodical behavior. But Figure 3.22 shows that tensile strengths of PCAT2 and PCAT5 decreased continuously during irradiation process. On the other hand, tensile strength of PCAT10 firstly decreased and then increased. All PCAT samples had lower tensile strength than neat polyester resin after irradiation.

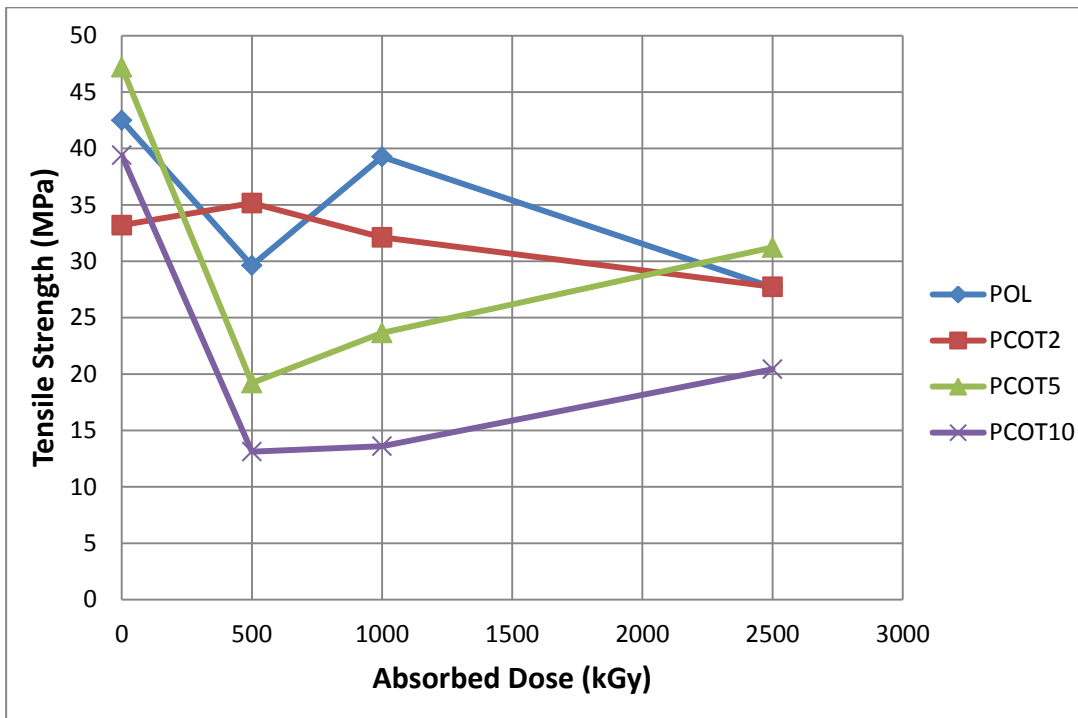


Figure 3.21: Tensile Strengths of PCOT Samples Irradiated by High Dose Rate Gamma Source under Vacuum

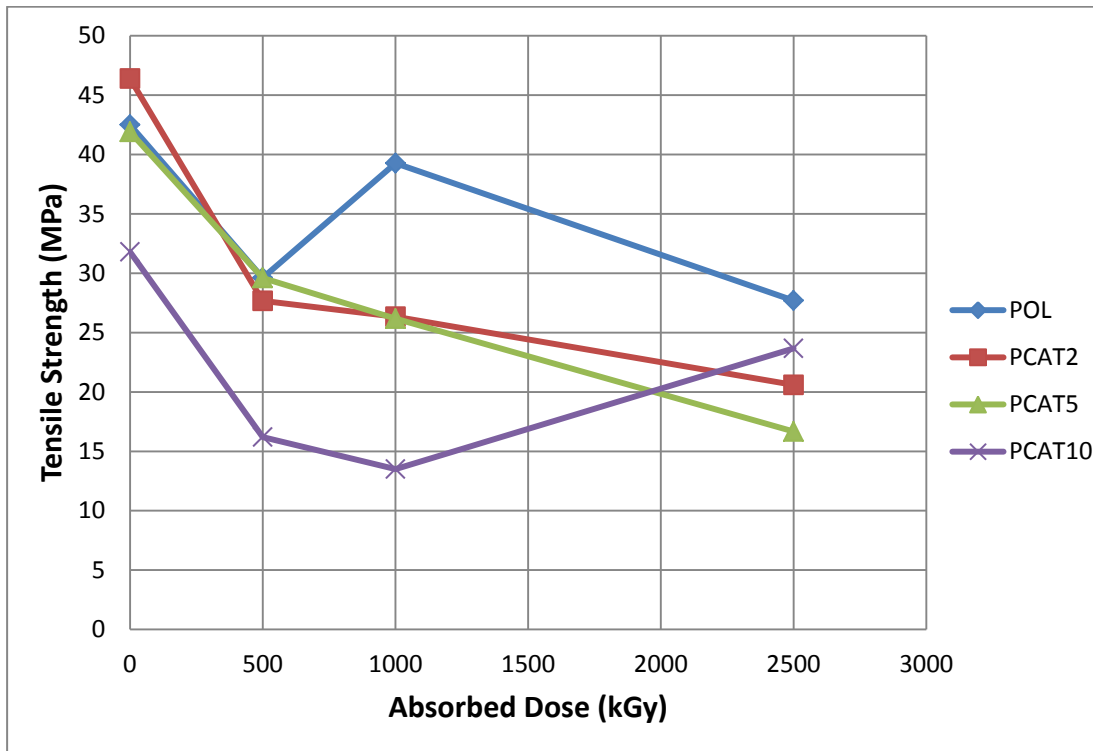


Figure 3.22: Tensile Strengths of PCAT Samples Irradiated by High Dose Rate Gamma Source under Vacuum

Tensile strengths of PCOL2 and PCOL10 decreased continuously during irradiation under vacuum and they had lower tensile strength than neat polyester resin after irradiation by high dose rate gamma source as it is shown in Figure 3.23. Tensile strength of PCOL5 was higher than that of neat polyester resin.

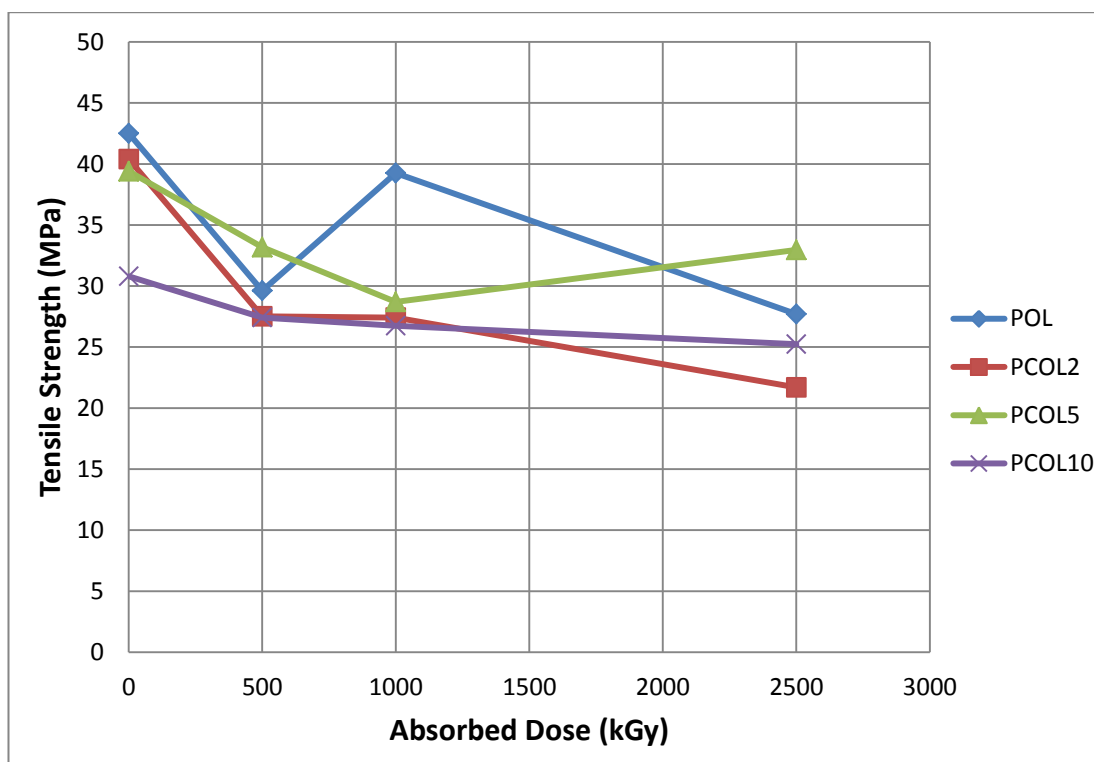


Figure 3.23: Tensile Strengths of PCOL Samples Irradiated by High Dose Rate Gamma Source under Vacuum

3.2.2.3. Elongation at Break

When PANB samples were irradiated under vacuum, elongation of PANB5 at break stayed constant and elongation of PANB10 at break increased sharply. But Figure 3.24 shows that elongation of PANB2 at break increased and then decreased. They all had lower elongation at break when compared with neat polyester resin.

Figure 3.25 shows that when polyester resin samples reinforced with concentrated tincal were irradiated under vacuum, elongation of PCOT2 and PCOT5 at break showed periodical behavior. On the other hand, elongation of PCOT10 at break decreased and then increased during irradiation process. Neat polyester resin was more ductile than PCOT samples after irradiation under vacuum.

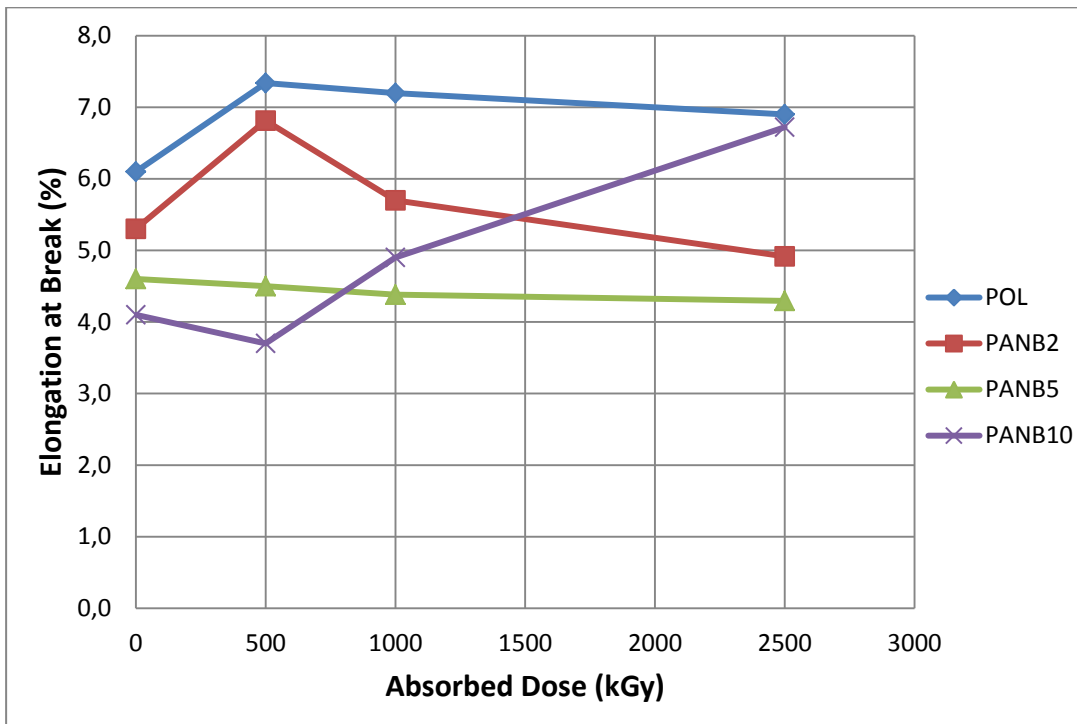


Figure 3.24: Elongation of PANB Samples at Break Irradiated by High Dose Rate Gamma Source under Vacuum

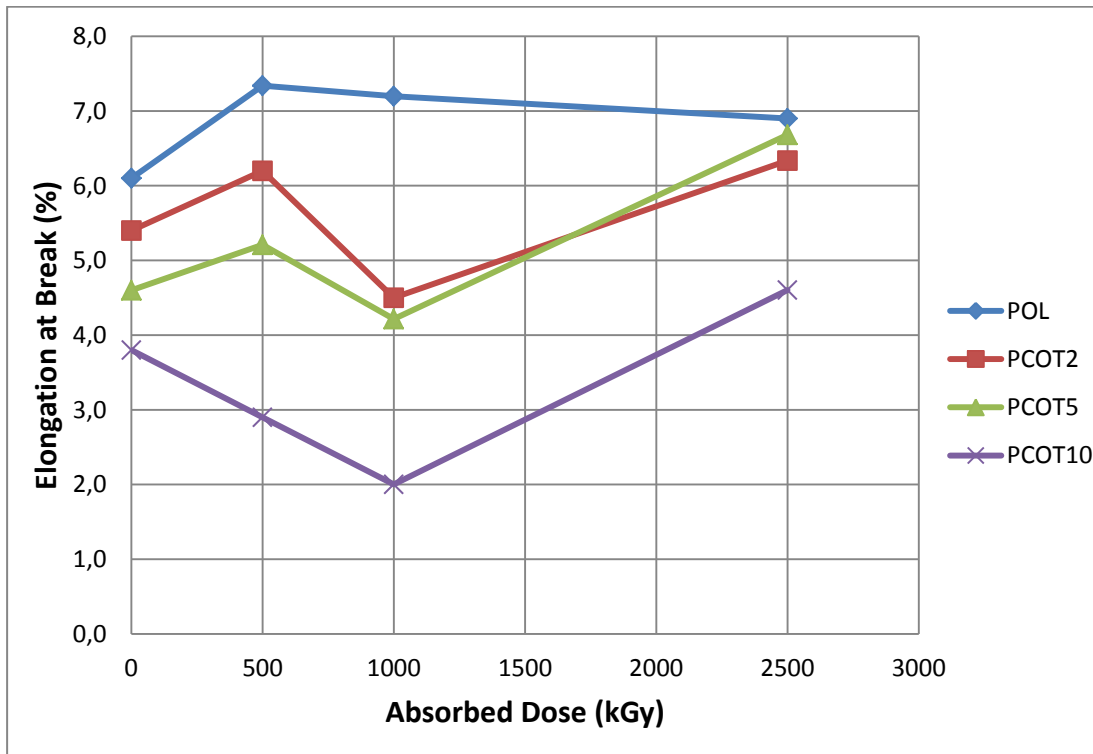


Figure 3.25: Elongation of PCOT Samples at Break Irradiated by High Dose Rate Gamma Source under Vacuum

Elongation of PCAT2 and PCAT5 samples at break increased with increase in total dose absorbed as can be seen from Figure 3.26. But elongation of PCAT10 at break decreased up to 1000 kGy and then it increased. Elongation of PCAT samples and neat polyester resin at break were close after irradiation under vacuum.

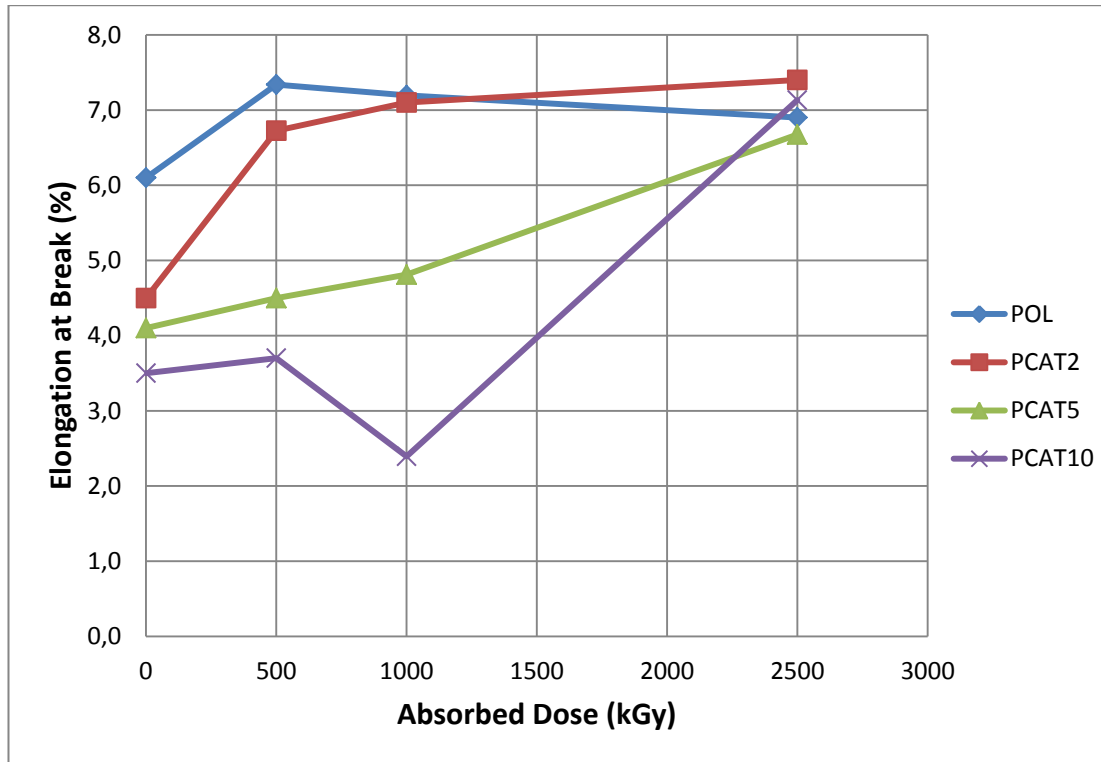


Figure 3.26: Elongation of PCAT Samples at Break Irradiated by High Dose Rate Gamma Source under Vacuum

Figure 3.27 shows that during high dose rate irradiation under vacuum, elongation of PCOL2 at break had increasing trend. PCOL5 and PCOL10 had also increasing trend up to 500 kGy but after that point, PCOL5 started to decrease when PCOL10 stayed almost constant. When reinforcing filler was raised from 2% to 5%, it gave composite some toughness. But additional increase in filler ratio made composite lose its strength because of poor dispersion. These results are compatible with tensile strength results.

When all results of tensile tests applied to the samples irradiated under vacuum were examined, it can be said that samples were not affected positively by absence of oxygen as expected. There were not any significant differences between mechanical test results of samples irradiated in air and under vacuum by high dose

rate gamma source. This situation can be clarified by oxidation of radicals, which were formed by irradiation, with oxygen trapped in composite network and with oxygen in polyester chains.

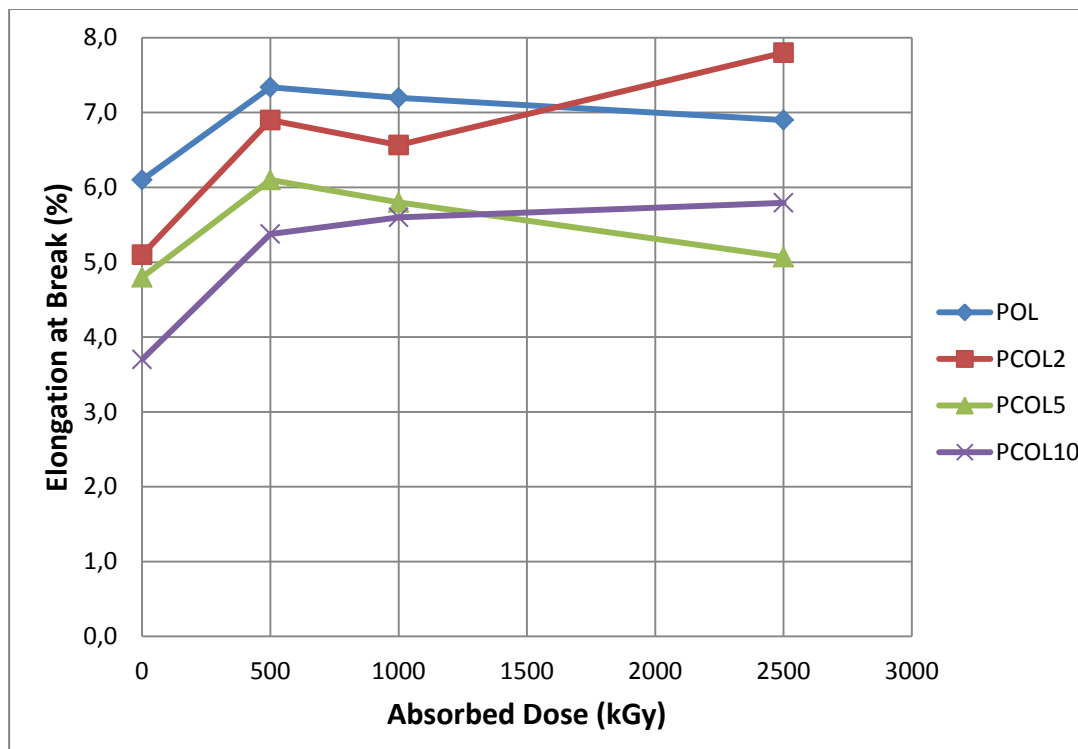


Figure 3.27: Elongation of PCOL Samples at Break Irradiated by High Dose Rate Gamma Source under Vacuum

When samples were irradiated up to 500 kGy, almost all samples were experienced a network destruction and after that point, they had some recovery on their mechanical properties because of crosslinking. But when total absorbed dose were reached to 2500 kGy, their mechanical properties were worse than their initial state.

3.3. Attenuated Total Reflectance - Fourier Transform Infrared Spectroscopy

ATR-FTIR results of polyester resin untreated and reinforced with boron minerals can be used to estimate chemical structure of samples and reactions occurred in structure via irradiation process. Normalized absorbance values of bands investigated in this section were given in Appendix D.

3.3.1. ATR-FTIR Results of Boron Minerals

The ability of boron minerals to form chain or network as mentioned in Chapter 1 enables FT-IR spectra of boron minerals to become complex.

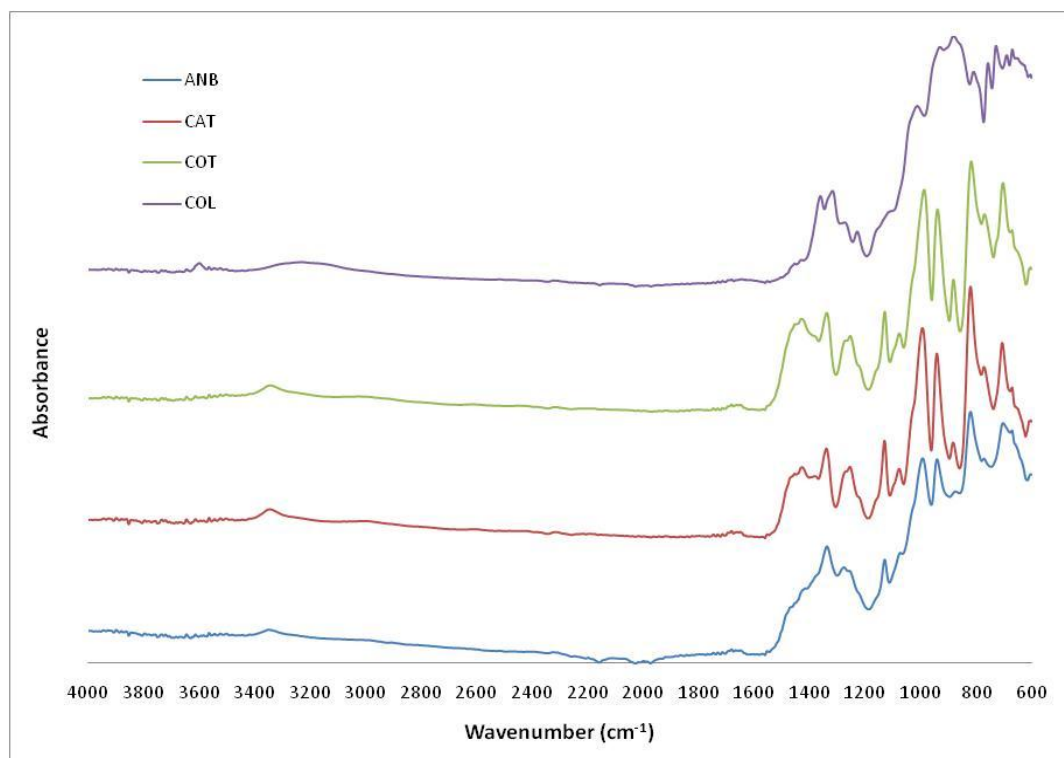


Figure 3.28: ATR-FTIR Spectra of Boron Minerals

Since anhydrous borax, calcined tincal and concentrated tincal have similar crystal structure; FT-IR spectra of ANB, CAT and COT samples are compatible with each other as can be seen from Figure 3.28. Band at 705 cm^{-1} represents B-O-B ring bending, and bands at 880 and 1255 cm^{-1} represent bending of B-OH. 880 and 1255 cm^{-1} bands could not be observed for ANB since it doesn't contain B-OH units. Stretching of tetragonal boron units (BO_4) can be observed at 820 , 990 , 1075 and at 1130 cm^{-1} at FT-IR spectra. Stretching of triangular boron groups (BO_3) give bands at 940 , 1340 and at 1425 cm^{-1} . Bending of O-H can be observed at 3345 cm^{-1} . [Weir, 1966, Peak et al., 2003, Park et al. 2007, Pavlyukevich et al., 2009, Çetin et al., 2012, Frost et al., 2013, Budak and Gönen, 2014].

FT-IR spectra of COL had differences with other boron minerals. Basic structure of COL is endless B-O chains. Bands mentioned above had 10 to 20 cm^{-1}

lower wavenumber in COL samples since differences in hydrogen bonding may cause shifting of bands. There were some extra bands in the region of 600-760 cm^{-1} which represents bending of B-OH. Band at 3600 cm^{-1} can be attributed to crystalline water in the structure of COL. Most significant differences of spectra of COL from other boron minerals are strong and wide bands at 880 and 940 cm^{-1} . Number of tetragonal units is lower than triangular units or B-OH units in crystal structure of COL in contrast to ANB, CAT or COT. This situation resulted in more intense BO_4 and B-OH bands.

3.3.2. ATR-FTIR Results of Samples Irradiated by Low Dose Rate Gamma Source

Characteristic FT-IR bands of unsaturated polyester resin can be summarized as out-of-plane bending of C-H in aromatic ring at 705, 795 and 875 cm^{-1} , in-plane bending of C-H in aromatic ring at 1370 cm^{-1} , out-of-plane bending of =CH groups in polyester backbone at 740 cm^{-1} , in-plane bending of =CH groups in polyester backbone at 1070 cm^{-1} , out-of-plane bending of polyester double bonds (C=C) at 975 cm^{-1} , stretching of polyester single bonds (C-C) at 1040 cm^{-1} , stretching of C-O bonds at 1110 and at 1255 cm^{-1} , stretching of aromatic double bonds (C=C) at 1450 and at 1600 cm^{-1} , stretching of C=O in ester groups at 1720 cm^{-1} , and stretching of -CH in aromatic ring at 2850-2960 cm^{-1} region [Choi and Kertesz, 1997, Jurkin and Pucic, 2006, Atta et al., 2007, and Czayka et al. 2007].

Crosslinking reactions does not complete entirely because of restriction of free radical mechanism as mentioned in Section 1.1.1.4. Some of unreacted styrene monomer exists and it may polymerize during irradiation [Czayka et al. 2007]. Polystyrene also tends to crosslinking when it is exposed to ionizing radiation [Ivanov, 1992]. Band at 795 cm^{-1} could be characteristic for styrene monomer and bands at 1450, 1600 and 2940 cm^{-1} could be characteristic for polystyrene [Delahaye et al., 1998, Czayka et al. 2007].

Relatively weak FT-IR bands are observed in the region of 3000-3100 cm^{-1} for the structures containing aromatic groups [Bellamy, 1975] and these bands represent unsaturated =CH groups [Mayo et al., 2004]. If these groups become

saturated (such as saturation of vinyl units in styrene after formation of polystyrene or crosslinks), mentioned bands get weaker and new bands are observed just below 3000 cm^{-1} which represents saturated $-\text{CH}$ groups [Mayo et al., 2004]. In the study, even though there were very small shoulders around 3070 cm^{-1} , bands in the region of $3000\text{-}3100\text{ cm}^{-1}$ became almost invisible after curing, because of low concentration of styrene in polyester resin and of consumption of this styrene during curing. In addition, $=\text{CH}$ stretching region may be masked in some cases when intramolecular bonds get involved [Bellamy, 1975].

Figure 3.29 shows ATR-FTIR spectra of neat polyester resins non-irradiated and irradiated by low dose rate gamma source. When these spectra were compared, most significant changes can be seen at 795 cm^{-1} , at 975 cm^{-1} , at 1450 cm^{-1} and at 1720 cm^{-1} . According to the Beer-Lambert law, absorbance in a spectrum is directly proportional to the concentration of the sample [Stuart, 2004]. In other words, increase in intensity of a band means increase in concentration of the type of bond represented by the band. Bands at 795 cm^{-1} and 1450 cm^{-1} gives information about aromatic ring as mentioned above and these bands increased up to 138 kGy and then they started to decrease. These changes showed breakage of crosslinks between polyester molecules and formation of polystyrene from free styrene molecules which had not entered crosslinking reactions. Band at 1720 cm^{-1} shows carbonyl groups ($\text{C}=\text{O}$) in polyester and since this band is reduced up to 138 kGy, formation of free carbonyl groups and lower molecular weight esters could be occurred [Kijchavengkul et al., 2010]. Increasing and decreasing trend at the band of 975 cm^{-1} could be assumed as breakage of crosslinks and then reformation of them through the mechanism mentioned in Chapter 1. These trends were also compatible with results of mechanical tests since breakage of crosslinks gives material some elasticity. All these results could have a meaning of degradation of polyester resin by irradiation up to 138 kGy and then reformation of polymer network since crosslinks are formed through ester $\text{C}=\text{C}$ double bonds as shown in Figure 1.2.

Figure 3.30 gives ATR-FTIR spectra of samples reinforced by 5% of boron mineral and irradiated by 245 kGy absorbed dose. Band of aromatic ring at 795 cm^{-1} , and at 1450 cm^{-1} were relatively lower when compared with neat polyester resin. Bands of carbonyl groups at 1720 cm^{-1} were slightly higher after reinforcement of

polyester resin by boron minerals. These showed that formation of free styrene and chain scission of polyester as a result of degradation were partially blocked and boron minerals had positive effect on shielding against gamma radiation. Lowest polystyrene band (at 1450 cm^{-1}) and lowest ester C=C band (at 975 cm^{-1}) were observed for PCAT5 and since it had the highest Young's modulus among these samples, this result was reasonable.

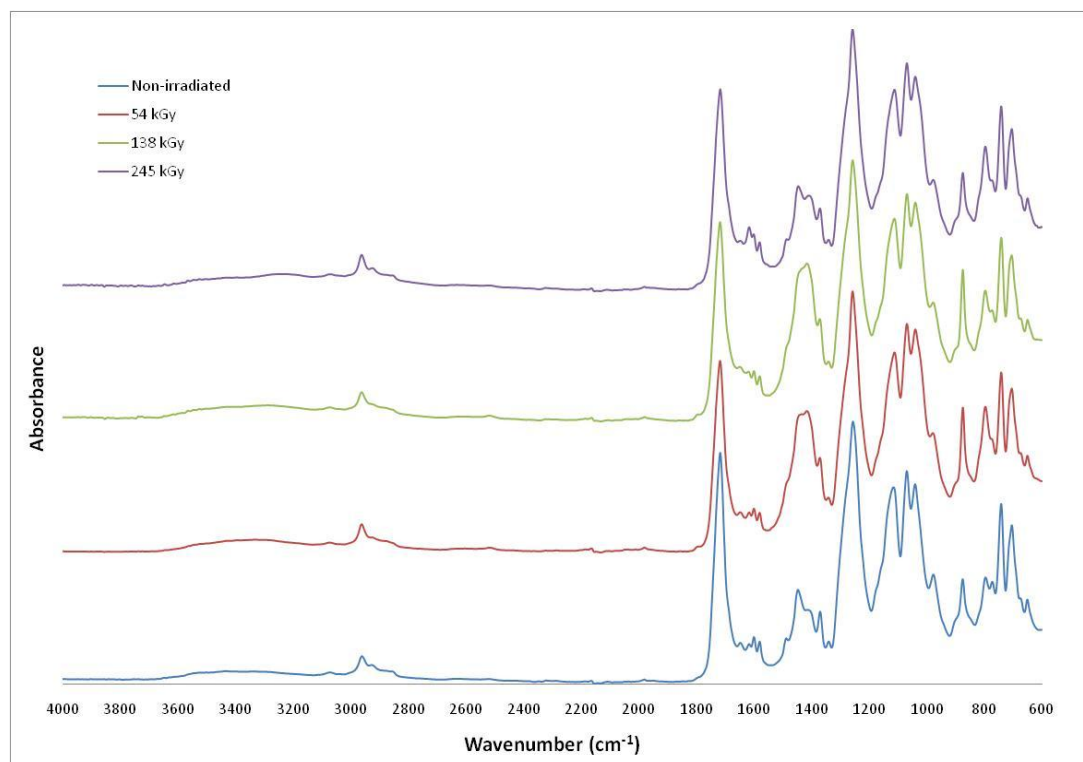


Figure 3.29: ATR-FTIR Spectra of POL Irradiated by Low Dose Rate Gamma Source

Figure 3.31 shows ATR-FTIR spectra of polyester resin reinforced with 2%, 5% and 10% of anhydrous borax and irradiated by 245 kGy to investigate the effect of amount of reinforcing filler in polyester resin. Significant decrease at 1450 cm^{-1} for reinforced samples when compared with neat polyester resin showed lower polystyrene formation. But PANB10 had higher intensity at 1450 cm^{-1} when compared with PANB2 and PANB5. It also had higher band for ester C=C double bonds at 975 cm^{-1} . Since crosslinks are formed through these bonds as shown in Section 1.1.1.4, this could be a sign of prevention of formation of crosslinks with higher amount of filler. Higher bands of carbonyl groups at 1720 cm^{-1} for PANB samples showed that composites became more resistant to degradation by irradiation.

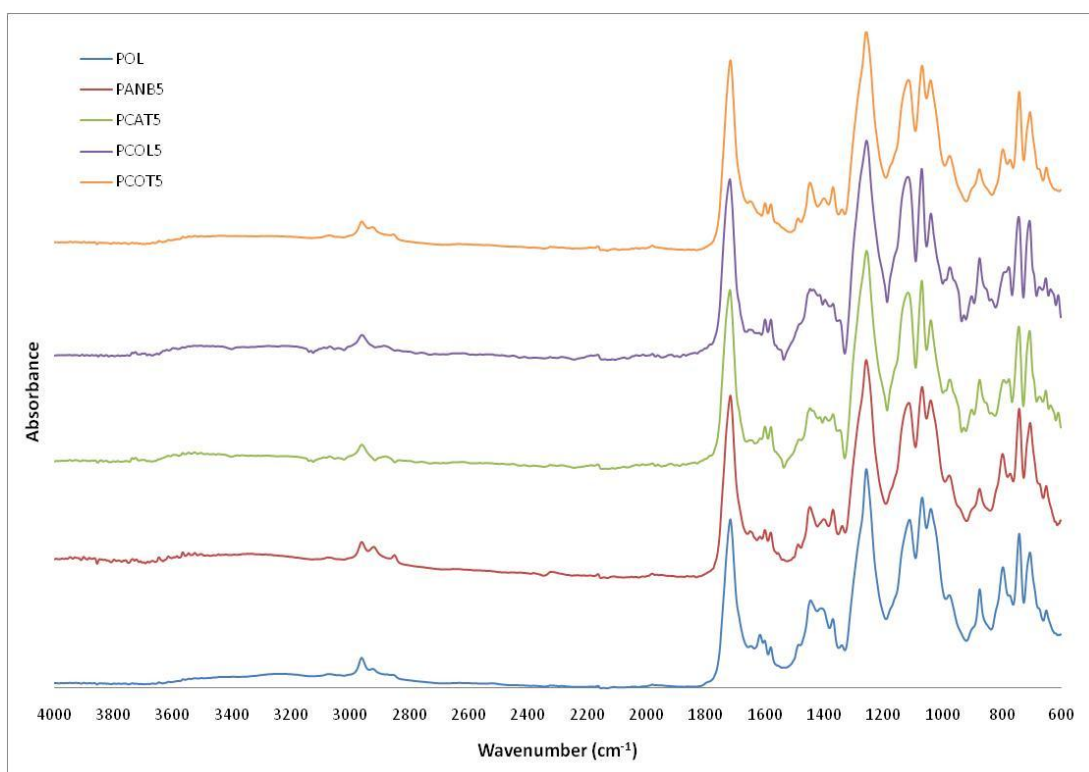


Figure 3.30: ATR-FTIR Spectra of Reinforced Samples Irradiated by Low Dose Rate Gamma Source

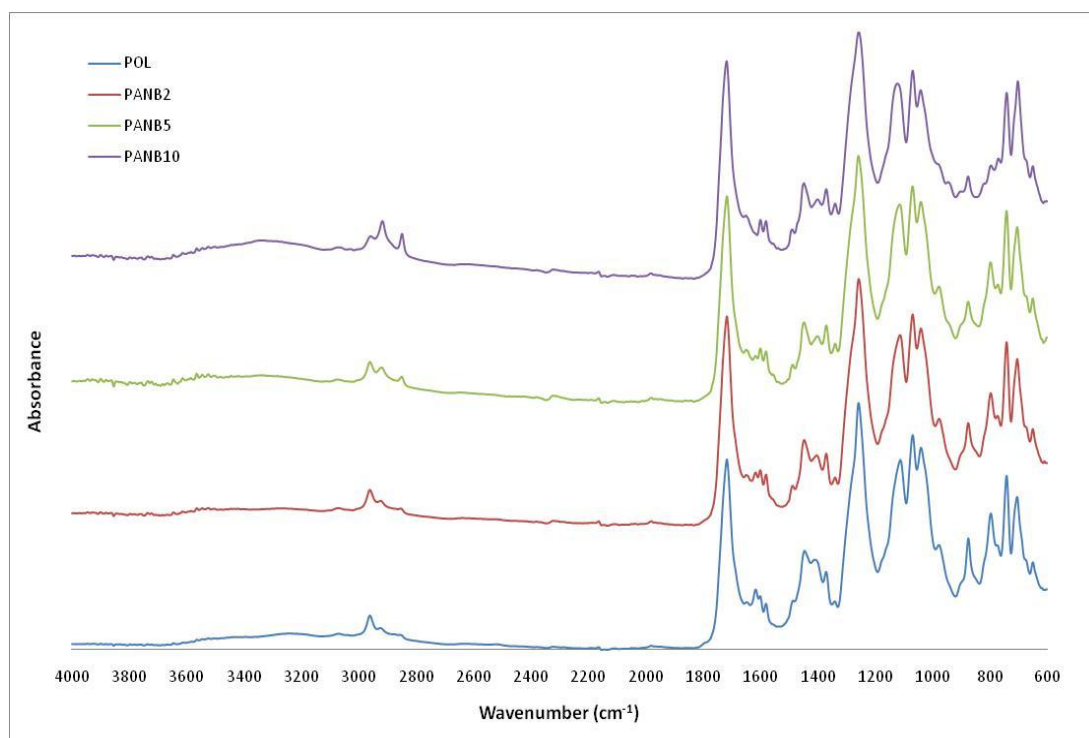


Figure 3.31: ATR-FTIR Spectra of PANB with Different Compositions Irradiated by Low Dose Rate Gamma Source

3.3.3. ATR-FTIR Results of Samples Irradiated by High Dose Rate Gamma Source Open to Atmosphere

Changes in the bands at 795 cm^{-1} , 975 cm^{-1} , 1370 cm^{-1} , at 1450 cm^{-1} and in the region of $2850\text{-}2960\text{ cm}^{-1}$ during irradiation of neat polyester resin by high dose rate gamma source can be seen from Figure 3.32. When absorbed dose was reached to 500 kGy , bands at 795 cm^{-1} (styrene), 975 cm^{-1} (ester C=C double bonds), and at 1450 cm^{-1} (polystyrene) decreased and this could be a sign of decomposition of polystyrene which may be formed during curing and formation of some crosslinks due to decrease in ester C=C double bonds. But after that point, there were sharp increases of bands representing polystyrene and ester double bonds when absorbed dose was reached to 2500 kGy . These results were probably led by destruction of polymer network. Mechanical test results confirmed these results. There are also additional bands in the region of $3500\text{-}4000\text{ cm}^{-1}$ after 1000 kGy irradiation as can be seen from the figure and these bands indicate formation of -OH groups. This can be interpreted as the oxidizing reactions and the formation of alcohol and carboxylic acid groups.

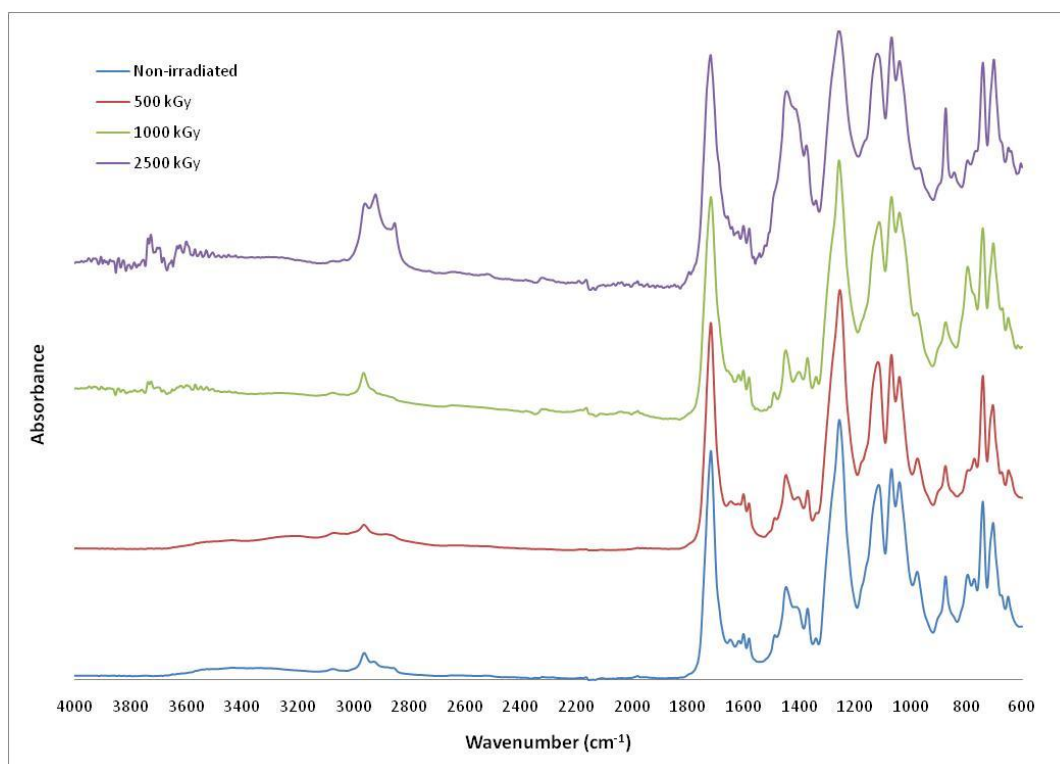


Figure 3.32: ATR-FTIR Spectra of POL Irradiated by High Dose Rate Gamma Source Open to Atmosphere

Figure 3.33 shows shielding effect of boron minerals on polyester resin after high dose rate irradiation. Intensities of polystyrene bands at 1450 cm^{-1} and in the region of $2850\text{-}2960\text{ cm}^{-1}$ were relatively lower when compared with neat polyester resin and this showed lower polystyrene formation. Bands of aromatic ring at 875 cm^{-1} , 1370 cm^{-1} , and in the region of $3500\text{-}4000\text{ cm}^{-1}$ were also lower than those of neat polyester resin. This was probably because of prevention of degradation and oxidizing reactions by boron minerals.

Effect of reinforcing filler ratio at high doses can be seen on Figure 3.34. Higher band at 975 cm^{-1} (ester C=C) for PANB samples indicated lower crosslink density. On the other hand, lower bands at 1450 cm^{-1} and in the region of $2850\text{-}2960\text{ cm}^{-1}$ were due to prevention of formation of polystyrene. Band of -OH groups in the region of $3500\text{-}4000\text{ cm}^{-1}$ was also lower for reinforced polyester resin. Polyester resin reinforced with 2% of anhydrous borax showed more resistance against radiation. Since the presence of filler could prevent crosslinking reactions, composite materials reinforced with higher ratio could be degraded heavier by irradiation.

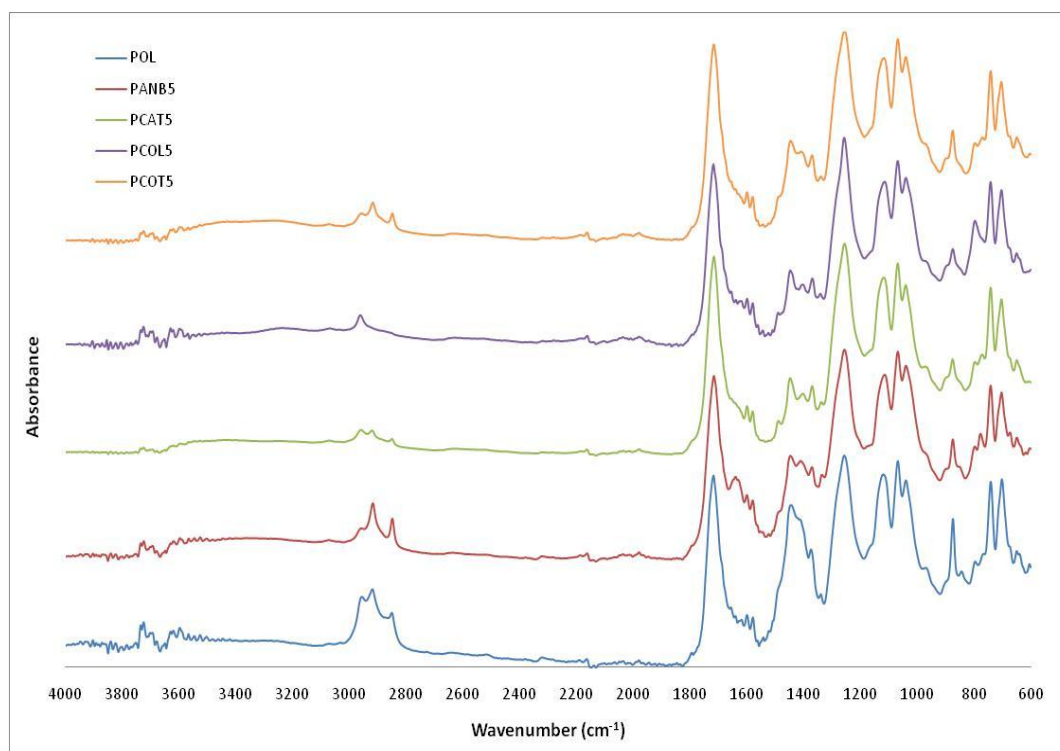


Figure 3.33: ATR-FTIR Spectra of Reinforced Samples Irradiated by High Dose Rate Gamma Source Open to Atmosphere

3.3.4. ATR-FTIR Results of Samples Irradiated by High Dose Rate Gamma Source under Vacuum

Effect of high doses on neat polyester resin under vacuum is shown in Figure 3.35. Most significant changes were observed in the bands at 975 cm^{-1} , 1040 cm^{-1} , 1070 cm^{-1} , 1450 cm^{-1} , and at 1600 cm^{-1} . 1450 cm^{-1} and 1600 cm^{-1} bands are particular to polystyrene and these bands had periodical behavior with increase in absorbed dose. Intensities of these bands increased when the samples were irradiated up to 500 kGy. At 1000 kGy, they decreased and then they increased again. These results showed formation and decomposition of polystyrene during irradiation periodically and this behavior was compatible with mechanical test results. Increase in ester C=C double bonds at 975 cm^{-1} , decrease in C-C single bonds at 1040 cm^{-1} and increase in =CH units at 1070 cm^{-1} at the end of irradiation process could be assumed as the proof of destruction of network structure.

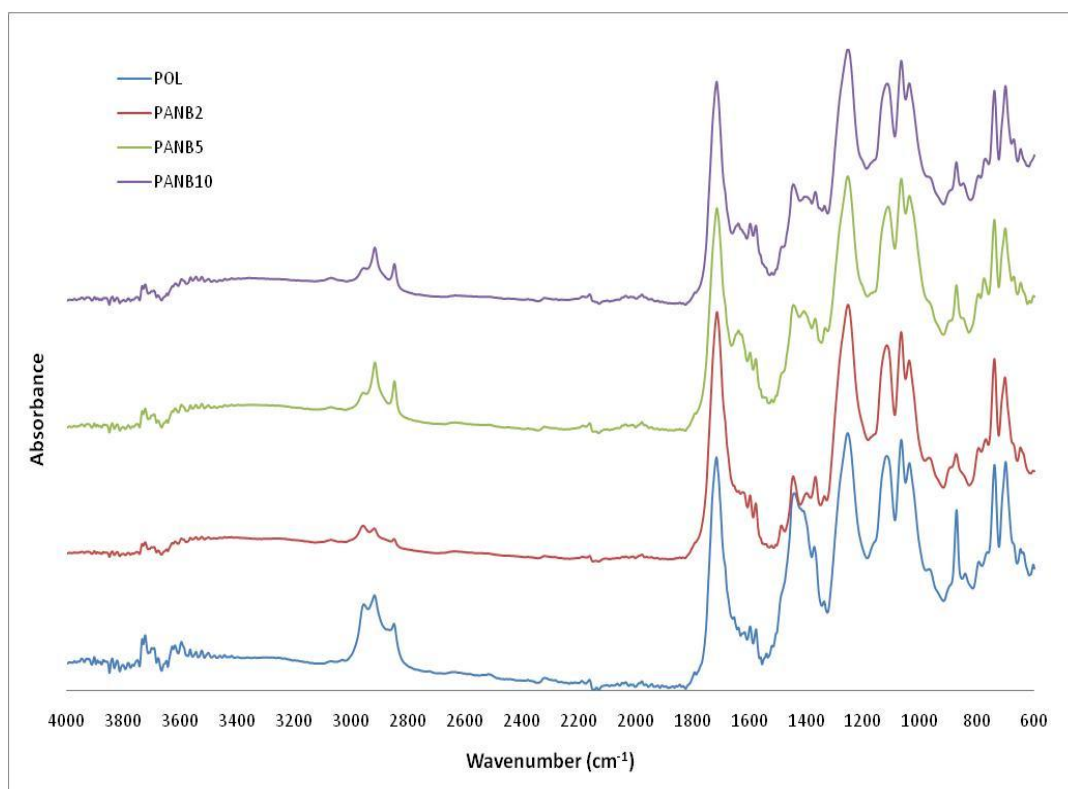


Figure 3.34: ATR-FTIR Spectra of PANB with Different Compositions Irradiated by High Dose Rate Gamma Source Open to Atmosphere

When FT-IR spectra given in Figure 3.36 were investigated, it can be said that bands which represent polystyrene at 1450 cm^{-1} and in the region of $2850\text{-}2960\text{ cm}^{-1}$ were increased for all reinforced samples except PCAT5 after irradiation by high dose rate gamma source under vacuum. These bands were lower for PCAT5 when compared with neat polyester resin. Carbonyl group ($\text{C}=\text{O}$) band at 1720 cm^{-1} was lower for all reinforced samples. Higher bands at 1040 cm^{-1} (ester $\text{C}-\text{C}$) and lower bands at 975 cm^{-1} (ester $\text{C}=\text{C}$) showed that reinforcement with boron minerals made polyester chains more resistant against irradiation.

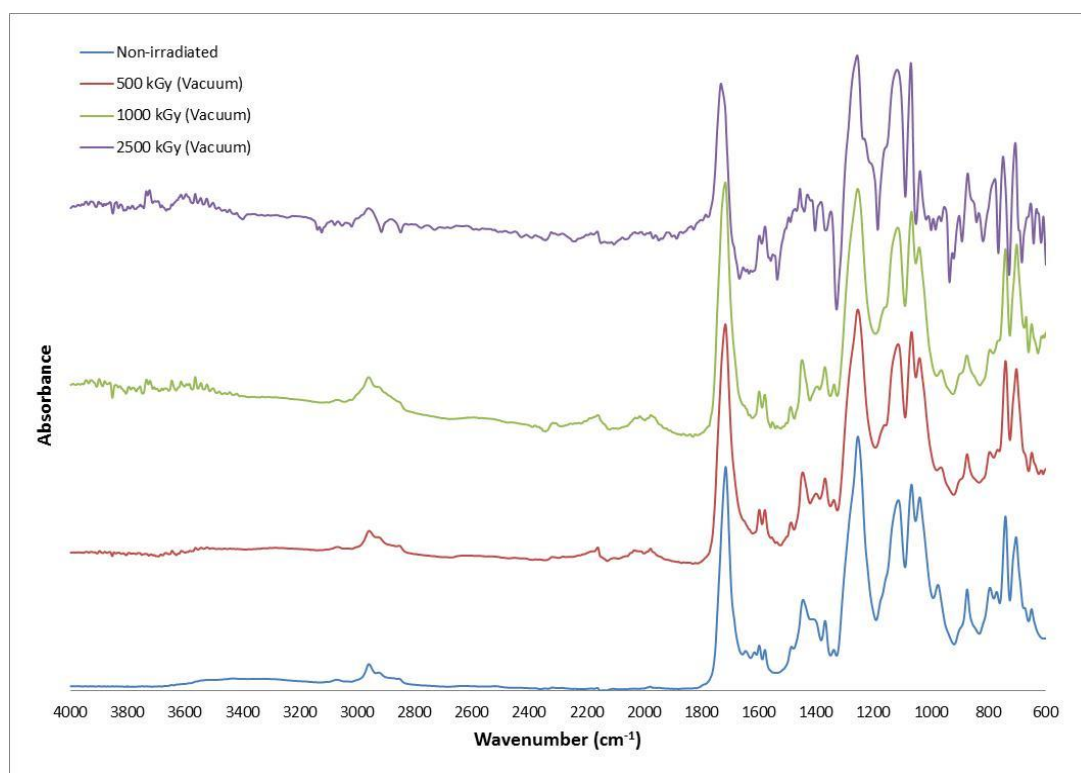


Figure 3.35: ATR-FTIR Spectra of POL Irradiated by High Dose Rate Gamma Source under Vacuum

Effect of filler concentration on FT-IR spectra was given in Figure 3.37. Highest styrene band at 795 cm^{-1} and lowest polystyrene band at 1450 cm^{-1} was observed for PANB5. This could be explanation of better mechanical properties than PANB2 and PANB10 for irradiation under vacuum with absorbed dose of 2500 kGy. Highest ester double bonds at 975 cm^{-1} of PANB10 showed decreasing crosslink concentration with high reinforcing filler ratio. Lowest 1720 cm^{-1} band of PANB10 also indicated formation of free carbonyl groups and lower molecular weight esters.

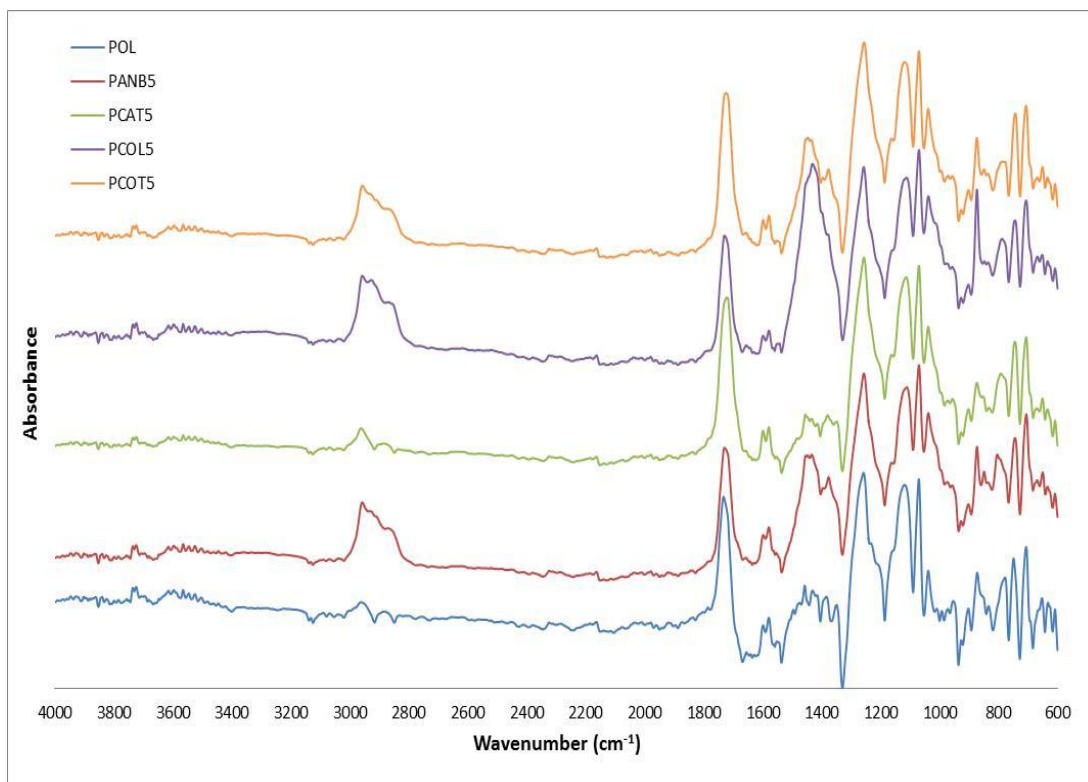


Figure 3.36: ATR-FTIR Spectra of Reinforced Samples Irradiated by High Dose Rate Gamma Source under Vacuum

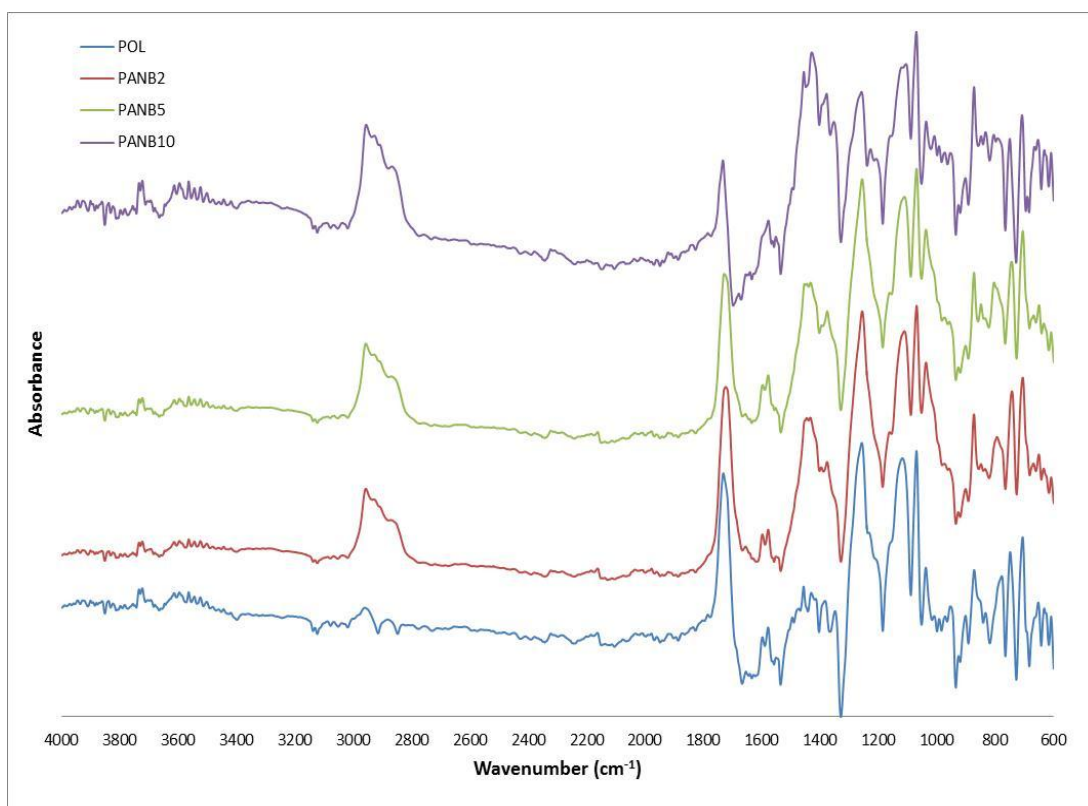


Figure 3.37: ATR-FTIR Spectra of PANB with Different Compositions Irradiated by High Dose Rate Gamma Source under Vacuum

3.4. Dynamic Mechanical Analysis

Viscoelastic behavior of materials can be observed by dynamic mechanical analysis (DMA). Glass transition temperature (T_g), which is very important parameter for polymeric materials, can also be determined by this technique. Loss factor ($\tan\delta$) vs. temperature graphs of neat and reinforced polyester resin samples non-irradiated and irradiated by gamma source are given in Figures 3.38 to 3.40.

3.4.1. DMA Results of Neat Polyester Resin Samples Non-irradiated and Irradiated

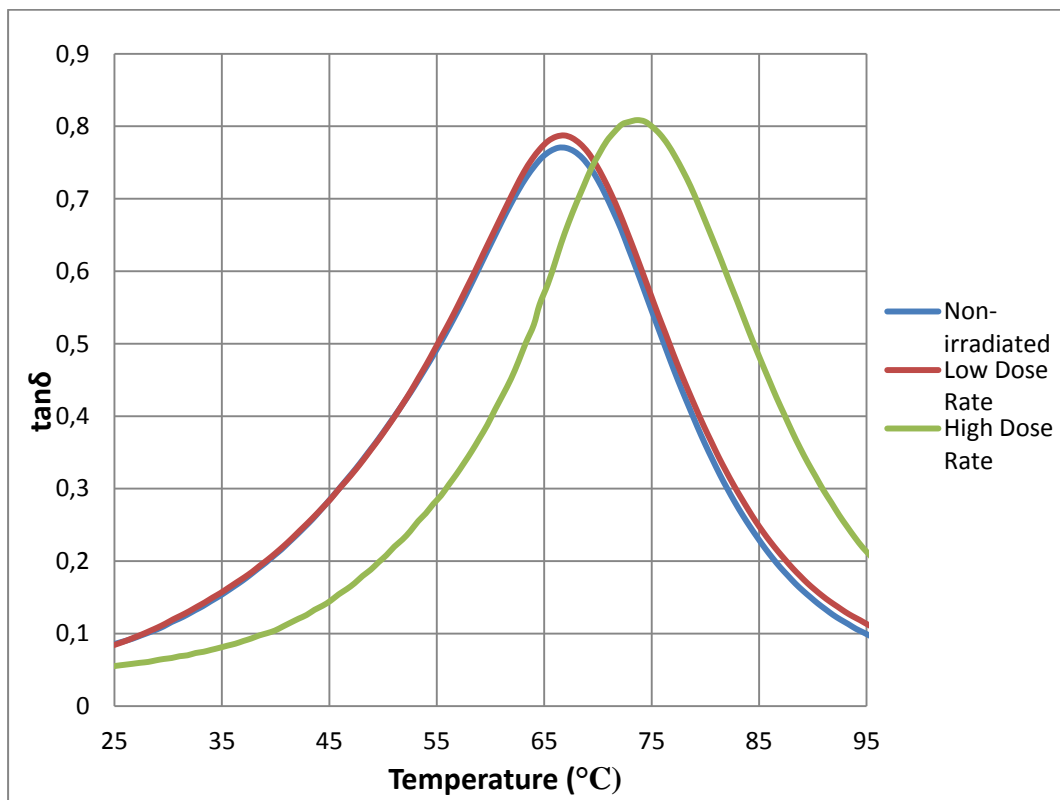


Figure 3.38: $\tan\delta$ Curves of Neat Polyester Resin Samples Non-irradiated and Irradiated

$\tan\delta$ curves of neat polyester resin samples non-irradiated, irradiated by low dose rate gamma source with absorbed dose of 245 kGy, and irradiated by high dose rate gamma source with absorbed dose of 2500 kGy were given in Figure 3.38. In this graph, peak gives T_g of the sample and according to this graph, T_g of samples

non-irradiated and irradiated by low dose rate gamma source were almost the same (66.3 °C and 67.0 °C, respectively). On the other hand, for the neat polyester resin irradiated by high dose rate gamma source, loss factor curve was shifted and T_g of the sample was increased to 74.3 °C. When Figure 3.29 and Figure 3.32 were investigated, it can be seen that polystyrene formation was much higher at high doses. Since polystyrene is a brittle material with higher T_g (about 100 °C) than that of unsaturated polyester, the increase with increase in polystyrene concentration [Hanemann et al., 2010] as shown in Figure 3.38 was an expected result.

In addition, loss factor curve gives information about crosslinking density. Height of peak is inversely proportional to crosslinking density [Sepe, 1997]. Increase in peak height of loss factor curve with increase in dose rate of irradiation showed that irradiation caused chain scission and polyester resin degraded.

3.4.2. DMA Results of Polyester Resin Reinforced with Different Boron Minerals

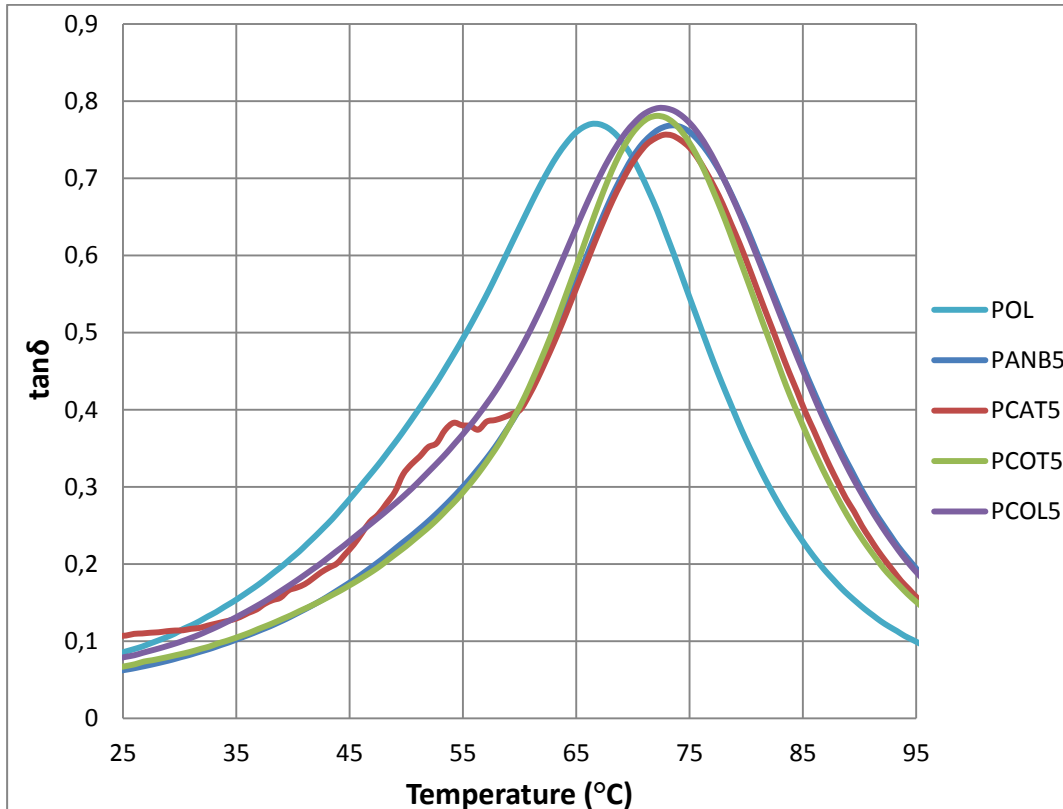


Figure 3.39: $\tan\delta$ Curves of Polyester Resin Reinforced with Different Boron Minerals

Loss factor vs. temperature graphs of non-irradiated polyester resin samples reinforced with 5% of boron minerals can be seen on Figure 3.39. All boron minerals gave an increase on glass transition temperature of composites. Boron minerals have highly crystalline structure and they are rigid materials. Since mobility of the chains near filler particles is reduced, these results could be presumable and higher moduli of reinforced samples than that of neat polyester resin as mentioned in Section 3.2.1 were favorable. T_g 's of PANB5, PCAT5, PCOT5 and of PCOL5 can be listed as 73.7 °C, 72.7 °C, 72.1 °C, and 72.3 °C, respectively.

When PCAT5, PCOL5 and PCOT5 had almost the same T_g , PANB5 had slightly higher T_g when compared with the rest. This could be related to lack of water in the structure of anhydrous borax. Presence of water can give some defects to the composite material.

3.4.3. DMA Results of Polyester Resin Reinforced with Different Compositions

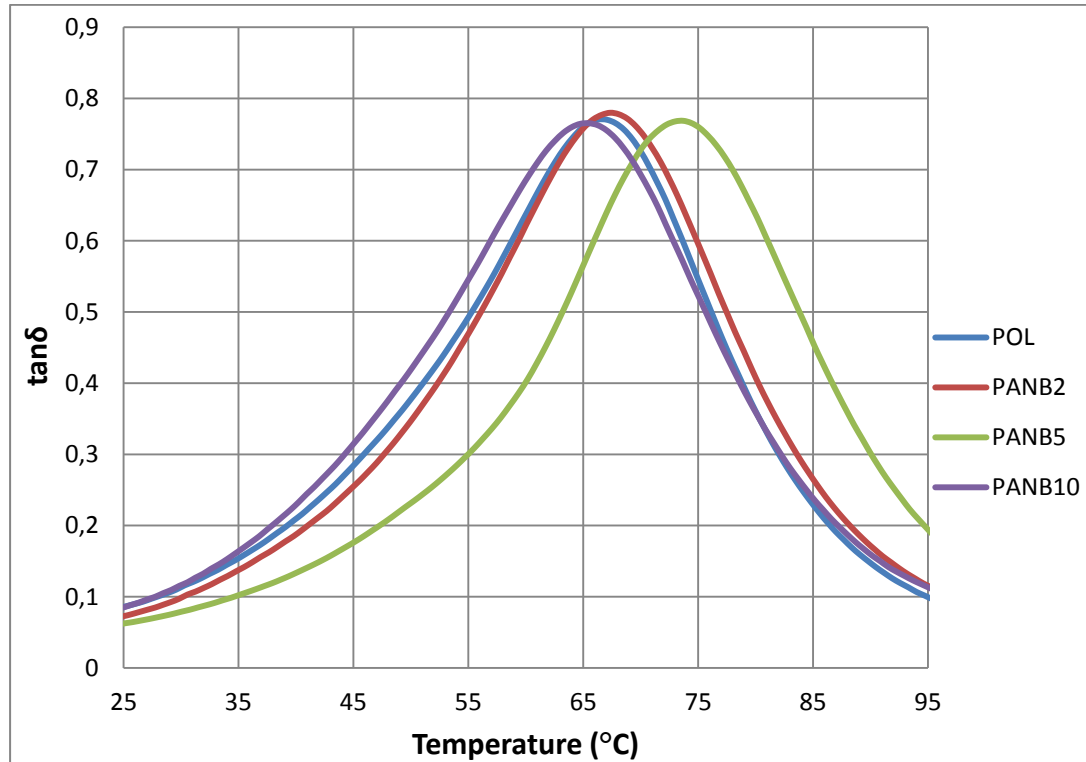


Figure 3.40: $\tan\delta$ Curves of Polyester Resin Reinforced with Anhydrous Borax in Different Compositions

Non-irradiated PANB samples with different compositions were analyzed by DMA technique to investigate effect of boron mineral composition on glass transition temperature of polyester resin and the results can be seen on Figure 3.40. After addition of 2% of anhydrous borax into polyester resin, T_g was increased slightly from 66.3 °C to 67.3 °C. When anhydrous borax composition was increased to 5%, there was a significant increase of T_g to 73.7 °C. But when the filler ratio was 10%, T_g of composite was decreased to 65.4 °C. These results can be explained as prevention of formation of crosslinks with increase in amount of reinforcing filler and this situation caused T_g of composite material to shift to lower temperatures. Comparable results were also observed in tensile tests and ATR-FTIR spectra.

3.5. Thermogravimetric Analysis

Thermogravimetric analysis (TGA) is a thermal analysis technique which gives information about chemical and physical properties of a material, such as phase transitions or thermal degradation, as a function of temperature. TGA thermograms of boron minerals and of neat and reinforced polyester resin samples which were non-irradiated and irradiated by gamma source are mentioned in this section.

3.5.1. TGA Results of Boron Minerals

Thermograms of boron minerals used in this study can be seen in Figure 3.41. Anhydrous borax was thermally stable during analysis up to 900 °C. A slight weight loss after 110 °C was probably due to moisture. Calcined tincal had sudden weight loss starting around 100 °C and after 150 °C, its weight was decreased with almost constant ratio up to 600-650 °C. It has lost 20% of its initial weight. Since theoretical water and OH⁻ content of calcined tincal is 15% by weight, moisture could contribute this extra weight loss. Concentrated tincal started to lose its weight at 75 °C and it was due to loss of lattice water in its structure. Concentrated tincal lost 41.5% of its initial weight and this showed that it could keep some OH⁻ groups since it had theoretical water and OH⁻ content of 47.2% by weight.

TGA thermogram of colemanite was quite different when compared with those of tincal samples. It was almost thermally stable up to 390 °C and it started to lose its

weight after this temperature. This result showed that its polymeric structure gives colemanite some extra stability. Its weight was decreased to 62.3% of its initial value and it lost water more than its theoretical water and OH⁻ content which is 21.9% by weight. Since colemanite sample had some moisture and impurities, this result is reasonable.

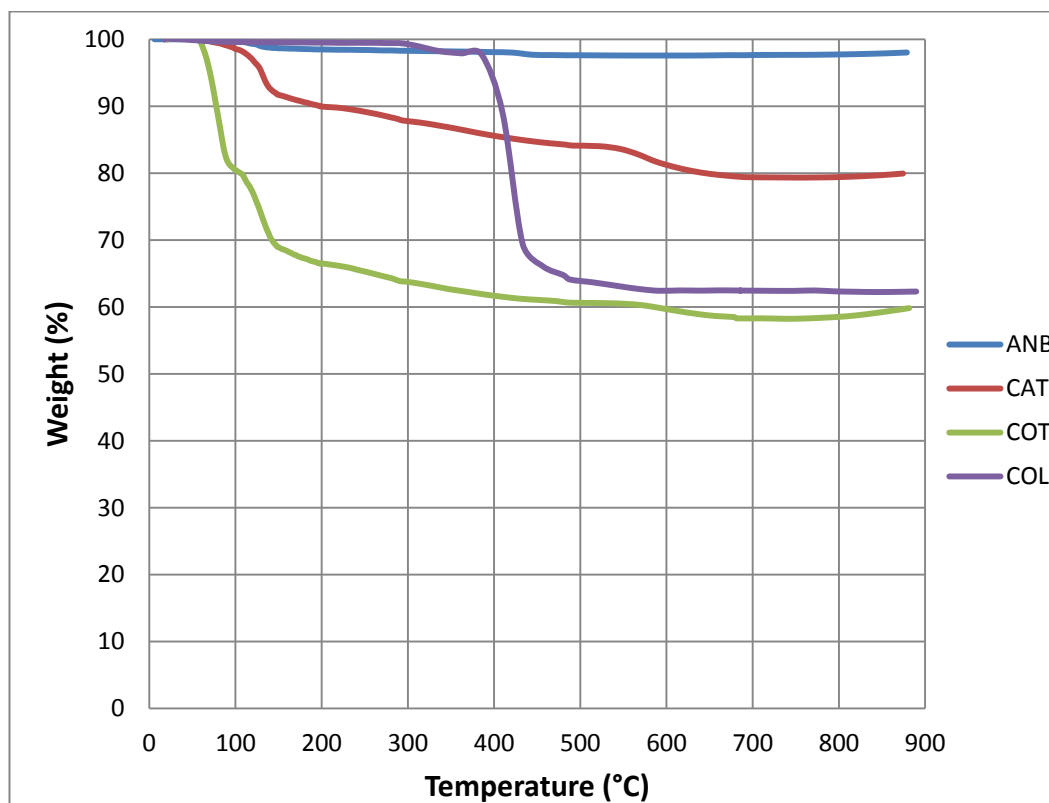


Figure 3.41: TGA Thermograms of Boron Minerals

Significant weight increase observed especially on COT and CAT samples at high temperatures and that could be attributed to buoyancy effect of gas flow in thermogravimetric analyzer. This effect could be explained as increasing force of the inert gas making an impact on crucibles with increasing velocity of gas flow at high temperatures.

3.5.2. TGA Results of Neat Polyester Resin Samples Non-irradiated and Irradiated

As seen from Figure 3.42, TGA thermograms of neat polyester resin samples non-irradiated, irradiated by low dose rate gamma source with absorbed dose of 245

kGy, and irradiated by high dose rate gamma source with absorbed dose of 2500 kGy in air and under vacuum were almost identical. Each sample showed similar thermal degradation behavior.

Thermogravimetric data can also be represented by derivative thermogravimetry (DTG) curve, which shows rate of mass loss with respect to time or temperature. Peaks on these curves show great thermal events.

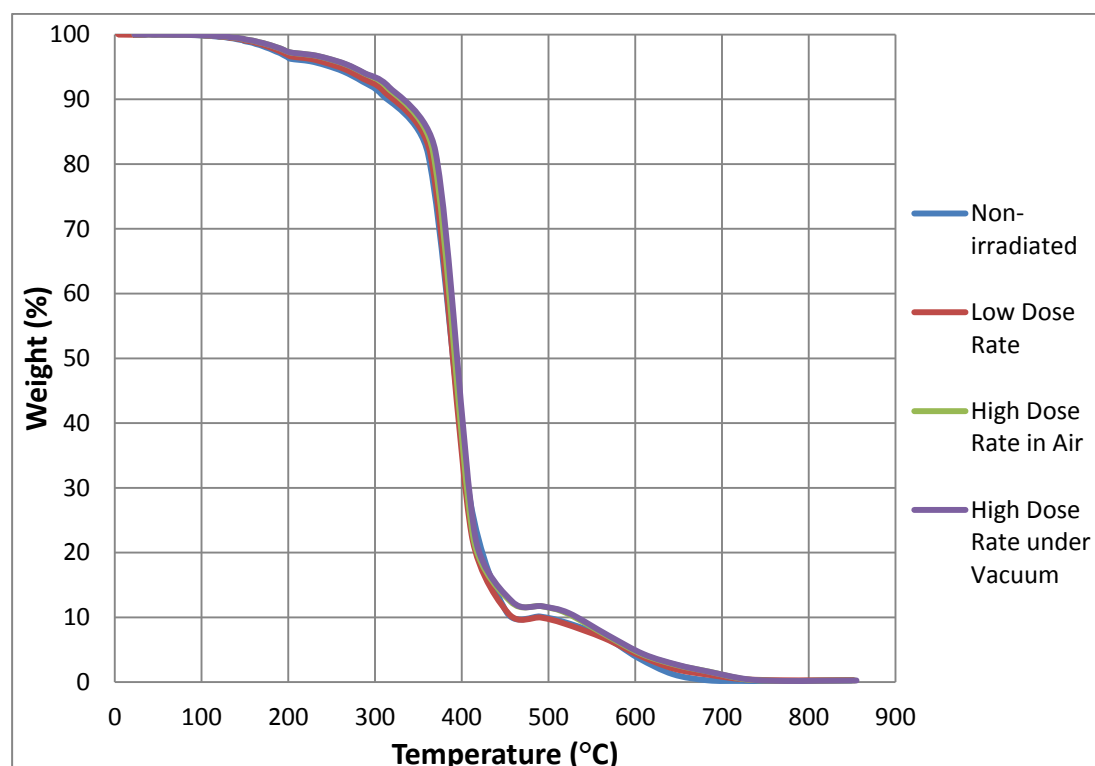


Figure 3.42: TGA Thermograms of Neat Polyester Resin Samples Non-irradiated and Irradiated

DTG curves of neat polyester resin samples were given in Figure 3.43 and these peaks were also identical with respect to irradiation process. There were 3 peaks in this figure. First peak was observed in 100-220 °C interval. Second peak gave its highest point at 410 °C while third peak was in between 500-720 °C. First peak showed water loss by dehydration. Main degradation was observed around 410 °C and chain scission of polyester chains, which leads to formation of its primary units, was occurred at this temperature. Final step of thermal degradation was after 500 °C and in this step, carbonaceous char formed in previous step was also

degraded. There was almost none of final residue after 700 °C. Irradiation procedure seemed not to have any significant effect on thermal stability of polyester resin.

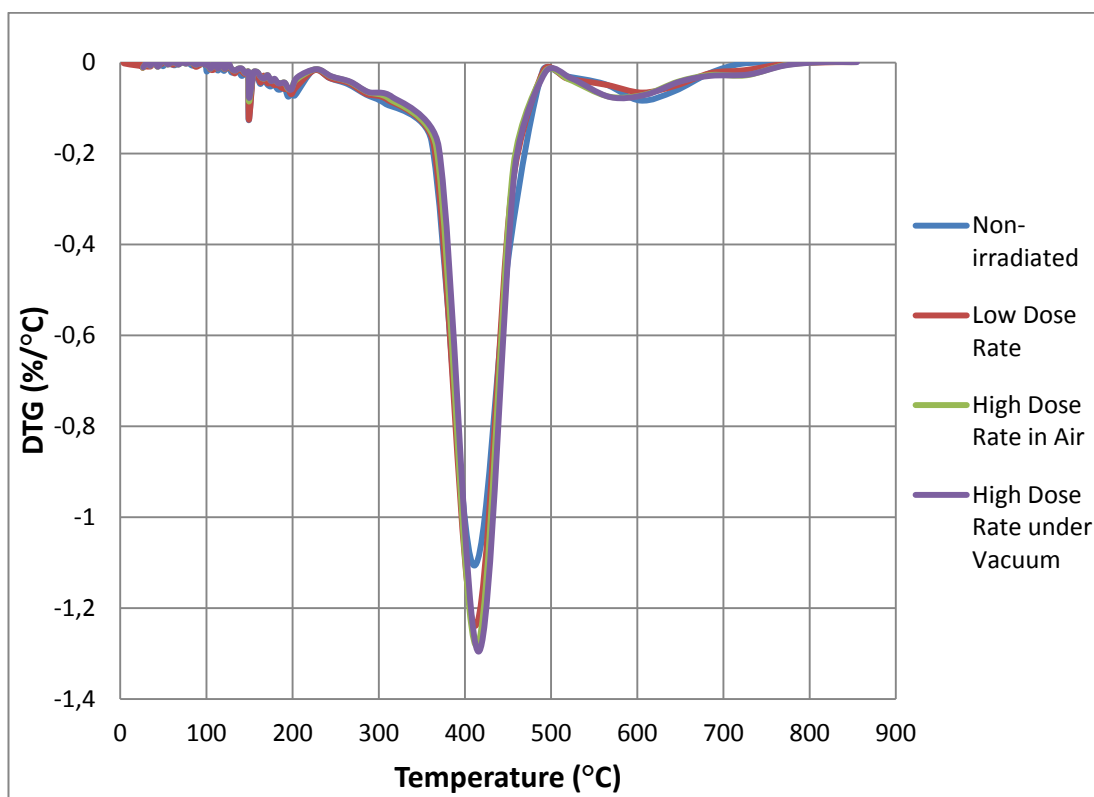


Figure 3.43: DTG Curves of Neat Polyester Resin Samples Non-irradiated and Irradiated

3.5.3. TGA Results of Polyester Resin Reinforced with Different Boron Minerals

TGA results of non-irradiated neat polyester resin and polyester resin reinforced with 5% of boron minerals were given in Figure 3.44. TGA curves of reinforced samples were identical during main degradation step. There was only 10-20 °C increase in main degradation temperature when compared with neat polyester resin. It can be said that thermal stability was not changed significantly with respect to boron minerals. This situation was attributed to lack of chemical bonding between polyester chains and boron minerals.

After degradation of polyester chains occurred, neat polyester resin went to complete decomposition and there was not char residue observed. But reinforced

samples had some yield and amount of this yield was proportional to boron content of reinforcing fillers.

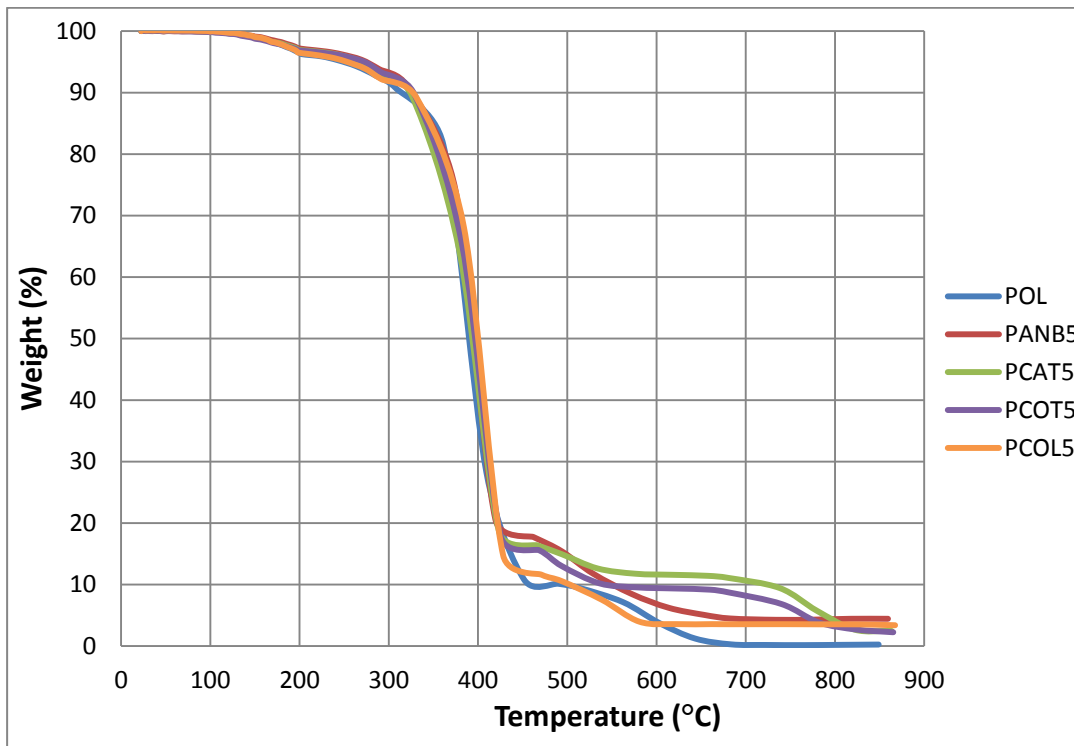


Figure 3.44: TGA Thermograms of Non-irradiated Polyester Resin Samples Reinforced with 5 % of Boron Minerals

3.5.4. TGA Results of Polyester Resin Reinforced with Different Compositions

Effect of anhydrous borax concentration on thermal stability of non-irradiated and reinforced polyester resin can be seen in Figure 3.45 and in Figure 3.46. Thermal degradation trends of composite samples mentioned in Figure 3.45 were quite similar since there was not any significant chemical bondage between filler and polymer matrix. Char residue of samples were proportional to the reinforcing filler ratio of composite materials.

Figure 3.46 shows that reinforcement gave composite materials some retardation before the initiation of chain scission of polyester chains. But once it started, decomposition of composite material underwent faster and it completed in slightly lower temperatures. This result was probably due to improved and effective heat transfer to the polyester matrix through the dispersed inorganic phase.

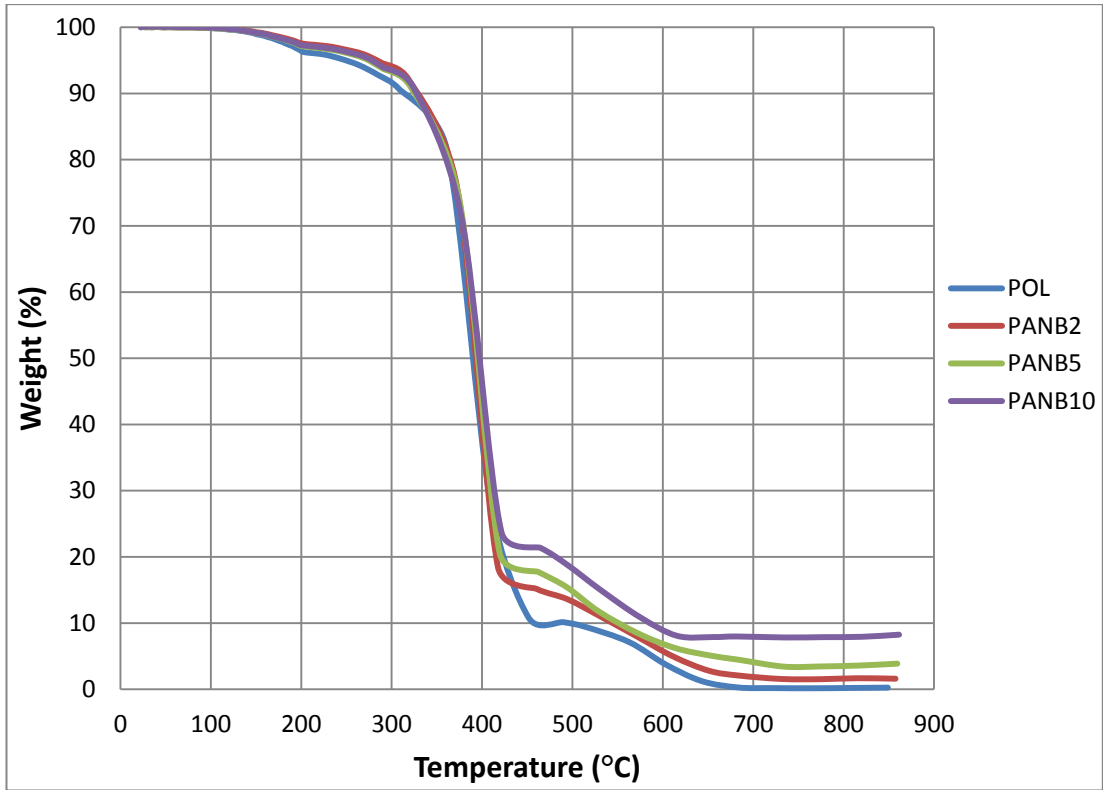


Figure 3.45: TGA Thermograms of Polyester Resin Reinforced with Anhydrous Borax in Different Compositions

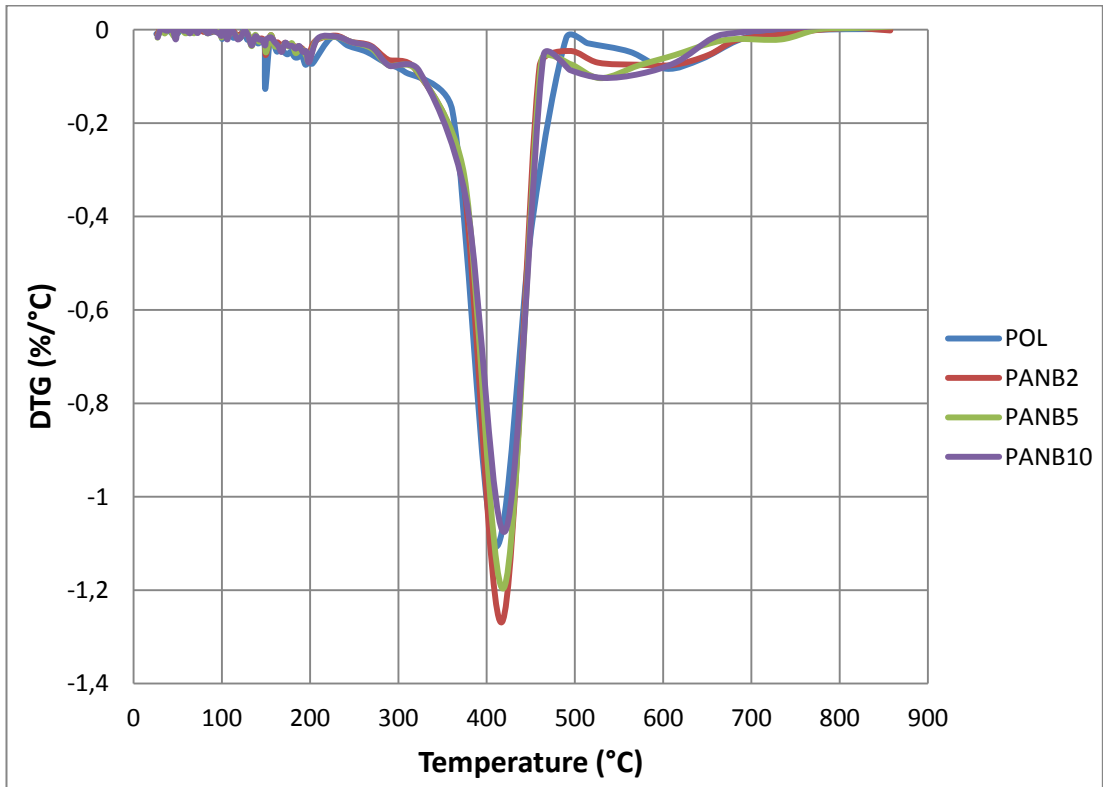


Figure 3.46: DTG Curves of Polyester Resin Reinforced with Anhydrous Borax in Different Compositions

3.6. Scanning Electron Microscopy Study

Scanning Electron Microscopy (SEM) technique gives information about surface properties of the sample and it is used in various applications such as fractured surfaces, surface toughness, networks or adhesive failures [Stuart, 2002]. SEM micrographs of neat and reinforced polyester resin samples non-irradiated and irradiated by gamma source are given below.

Figure 3.47 shows outer surface of neat polyester resin before irradiation. Surface of the sample was quite smooth and there was not any roughness or fracture on it. On the other hand, some facial changes occurred after it was irradiated with low dose rate gamma source up to absorbed dose of 54 kGy. Formation of some micro cracks on the surface can be seen in Figure 3.48. Gamma radiation caused radical formation and by this way, the network structure was damaged.

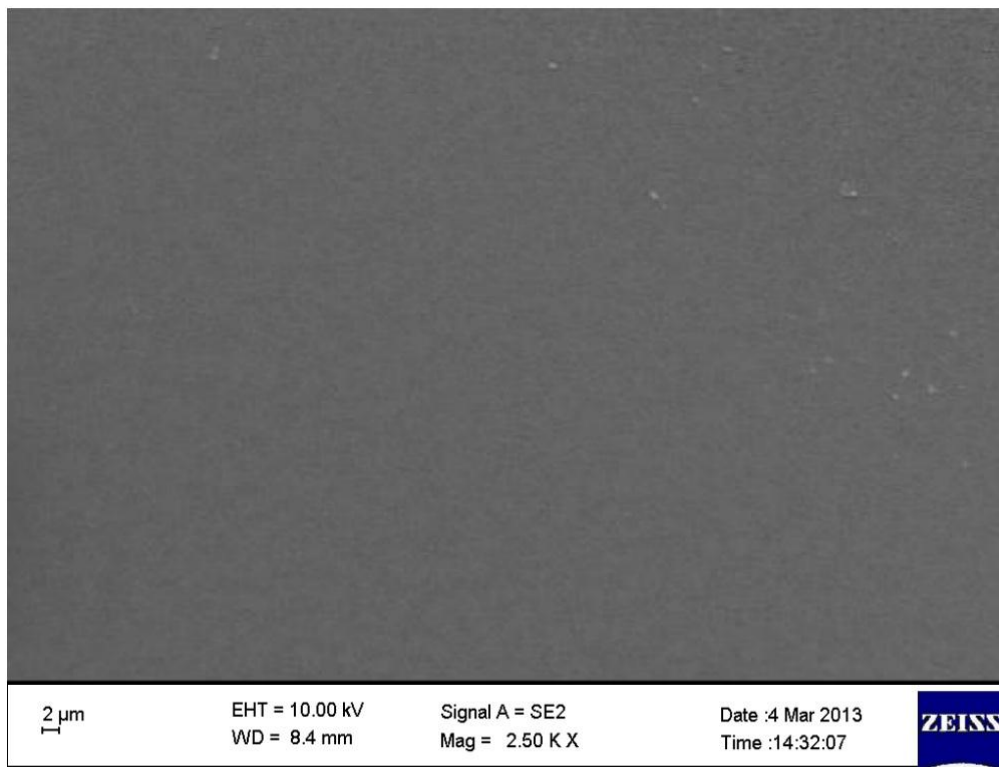


Figure 3.47: SEM Micrograph of Non-irradiated Neat Polyester Resin

SEM micrograph of non-irradiated PCOT5 sample was given in Figure 3.49. There was some extrusion of boron minerals out of polyester resin surface and boron

mineral clusters could be recognized. Relatively evenly distribution of reinforcing fillers was observed. Surface of PCOT5 was rougher when compared with the surface of neat polyester resin. This could be due to higher viscosity and prevention of polyester chains to move freely by boron minerals presented before curing was concluded.

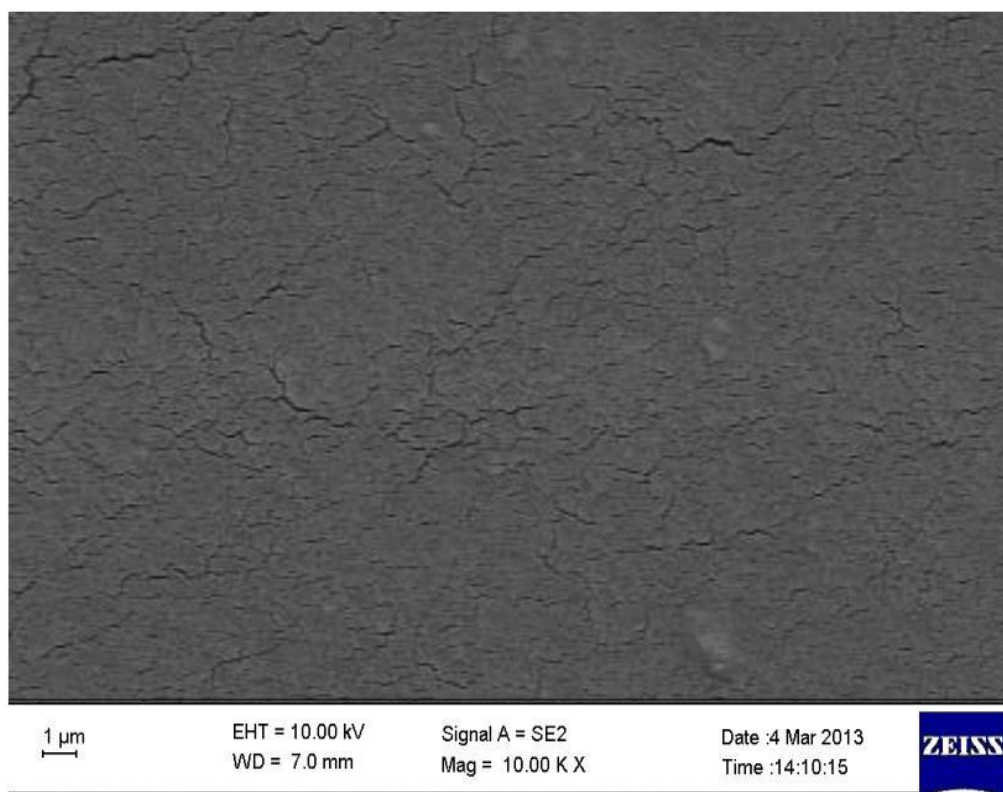


Figure 3.48: SEM Micrograph of Neat Polyester Resin Irradiated by Low Dose Rate Gamma Source with Absorbed Dose of 54 kGy

After irradiation of PCOT5 sample with low dose rate gamma source, micro cracks were also formed. But these micro cracks were intense around tincal clusters as can be seen from Figure 3.50. Lack of adhesion between polymer matrix and fillers may cause formation of these weak zones.

Wavy appearance of surface of reinforced sample was also observed for PCOT10 sample as given in Figure 3.51. But the surface seemed to become rougher with increasing reinforcing filler ratio. The higher the filler ratio, the higher the viscosity and the rougher the composite surface.

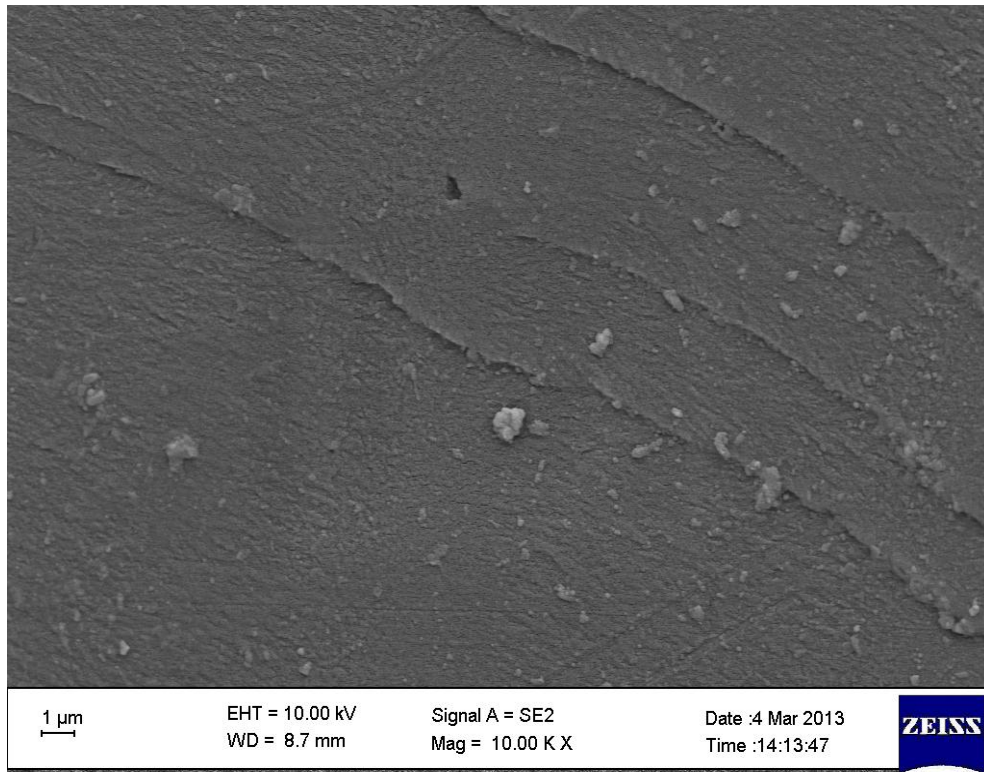


Figure 3.49: SEM Micrograph of Non-irradiated PCOT5

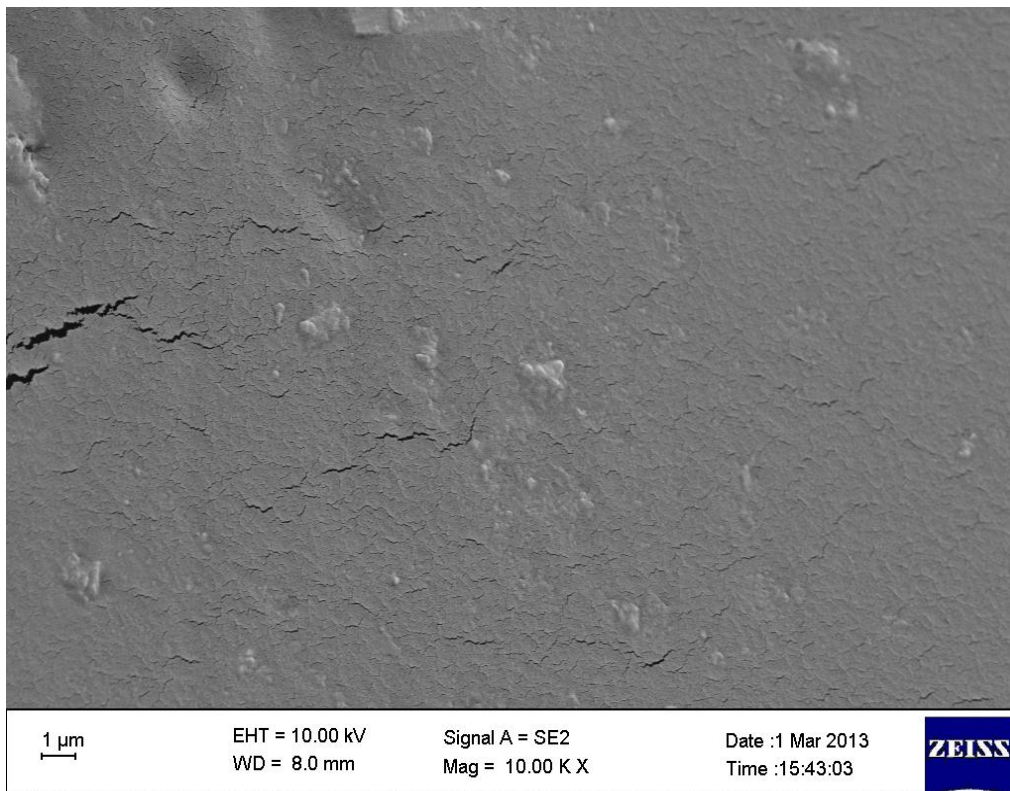


Figure 3.50: SEM Micrograph of PCOT5 Irradiated by Low Dose Rate Gamma Source with Absorbed Dose of 54 kGy

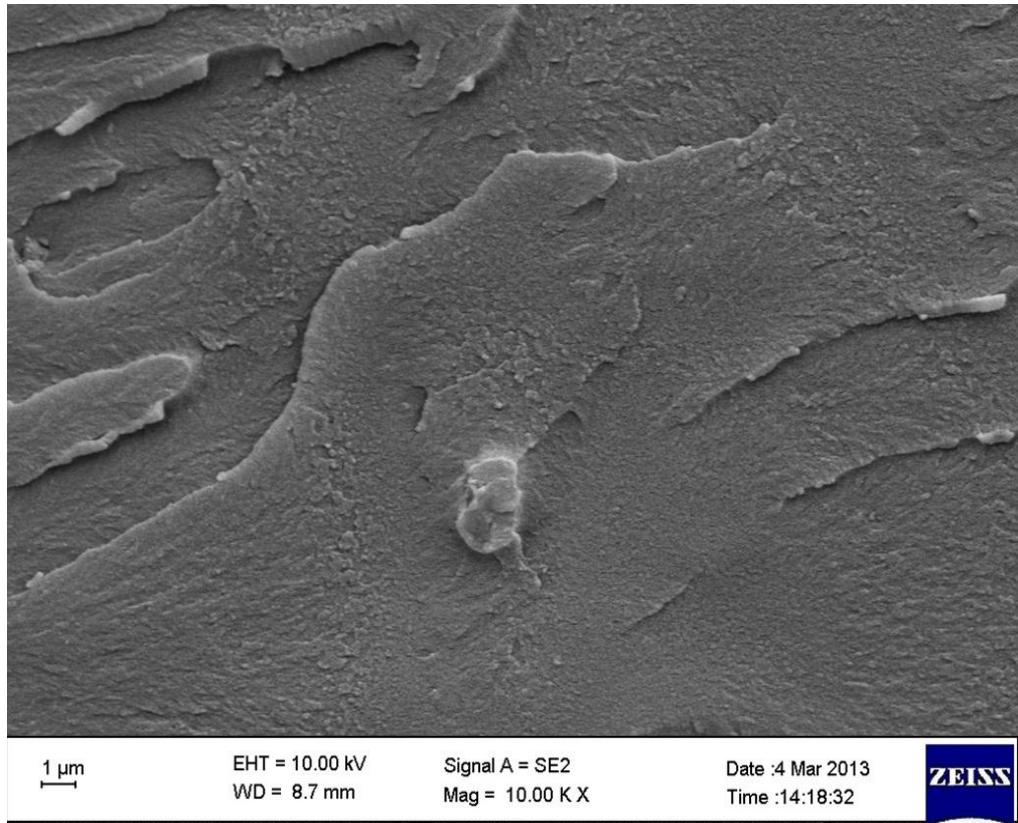


Figure 3.51: SEM Micrograph of Non-irradiated PCOT10

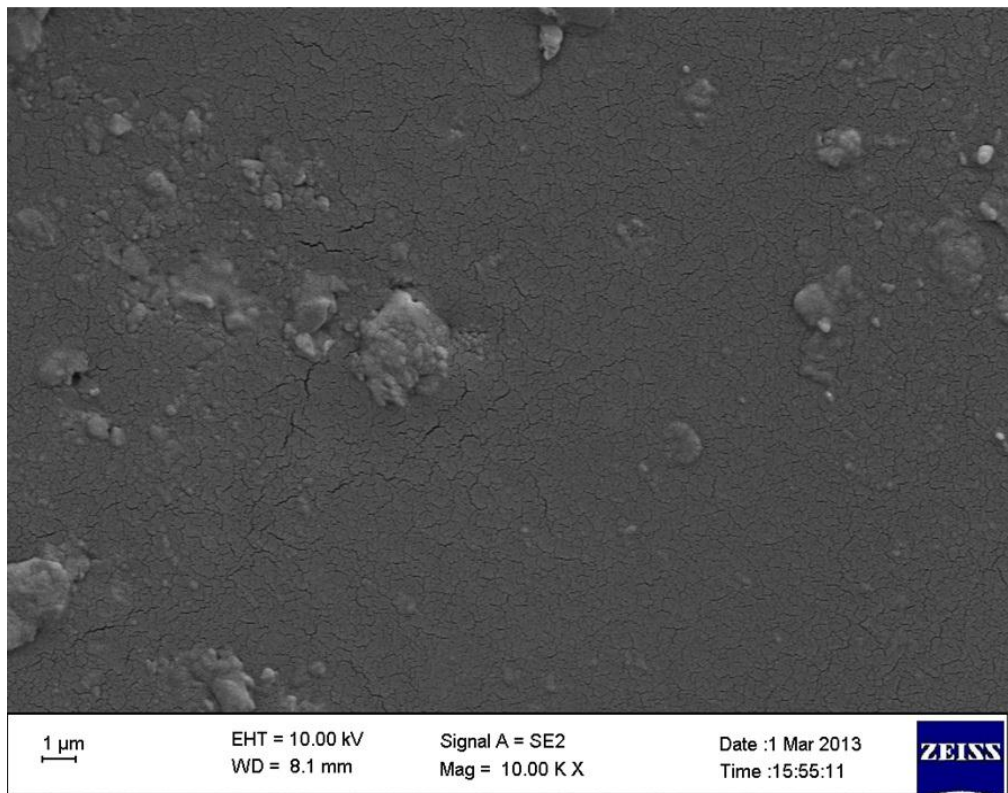


Figure 3.52: SEM Micrograph of PCOT10 Irradiated by Low Dose Rate Gamma Source with Absorbed Dose of 54 kGy

It can be seen from Figure 3.52 that it was hard to talk about evenly distribution of filler particles for PCOT10. Non-uniform dispersion led to some agglomeration and this situation disrupts homogeneity of the composite. Micro cracks were also observed around boron clusters and these micro cracks were the main reason of the loss in tensile strength.

CHAPTER 4

CONCLUSIONS

Unsaturated polyester resin is one of the mostly used resins around the world and has wide range of application areas from manufacture of furniture to building of ships. Exposure to radiation in everyday life increases with fast development of technology. Protection from radiation becomes more essential and this study aimed to manufacture an alternate composite material to use for radiation protection.

When the results of this study were investigated, following conclusions can be reached:

- Irradiation dose rate is an important parameter that leads different effects on same polymer through different mechanisms such as crosslinking or chain scission.
- Boron minerals gave resistance against low doses since composite materials had better mechanical properties. On the other hand, boron minerals were not effective against high doses. Degradation was the dominant mechanism and boron minerals could not show any significant shielding effect. As a result, polyester-boron composites manufactured in this study can be used in low level radioactive applications.
- Absence of oxygen did not have positive effect on mechanical properties since there were not any significant differences between mechanical test results of samples irradiated in air and under vacuum by high dose rate gamma source. This situation can be clarified by oxidation of radicals formed by irradiation with oxygen trapped in composite network and with oxygen in polyester chains.

- High amount of reinforcing filler could prevent formation of crosslinks. Defects in filler-polyester interface enhanced degradative effects of radiation.
- Most satisfying results were obtained for composites reinforced with anhydrous borax. Its highest boron content made composite material able to resist against radiation. On the other hand, colemanite had the worst performance on the contrary of its moderate boron content. Molecules of colemanite were much bigger than other boron minerals used in this study and they could interrupt curing and crosslinking of polyester resin.
- ATR-FTIR results gave information about transformations occurred during irradiation. Formation or breakage of crosslinks, degradation of polyester chains, and formation of polystyrene from unreacted styrene monomer could be observed from ATR-FTIR spectra. Especially 975 cm^{-1} (ester double bonds, C=C), 1450 cm^{-1} (polystyrene), 1720 cm^{-1} (carbonyl groups, C=O) and region of $3500\text{-}4000\text{ cm}^{-1}$ (-OH groups) bands shown the change in the structure.
- DMA results showed that irradiation by low dose rate gamma source did not have significant effect on glass transition temperature of samples. But irradiation by high dose rate gamma source shifted T_g to higher temperatures due to higher polystyrene formation since polystyrene has higher T_g than unsaturated polyester. Boron minerals also gave an increase on T_g of composites. They are rigid materials and T_g was expected to increase since mobility of the polymer chains near these rigid particles is hindered.
- Thermal stability of composites was not affected by irradiation as seen from TGA results. Thermal stability also was not changed significantly with respect to boron minerals due to lack of chemical bonding between polyester chains and boron minerals. Char residue was proportional to the amount of filler in composite materials.
- SEM results showed that boron minerals affected surface morphology of composites. Formation of fractures after irradiation could be observed from SEM micrographs. Higher amount of reinforcing filler in composites tend to agglomeration.

REFERENCES

1. Abdelghany, A.M., ElBatal, F.H., ElBatal, H.A., and EzzElDin, F.M., “Optical and FTIR Structural Studies of CoO-doped Sodium Borate, Sodium Silicate and Sodium Phosphate Glasses and Effects of Gamma Irradiation – A Comparative Study”, *Journal of Molecular Structure*, vol. 1074, pp 503-510. (2014)
2. Ajjji, Z., “Preparation of polyester/gypsum/composite using gamma radiation, and its radiation stability”, *Radiation Physics and Chemistry*, vol. 73, pp 183-187. (2005)
3. Ateş, E., and Barnes, S., “The effect of elevated temperature curing treatment on the compression strength of composites with polyester resin matrix and quartz filler”, *Materials and Design*, vol. 34, pp 435-443. (2012)
4. Atta, A.M., Nassar, I.F., and Bedawy, H.M., “Unsaturated Polyester Resins Based on Rosin Maleic Anhydride Adduct as Corrosion Protections of Steel”, *Reactive & Functional Polymers*, vol. 67, pp 617-626. (2007)
5. Aytaç, A., Şen, M., Deniz, V., and Güven, O., “Effect of gamma irradiation on the properties of tyre cords”, *Nuclear Instruments and Methods in Physics Research B*, vol. 267, pp 271-275. (2007)
6. Baştuğ, A., Gürol, A., İçelli, O., and Şahin Y., “Effective atomic numbers of some composite mixtures including borax”, *Annals of Nuclear Energy*, vol. 37, pp. 927-933. (2010)
7. Bellamy, L.J., *The Infra-red Spectra of Complex Molecules*, Chapman and Hall Ltd., London, UK. (1975)

8. Bessadok, A., Roudesli, S., Marais, S., Follain, N., and Lebrun, L., "Alfa fibres for unsaturated polyester composites reinforcement: Effects of chemical treatments on mechanical and permeation properties", *Composites: Part A*, vol. 40, pp 184-195. (2009)
9. Binici, H., Aksoğan, O., Sevinç, A.H., and Küçükönder, A., "Mechanical and radioactivity shielding performances of mortars made with colemanite, barite, ground basaltic pumice and ground blast furnace slag", *Construction and Building Materials*, vol. 50, pp. 177-183. (2014)
10. Biron, M., *Thermosets and Composites*, Elsevier Ltd., Oxford, UK. (2004)
11. Bor Ürünleri (2012), Available at: http://www.etimaden.gov.tr/tr/0_sayfa_ortakSayfa.asp?hangisayfa=4_sayfa_a_4 (Accessed April 27th 2012)
12. Budak, A., and Gönen, M., "Extraction of Boric Acid from Colemanite Mineral by Supercritical Carbon Dioxide", *Journal of Supercritical Fluids*, vol. 92, pp. 183-189. (2014)
13. Büyük, B., and Tuğrul, A.B., "Gamma and Neutron Attenuation Behaviours of Boron Carbide-Silicon Carbide Composites", *Annals of Nuclear Energy*, vol. 71, pp. 46-51. (2014)
14. Cherian, A.B., Varghese, L.A., and Thachil, E.T., "Epoxy-modified, unsaturated polyester hybrid networks", *European Polymer Journal*, vol. 43, pp 1460-1469. (2007)
15. Choi, C.H., and Kertesz, M., "Conformational Information from Vibrational Spectra of Styrene, *trans*-Stilbene, and *cis*-Stilbene", *The Journal of Physical Chemistry A*, vol. 101, pp 3823-3831. (1997)
16. Clegg, D.W., and Collyer, A.A., *Irradiation Effects on Polymers*, Elsevier Science Publishers Ltd., Essex, UK. (1991)

17. Croonenborghs, B., Smith, M.A., and Strain, P., "X-ray versus gamma irradiation effects on polymers", *Radiation Physics and Chemistry*, vol. 76, pp 1676-1678. (2007)
18. Czayka, M., Fisch, M., Uribe, R.M., and Vargas-Aburto, C., "Radiation-thickening of iso-polyester resin", *Radiation Physics and Chemistry*, vol. 76, pp 1058-1068. (2007)
19. Çetin, B., Ünal, H.İ., Erol, Ö., "Synthesis, Characterization and Electrokinetic Properties of Polyindene/Colemanite Conducting Composite", *Clays and Clay Minerals*, vol. 60, pp. 300-314. (2012)
20. Delahaye, N., Malais, S., Saiter, J.M., and Metayer, M., "Characterization of unsaturated polyester resin cured with styrene", *Journal of Applied Polymer Science*, vol. 67, pp 695-703. (1998)
21. Demir, F., "Determination of mass attenuation coefficients of some boron ores at 59.54 keV by using scintillation detector", *Applied Radiation and Isotopes*, vol. 68, pp. 175-179. (2010)
22. Demir, F., and Un, A., "Radiation transmission of colemanite, tincalconite and ulexite for 6 and 18 MV X-rays by using linear accelerator", *Applied Radiation and Isotopes*, vo. 72, pp. 1-5. (2013)
23. Derun, E.M., and Kıpçak, A.S., "Characterization of some boron minerals against neutron shielding and 12 year performance of neutron permeability", *Journal of Radioanalytical and Nuclear Chemistry*, vol. 292, pp. 871-878. (2012)
24. Evans, S.J., Haines, P.J., and Skinner, G.A., "The thermal degradation of polyester resins II: The effects of cure and of fillers on degradation", *Thermochimica Acta*, vol. 291, pp 43-49. (1997)

25. Evora, V.M.F., and Shukla, A., "Fabrication, characterization and dynamic behavior of polyester/TiO₂ nanocomposites", *Materials Science and Engineering A*, vol. 361, pp 358-366. (2003)
26. Fernandes Jr., V.J., Fernandes, N.S., Fonseca, V.M., Araujo, A.S., and Silva, D.R., "Kinetic evaluation of decabromodiphenil oxide as a flame retardant for unsaturated polyester", *Thermochimica Acta*, vol. 388, pp 283-288. (2002)
27. Fintzou, A.T., Kontominas, M.G., Badeka, A.V., Stahl, M.R., and Riganakos, K.A., "Effect of electron-beam and gamma-irradiation on physicochemical and mechanical properties of polypropylene syringes as a function of irradiation dose: Study under vacuum", *Radiation Physics and Chemistry*, vol. 76, pp 1147-1155. (2007)
28. Frost, R.L., Xi, Y., Scholz, R., Belotti, F.M., and Filho, M.C., "Infrared and Raman Spectroscopic Characterization of the Borate Mineral Colemanite – CaB₃O₄(OH)₃.H₂O – Implications for the Molecular Structure", *Journal of Molecular Structure*, vol. 1037, pp 23-28. (2013)
29. Garrett, D.E., *Borates: Handbook of Deposits, Processing, Properties and Use*, Academic Press, San Diego, USA. (1998)
30. Goodman, S.H., *Handbook of Thermoset Plastics*, Noyes Publications, New Jersey, USA. (1998)
31. Gu, H., "Degradation of glass fibre/polyester composites after ultraviolet radiation", *Materials and Design*, vol. 29, pp 1476-1479. (2008)
32. Hacıoğlu, F., "Degradation of EPDM via Gamma Irradiation and Possible Use of EPDM in Radioactive Waste Management", M.Sc. Thesis in Polymer Science and Technology, Middle East Technical University, Ankara, Turkey. (2010)

33. Hanemann, T., Schumacher, B., and Hausselt, J., "Polymerization conditions influence on the thermomechanical and dielectric properties of unsaturated polyester-styrene-copolymers", *Microelectric Engineering*, vol. 87, pp 15-19. (2010)
34. Hassan, S.B., Oghenevweta, J.E., and Aigbodion, V.S., "Morphological and mechanical properties of carbonized waste maize stalk as reinforcement for eco-composites", *Composites: Part B*, vol. 43, pp 2230-2236. (2012)
35. Ivanov, V.S., *Radiation Chemistry of Polymers*, Koninklijke, B.V., Utrecht, The Netherlands. (1992)
36. Jurkin, T., and Pucic, I., "Post-irradiation crosslinking of partially cured unsaturated polyester resin", *Radiation Physics and Chemistry*, vol. 75, pp 1060-1068. (2006)
37. Kıpçak, A.S., Baysoy, D.Y., Derun, E.M., and Pişkin, S., "Characterization and neutron shielding behavior of dehydrated magnesium borate minerals synthesized via solid-state method", *Advances in Materials Science and Engineering*, vol. 2013, pp. 1-9. (2013)
38. Kıpçak, A.S., Derun, E.M., and Pişkin, S., "Characterization and determination of neutron transmission properties of sodium-calcium and sodium borates from different regions of Turkey", *Journal of Radioanalytical and Nuclear Chemistry*, vol. 301, pp. 175-188. (2014)
39. Kijchavengkul, T., Auras, R., Rubino, M., Alvarado, E., Montero, J.R.C., and Rosales, J.M., "Atmospheric and soil degradation of aliphatic-aromatic polyester films", *Polymer Degradation and Stability*, vol. 95, pp 99-107. (2010)
40. Kirk-Othmer Encyclopedia of Chemical Technology, John Wiley & Sons Ltd., New York. (2001)

41. Kojima, K., Kumafuji, H., and Ueno, K., “Discoloration of plasticized PVC by irradiation”, *Radiation Physics and Chemistry*, vol. 18, pp 859-863. (1981)
42. Korkut, T., Karabulut, A., Budak, G., Aygün, B., Gencil, O., and Hançerlioğulları, A., “Investigation of neutron shielding properties depending on number of boron atoms for colemanite, ulexite and tincal ores by experiments and FLUKA Monte Carlo simulations”, *Applied Radiations and Isotopes*, vol. 70, pp. 341-345. (2012)
43. Lipatov, Y.S., *Polymer Reinforcement*, ChemTec Publishing, Ontario, Canada. (1995)
44. Madugu, I.A., Abdulwahab, M., and Aigbodion, V.S., “Effect of iron fillings on the properties and microstructure of cast fiber–polyester/iron filings particulate composite”, *Journal of Alloys and Compounds*, vol. 476, pp 807-811. (2009)
45. Mansour, E., “FTIR Spectra of Pseudo-binary Sodium Borate Glasses Containing TeO₂”, *Journal of Molecular Structure*, vol. 1014, pp 1-6. (2012)
46. Marais, S., Metayer, M., Labbe, M., Valleton, J.M., Alexandre, S., Saiter, J.M., and Poncin-Epaillard, F., “Surface Modification by Low-pressure Glow Discharge Plasma of an Unsaturated Polyester Resin: Effect on Water Diffusivity and Permeability”, *Surface and Coatings Technology*, vol. 122, pp 247-259. (1999)
47. Mark, H.F., *Encyclopedia of Polymer Science and Technology*, vol.11, John Wiley & Sons Ltd., New York. (2003)
48. Mark, J.E., *Physical Properties of Polymers Handbook*, Springer Science, New York. (2007)

49. Martinez-Barrera, G., Villarruel, U.T., and Viguera-Santiago, E., "Compressive Strength of Gamma-irradiated Polymer Concrete", *Polymer Composites*, vol. 29, pp 1210-1217. (2008)
50. Mayo, D.W., Miller, F.A., and Hannah, R.W., *Course Notes on the Interpretation of Infrared and Raman Spectra*, John Wiley & Sons, New Jersey, USA. (2003)
51. Mishra, S., Mohanty, A.K., Drzal, L.T., Misra, M., Parija, S., Nayak, S.K., and Tripathy, S.S., "Studies on mechanical performance of biofibre/glass reinforced polyester hybrid composites", *Composites Science and Technology*, vol. 63, pp 1377-1385. (2003)
52. Mulinari, D.R., Baptista, C.A.R.P., Souza, J.V.C., and Voorwald, H.J.C., "Mechanical Properties of Coconut Fibers Reinforced Polyester Composites", *Procedia Engineering*, vol. 10, pp 2074-2079. (2011)
53. Murray, R.L, *Nuclear Energy: An Introduction to the Concepts, Systems, and Applications of Nuclear Processes*, Butterworth-Heinemann, Boston, USA. (2000)
54. Park, E.H., Jeong, S.U., Jung, U.H., Kim, S.H., Lee, J., Nam, S.W., Lim, T.H., Park, Y.J., and Yu, Y.H., "Recycling of Sodium Metaborate to Borax", *International Journal of Hydrogen Energy*, vol. 32, pp. 2982-2987. (2007)
55. Pavlyukevich, Y. G., Levitskii, I. A., and Mazura, N. V., "Use of Colemanite in Glass Fiber Production", *Glass and Ceramics*, vol. 66, pp. 345-349. (2009)
56. Peacock, A.J., and Calhoun, A., *Polymer Chemistry: Properties and Applications*, Hanser Gardner Publications, Munich, Germany. (2006)
57. Peak, D., Luther III, G.W. and Sparks, D.L., "ATR-FTIR Spectroscopic Studies of Boric Acid Adsorption on Hydrous Ferric Oxide", *Geochimica et Cosmochimica Acta*, vol. 67, pp. 2551-2560. (2003)

58. Peng, G., Li, Q., Yang, Y., Wang, H., and Li, W., "Effect of nano ZnO on strength and stability of unsaturated polyester composites", *Polymers for Advanced Technologies*, vol. 19, pp 1629-1634. (2008)
59. Ramanaiah, K., Prasad, A.V.R., and Reddy, K.H.C., "Thermal and mechanical properties of waste grass broom fiber-reinforced polyester composites", *Materials and Design*, vol. 40, pp 103-108. (2012)
60. Sastri, V.R., *Plastics in Medical Devices*, William Andrew Publishing, New York. (2010)
61. Sathishkumar, T.P., Navaneethakrishnan, P., and Shankar, S., "Tensile and flexural properties of snake grass natural fiber reinforced isophthallic polyester composites", *Composites Science and Technology*, vol. 72, pp 1183-1190. (2012)
62. Sawpan, M.A., Pickering, K.L., and Fernyhough, A., "Flexural properties of hemp fibre reinforced polylactide and unsaturated polyester composites", *Composites: Part A*, vol. 43, pp 519-526. (2012)
63. Schiers, J., and Long, T.E., *Modern Polyesters: Chemistry and Technology of Polyesters and Copolyesters*, John Wiley & Sons Ltd., Wiltshire, Great Britain. (2003)
64. Scott, G., *Mechanisms of Polymer Degradation and Stabilisation*, Elsevier, NY, USA. (1990)
65. Segovia, F., Ferrer, C., Salvador, M.D., and Amigo, V., "Influence of processing variables on mechanical characteristics of sunlight aged polyester-glass fibre composites", *Polymer Degradation and Stability*, vol. 71, pp 179-184. (2001)

66. Seki, Y., Sever, K., Sarikanat, M., Sakarya, A., and Elik, E., "Effect of huntite mineral on mechanical, thermal and morphological properties of polyester matrix", *Composites: Part B*, vol. 45, pp 1534-1540. (2013)
67. Sepe, M.P., *Thermal Analysis of Polymers*, Rapra Technology, Poland. (1997)
68. Simitzis, J., Stamboulis, A., Tsoros, D., and Martakis, N., "Kinetics of Curing of Unsaturated Polyesters in the Presence of Organic and Inorganic Fillers", *Polymer International*, vol. 43, pp 380-384. (1997)
69. Smith, B.C., *Fundamentals of Fourier Transform Infrared Spectroscopy*, Taylor & Francis, Florida, USA. (2011)
70. Sorenson, W.R., Sweeny, F., and Campbell, T.W., *Preparative Methods of Polymer Chemistry*, John Wiley & Sons, NY, USA. (2001)
71. Sreekumar, P.A., Joseph, K., Unnikrishnan, G., and Thomas, S., "A comparative study on mechanical properties of sisal-leaf fibre-reinforced polyester composites prepared by resin transfer and compression moulding techniques", *Composites Science and Technology*, vol. 67, pp 453-461. (2007)
72. Sreenivasan, V.S., Ravindran, D., Manikandan, V., and Narayanasamy, R., "Influence of fibre treatments on mechanical properties of short *Sansevieria cylindrica*/polyester composites", *Materials and Design*, vol. 37, pp 111-121. (2012)
73. Stuart, B.H., *Polymer Analysis*, John Wiley & Sons, NY, USA. (2002)
74. Stuart, B.H., *Infrared Spectroscopy: Fundamentals and Applications*, John Wiley & Sons, West Sussex, England. (2004)

75. Şen, S., and Nugay, N., "Tuning of final performances of unsaturated polyester composites with inorganic microsphere/platelet hybrid reinforcers", *European Polymer Journal*, vol. 37, pp 2047-2053. (2001)
76. Tibiletti, L., Longuet, C., Ferry, L., Coutelen, P., Mas, A., Robin, J., and Lopez-Cuesta, J., "Thermal degradation and fire behaviour of unsaturated polyesters filled with metallic oxides", *Polymer Degradation and Stability*, vol. 96, pp 67-75. (2011)
77. Un, A., and Şahin, Y., "Determination of mass attenuation coefficients, effective atomic and electron numbers, mean free paths and keramas for PbO, barite and some boron ores", *Nuclear Instruments and Methods in Physics Research B*, vol. 269, pp. 1506-1511. (2011)
78. Waigaonkar, S., Babu, B.J.C., and Rajput, A., "Curing Studies of Unsaturated Polyester Resin Used in FRP Products", *Indian Journal of Engineering & Materials Sciences*, vol. 18, pp 31-39. (2011)
79. Weir, C.E., "Infrared Spectra of the Hydrated Borates", *Journal of Research of the National Bureau of Standards – A. Physics and Chemistry*, vol. 70A, pp. 153-164. (1966)
80. Zhang, M., and Singh, R.P., "Mechanical reinforcement of unsaturated polyester by Al₂O₃ nanoparticles", *Materials Letters*, vol. 58, pp 408-412. (2004)

APPENDIX A

CONTENTS OF BORON MINERALS USED IN THE STUDY

Table A.1: Contents of Etibor-68 (Anhydrous Borax)

Content	Unit	Amount
B ₂ O ₃	%	68.00 (min.)
Na ₂ O	%	30.27 (min.)
SO ₄	ppm	200 (max.)
Cl	ppm	105 (max.)
Fe	ppm	150 (max.)
Insolubles in Water	ppm	920 (max.)

Table A.2: Contents of Calcined Tincal

Content	Unit	Amount
B ₂ O ₃	%	52.00 (min.)
Na ₂ O	%	23.00 (min.)
SO ₄	%	0.15 (max.)
Fe	%	0.11 (max.)
SiO ₂	%	3.00 (max.)
CaO	%	3.25 (max.)
MgO	%	3.00 (max.)

Table A.3: Contents of Concentrated Tincal

Content	Unit	Amount
B ₂ O ₃	%	29.00
Na ₂ O	%	12.80
As	ppm	9
SiO ₂	%	2.50
CaO	%	2.80
MgO	%	2.70

Table A.4: Contents of Ground Colemanite

Content	Unit	Amount
B ₂ O ₃	%	40.00 ± 0.50
CaO	%	27.00 ± 1.00
SiO ₂	%	4.00-6.50
SO ₄	%	0.60 (max.)
As	ppm	35 (max.)
Fe ₂ O ₃	%	0.08 (max.)
Al ₂ O ₃	%	0.40 (max.)
MgO	%	3.00 (max.)
SrO	%	1.50 (max.)
Na ₂ O	%	0.35 (max.)
Loss on Ignition	%	24.60 (max.)

APPENDIX B

PROPERTIES OF UNSATURATED POLYESTER RESIN USED IN THE STUDY

Table B.1: Properties of Unsaturated Polyester Resin

Manufacturer	Eskim A.Ş. (Eskişehir, Turkey)
Type	Orthophthalic based cast type
Commercial Name	ES 1060 DK
Density (at 20 °C)	$1,15 \pm 0,02 \text{ g/cm}^3$
Viscosity (at 25 °C)	$450 \pm 80 \text{ cp}$
Solid Content	$65 \pm 2 \%$
Monomer Content	$35 \pm 2 \%$
Acid Number	$25 \pm 5 \text{ mg KOH/g}$
Gel Time	$6 \pm 1 \text{ min}$

APPENDIX C

TABLES OF TENSILE TEST RESULTS

Table C.1: Young's Modulus Results of Tensile Tests*

Sample	Non-irradiated	Low Dose Rate Irradiation in Air			High Dose Rate Irradiation in Air			High Dose Rate Irradiation under Vacuum		
		LDR1	LDR2	LDR3	HDR1	HDR2	HDR3	HDR1	HDR2	HDR3
POL	1071.5	756.0	540.7	839.6	1151.4	1009.9	740.4	634.1	834.3	693.9
PANB2	1351.6	943.6	833.5	1099.4	1203.6	1085.5	631.2	528.0	981.8	916.9
PANB5	1309.5	1061.7	888.3	1119.0	1242.4	1226.5	703.9	1359.1	1208.5	1043.0
PANB10	1234.3	1148.6	1088.1	1254.8	1176.8	1278.2	726.2	644.2	724.1	569.7
PCAT2	1569.9	1094.4	1202.6	915.0	636.9	689.4	604.0	595.7	468.1	377.4
PCAT5	1286.5	1310.1	1254.1	1188.9	754.8	801.1	679.7	677.4	726.7	438.7
PCAT10	1107.3	1196.4	1705.3	1463.7	1077.8	982.0	881.2	796.8	1062.8	477.1
PCOL2	916.6	782.6	680.0	799.8	720.7	736.7	609.2	553.9	578.5	422.5
PCOL5	937.5	845.6	770.2	858.4	1214.2	1092.0	712.5	1008.5	852.5	872.9
PCOL10	996.3	1233.5	1064.3	1259.7	916.9	939.5	666.2	730.5	669.2	673.9
PCOT2	1170.3	1392.2	1040.2	1141.9	1485.0	1003.1	720.8	733.0	1009.0	723.3
PCOT5	1250.0	1458.9	1161.9	1096.1	1062.0	949.8	833.9	996.5	1016.6	811.0
PCOT10	1486.5	1775.2	1391.0	1345.4	1286.8	1067.4	838.0	1138.0	1084.1	892.7

* All results are in units of MPa.

Table C.2: Tensile Strength Results of Tensile Tests*

Sample	Non-irradiated	Low Dose Rate Irradiation in Air			High Dose Rate Irradiation in Air			High Dose Rate Irradiation under Vacuum		
		LDR1	LDR2	LDR3	HDR1	HDR2	HDR3	HDR1	HDR2	HDR3
POL	42.5	27.6	24.3	22.7	39.6	34.9	36.0	29.6	39.3	27.7
PANB2	42.3	31.4	33.4	32.6	32.0	30.3	29.1	30.0	37.2	27.6
PANB5	40.2	29.5	29.6	28.1	29.4	29.1	20.3	36.7	41.6	30.7
PANB10	37.3	30.9	31.6	29.1	26.5	22.1	18.2	23.6	32.5	19.9
PCAT2	46.4	32.6	29.5	21.7	27.7	24.3	26.2	27.7	26.3	20.6
PCAT5	41.9	35.8	25.3	17.4	28.7	26.9	25.3	29.6	26.2	16.7
PCAT10	31.8	24.2	27.8	20.9	30.4	29.7	22.2	16.2	13.5	23.7
PCOL2	40.4	30.4	21.9	22.1	33.2	28.2	26.9	27.5	27.4	21.7
PCOL5	39.4	30.5	22.0	27.6	44.4	33.5	33.6	33.2	28.7	33.0
PCOL10	30.8	29.9	26.0	30.2	32.3	27.5	23.2	27.4	26.7	25.2
PCOT2	33.2	29.1	27.7	29.0	35.3	32.2	26.9	35.2	32.1	27.7
PCOT5	47.2	31.4	30.7	30.2	31.2	25.2	24.0	19.2	23.6	31.2
PCOT10	39.4	33.8	26.5	25.8	18.1	15.0	19.3	13.1	13.6	20.4

* All results are in units of MPa.

Table C.3: Elongation at Break Results of Tensile Tests*

Sample	Non-irradiated	Low Dose Rate Irradiation in Air			High Dose Rate Irradiation in Air			High Dose Rate Irradiation under Vacuum		
		LDR1	LDR2	LDR3	HDR1	HDR2	HDR3	HDR1	HDR2	HDR3
POL	6.1	6.3	7.3	4.5	5.7	6.6	8.1	7.3	7.2	6.9
PANB2	5.3	5.9	5.8	4.6	5.3	5.6	7.6	6.8	5.7	4.9
PANB5	4.6	5.3	4.9	4.4	4.5	4.6	5.7	4.5	4.4	4.3
PANB10	4.1	3.7	4.6	4.2	3.7	3.3	4.9	3.7	4.9	6.7
PCAT2	4.5	4.2	4.1	4.5	6.9	6.3	6.6	6.7	7.1	7.4
PCAT5	4.1	4.1	3.2	3.1	5.7	5.1	5.6	4.5	4.8	6.7
PCAT10	3.5	4.0	3.1	3.6	5.1	3.7	5.3	3.7	2.4	7.1
PCOL2	5.1	5.5	5.0	5.9	6.7	4.9	8.8	6.9	6.6	7.8
PCOL5	4.8	5.1	4.6	6.2	5.9	4.7	8.3	6.1	5.8	5.1
PCOL10	3.7	3.8	4.0	5.1	5.4	4.2	7.5	5.4	5.6	5.8
PCOT2	5.4	4.3	4.8	4.3	4.0	5.3	5.9	6.2	4.5	6.3
PCOT5	4.6	4.1	4.0	4.1	3.8	4.9	4.5	5.2	4.2	6.7
PCOT10	3.8	3.6	3.7	3.5	2.8	3.8	3.8	2.9	2.0	4.6

* All results are in units of % .

APPENDIX D

TABLES OF NORMALIZED ABSORBANCE VALUES OF ATR- FTIR SPECTRA

Table D.1: ATR-FTIR Results of Boron Minerals

FT-IR Band	Structure	Normalized Absorbance			
		ANB	CAT	COT	COL
880 cm ⁻¹	B-OH	0,68	0,38	0,53	1,16
940 cm ⁻¹	BO ₃	0,81	0,73	0,81	1,12

Table D.2: ATR-FTIR Results of POL Irradiated by Low Dose Rate Gamma Source

FT-IR Band	Structure	Normalized Absorbance			
		Non-Irradiated	LDR1	LDR2	LDR3
795 cm ⁻¹	Styrene	0,41	0,50	0,58	0,55
975 cm ⁻¹	Ester C=C	0,42	0,45	0,46	0,47
1450 cm ⁻¹	Polystyrene	0,36	0,53	0,57	0,40
1720 cm ⁻¹	C=O	0,88	0,76	0,73	0,77

Table D.3: ATR-FTIR Results of Reinforced Samples Irradiated by Low Dose Rate Gamma Source (Absorbed Dose of 245 kGy)

FT-IR Band	Structure	Normalized Absorbance				
		POL	PANB5	PCAT5	PCOL5	PCOT5
795 cm ⁻¹	Styrene	0,55	0,52	0,40	0,40	0,46
975 cm ⁻¹	Ester C=C	0,47	0,45	0,41	0,42	0,43
1450 cm ⁻¹	Polystyrene	0,40	0,33	0,28	0,32	0,31
1720 cm ⁻¹	C=O	0,77	0,84	0,80	0,82	0,87

Table D.4: ATR-FTIR Results of PANB with Different Compositions Irradiated by Low Dose Rate Gamma Source (Absorbed Dose of 245 kGy)

FT-IR Band	Structure	Normalized Absorbance			
		POL	PANB2	PANB5	PANB10
975 cm ⁻¹	Ester C=C	0,42	0,43	0,45	0,48
1450 cm ⁻¹	Polystyrene	0,40	0,34	0,33	0,38
1720 cm ⁻¹	C=O	0,77	0,85	0,84	0,88

Table D.5: ATR-FTIR Results of POL Irradiated by High Dose Rate Gamma Source Open to Atmosphere

FT-IR Band	Structure	Normalized Absorbance			
		Non-Irradiated	HDR1	HDR2	HDR3
795 cm ⁻¹	Styrene	0,41	0,31	0,59	0,50
975 cm ⁻¹	Ester C=C	0,42	0,35	0,41	0,47
1450 cm ⁻¹	Polystyrene	0,36	0,29	0,37	0,77

Table D.6: ATR-FTIR Results of Reinforced Samples Irradiated by High Dose Rate Gamma Source Open to Atmosphere (Absorbed Dose of 2500 kGy)

FT-IR Band	Structure	Normalized Absorbance				
		POL	PANB5	PCAT5	PCOL5	PCOT5
875 cm ⁻¹	C-H (Aro.)	0,70	0,48	0,45	0,47	0,53
1370 cm ⁻¹	C-H (Aro.)	0,56	0,34	0,33	0,33	0,41
1450 cm ⁻¹	Polystyrene	0,77	0,40	0,37	0,37	0,48
2940 cm ⁻¹	Polystyrene	0,33	0,14	0,12	0,14	0,16

Table D.7: ATR-FTIR Results of PANB with Different Compositions Irradiated by High Dose Rate Gamma Source Open to Atmosphere (Absorbed Dose of 2500 kGy)

FT-IR Band	Structure	Normalized Absorbance			
		POL	PANB2	PANB5	PANB10
975 cm ⁻¹	Ester C=C	0,47	0,40	0,42	0,50
1450 cm ⁻¹	Polystyrene	0,77	0,33	0,40	0,47
2940 cm ⁻¹	Polystyrene	0,33	0,14	0,14	0,16

Table D.8: ATR-FTIR Results of POL Irradiated by High Dose Rate Gamma Source under Vacuum

FT-IR Band	Structure	Normalized Absorbance			
		Non-Irradiated	HDR1	HDR2	HDR3
975 cm ⁻¹	Ester C=C	0,42	0,37	0,24	0,36
1040 cm ⁻¹	Ester C-C	0,76	0,81	0,74	0,55
1070 cm ⁻¹	Ester =CH	0,81	0,91	0,88	0,95
1450 cm ⁻¹	Polystyrene	0,36	0,38	0,29	0,39
1600 cm ⁻¹	Polystyrene	0,18	0,21	0,18	0,29

Table D.9: ATR-FTIR Results of Reinforced Samples Irradiated by High Dose Rate Gamma Source under Vacuum (Absorbed Dose of 2500 kGy)

FT-IR Band	Structure	Normalized Absorbance				
		POL	PANB5	PCAT5	PCOL5	PCOT5
975 cm ⁻¹	Ester C=C	0,36	0,46	0,34	0,47	0,38
1040 cm ⁻¹	Ester C-C	0,55	0,77	0,68	0,78	0,69
1450 cm ⁻¹	Polystyrene	0,39	0,48	0,26	0,87	0,56
1720 cm ⁻¹	C=O	0,89	0,61	0,78	0,59	0,74
2940 cm ⁻¹	Polystyrene	0,36	0,41	0,19	0,43	0,39

Table D.10: ATR-FTIR Results of PANB with Different Compositions Irradiated by High Dose Rate Gamma Source under Vacuum (Absorbed Dose of 2500 kGy)

FT-IR Band	Structure	Normalized Absorbance			
		POL	PANB2	PANB5	PANB10
795 cm ⁻¹	Styrene	0,44	0,52	0,56	0,51
975 cm ⁻¹	Ester C=C	0,36	0,42	0,46	0,56
1450 cm ⁻¹	Polystyrene	0,39	0,56	0,48	0,85
1720 cm ⁻¹	C=O	0,89	0,67	0,61	0,52

CURRICULUM VITAE

PERSONAL INFORMATION

Surname, Name: Akgün, Aydın Mert

Nationality: Turkish (T.C.)

Date and Place of Birth: 6 February 1981, Ankara

Marital Status: Single

Phone: +90 532 562 86 05

e-mail: mert_akgun@yahoo.com

EDUCATION

Degree	Institution	Year of Graduation
MS	METU – Chemical Engineering	2005
BS	Anadolu Uni. – Business Administration	2011
BS	Gazi Uni. – Chemical Engineering	2003
High School	Anıttepe High School, Ankara	1998

WORK EXPERIENCE

Year	Place	Enrollment
2006-Present	Maden Tetkik ve Arama Genel Md.	Chemical Engineer
2002 June	ELROKSAN Elmadağ Roket San.	Intern Engineering Student
2001 June	Anadolu Efes Bira. ve Malt San.	Intern Engineering Student

FOREIGN LANGUAGES: English

ORAL PRESENTATIONS

1. Babucuođlu, Y., Akgn, A.M., Demirtař, G., and Yksel, B., “Trkiye ve Dnya Maden Aramacılıđında MTA Analiz Laboratuvarlarının Yeri ve nemi”, VI. Geochemistry Symposium, Mersin Turkey, 2014.
2. Akgn, A.M., Babucuođlu, Y., Babucuođlu, A., and Arslan, Y., “Burdur Gl Toprak Yapısının Kaplıca Toprakları ile Element İeriđi Aısından Benzerliđi”, XIII. National Spectroscopy Congress, Burdur Turkey, 2013.
3. Babucuođlu, Y., and Akgn, A.M., “Jeokimyasal Aramalarda Analiz Yntemleri”, I. Symposium of Geosciences, Isparta Turkey, 2012.
4. Babucuođlu, Y., and Akgn, A.M., “Dnyada ve Trkiye’de Jeokimyasal Analiz alıřmaları”, ES-AN 2012, Trabzon Turkey, 2012.

POSTER PRESENTATIONS

1. Bahadır Cořkun, A., Babucuođlu, A., Akgn, A.M., and Babucuođlu, Y., “Investigation of Mineralogical Matrix Effect on XRF Analysis of Geological Samples”, 6th Black Sea Basin Conference on Analytical Chemistry, Trabzon Turkey, 2013.
2. Akgn, A.M., Kaplan, E., Babucuođlu, Y., Arslan, Y., and Kendzler, E., “Determination of Some Heavy Metals in Soil Samples”, VIII. Aegean Analytical Chemistry Days, İzmır Turkey, 2012.
3. Akgn, A.M., Babucuođlu, Y., Babucuođlu, A., and Arslan, Y., “Jeokimyasal rneklerde özme Yntemlerinin Karřılařtırılması”, ES-AN 2012, Trabzon Turkey, 2012.
4. Yzer Demirhisar, D., Akgn, A.M., and Demirel, V., “Farklı Asit Karıřımları ile Mikrodalga özme Yntemi Kullanılarak ICP-OES ile Eser Element Analizi”, 25th National Chemistry Congress, Erzurum Turkey, 2011.
5. Akgn, A.M., Babucuođlu, Y., and Arslan, Y., “Jeokimyasal Analiz Srecinde Dere Sedimanı rnekleri ierisindeki Bazı Elementlerin Deriřimlerinin Zaman Bađlı Olarak Deđiřimlerinin ICP-OES Tekniđi ile İncelenmesi”, XII. National Spectroscopy Congress, Antalya Turkey, 2011.

HOBBIES

Movies, Computer Technologies, Literature, Comics, Formula 1